Spring 5-17-2010

POLYMERSOMES: MULTI-FUNCTIONAL TOOLS FOR IN VIVO CANCER THERANOSTIC APPLICATIONS

Dalia H. Levine
University of Pennsylvania, daliahl@seas.upenn.edu

POLYMERSOMES: MULTI-FUNCTIONAL TOOLS FOR IN VIVO CANCER THERANOSTIC APPLICATIONS

Abstract
ABSTRACT

POLYMERSOMES: MULTI-FUNCTIONAL TOOLS FOR IN VIVO CANCER THERANOSTIC APPLICATIONS

Dalia Hope Levine

Dr. Daniel A. Hammer

Nanoparticles are currently being developed as delivery vehicles for therapeutic and contrast imaging agents. Polymersomes (mesoscopic polymer vesicles) possess a number of attractive biomaterial properties, including greater biocompatibility, prolonged circulation times, and increased mechanical stability, that make them ideal for these applications. The polymersome architecture, with its large hydrophilic reservoir and thick hydrophobic lamellar membrane, provides significant storage capacity for water soluble and insoluble substances.

The primary thesis aims are to develop multi-functional polymersomes for combination therapeutic applications, as well as simultaneous therapeutic and diagnostic applications. These multi-functional vesicles are capable of simultaneously loading both therapeutic agents, such as doxorubicin and combretastatin, and optical imaging agents, such as porphyrin-based near infrared (NIR) fluorophores, into their hydrophobic and hydrophilic regions.

Doxorubicin, an anti-neoplastic agent, was encapsulated into PEO-b-PCL polymersomes and its release was characterized in situ. In vitro and in vivo studies confirmed the therapeutic potential of doxorubicin loaded polymersomes. Furthermore, the in vitro therapeutic efficacy of polymersomes loaded with combretastatin, an anti-vascular agent, was established with and without co-doxorubicin loading. The co-encapsulation of DOX and combretastatin into polymeric vesicles, generates a multi-functional drug loaded polymersome with the potential to eliminate tumorigenic cells an endothelial cells, respectively.

The use of near infrared (NIR) emissive porphyrin polymersomes, loaded with porphyrin, for biodistribution studies, to non-invasively track the location of the polymersomes in tumor bearing mice was demonstrated using a noninvasive small animal optical imaging instrument which detects NIR fluorescence signal. Passive accumulation of drug loaded NIR-emissive polymersomes in tumor tissues of mice, as well as other organs, was observed. The study findings suggest the potential utility of NIR-emissive porphyrin polymersome in clinical diagnostic applications. Furthermore, preliminary results utilizing drug loaded porphyrin polymersomes to retard tumor growth and monitor vesicle location suggest these vesicles may have great future clinical utility.

The ability to load components into the polymersome membrane and core shows enormous promise for future dual modality polymersomes with potential to be nanostructured biomaterials for future theranostic applications which provide both therapy and diagnosis.

POLYMERSOMES: MULTI-FUNCTIONAL TOOLS FOR *IN VIVO* CANCER THERANOSTIC APPLICATIONS

Dalia Hope Levine

A DISSERTATION

In

Chemical and Biomolecular Engineering

Presented to the Faculties of the University of Pennsylvania in Partial Fulfillment of the Requirements for the Degree of Doctor of Philosophy

2010

Supervisor of Dissertation Daniel A. Hammer, Ph.D. Depts. of Chemical and Biomolecular Engineering and Bioengineering, Professor	Graduate Group Chairperson Raymond J. Gorte, Ph.D. Dept. of Chemical and Biomolecular Engineering, Professor
Dissertation Committee Members: Scott L. Diamond, Ph.D. Depts. of Chemical and Biomolecular Engineering and Bioengineering, Professor	Kathleen J. Stebe, Ph.D. Dept. of Chemical and Biomolecular Engineering, Professor and Chair
Jason A. Burdick, Ph.D. Dept. of Bioengineering, Assistant Professor	Lewis A. Chodosh, M.D., Ph.D. Dept. of Cancer Biology, Professor and Chair

POLYMERSOMES: MULTI-FUNCTIONAL TOOLS FOR *IN-VIVO* CANCER THERANOSTIC APPLICATIONS

Dedicated in loving memory of my family that perished during the Holocaust and my beloved stepfather. Your memories will always live on with me

Dedicated to my mother; simply said, I would never have completed this without you.

ACKNOWLEDGEMENT

Many people believe that completing a PhD is a solitary journey of growth and exploration. However, after over five years at Penn, and a lifetime in the making, I can unequivocally say that it is not. Along the journey there have been a number of outstanding individuals who have helped me by providing me with their time, encouragement, support, and ideas.

My thesis advisor, Dr. Daniel Hammer, deserves immeasurable thanks for his guidance, support, dedication, and patience throughout my PhD. His advising style, hands-off, yet always "on top of things", has provided me with a wonderful opportunity to grow as a scientist by learning through thinking and doing rather than by simply carrying out his directions. I am thankful to have been a part of his laboratory and for the opportunity to explore such ground breaking research. I must also express my immeasurable gratitude to Dr. P. Peter Ghoroghchian, my mentor and friend, for always providing encouragement, support, and brilliant suggestions; you were instrumental to this thesis both scientifically and personally. I am indebted to Eric Johnston for his technical knowledge and for putting up with my never ending purchase order and lab requests. Dr. Paul Frail must be thanked for his willingness to share his endless spectroscopy knowledge, his insightful suggestions, and of course, his porphyrins!

To my thesis committee, Dr. Kathleen Stebe, Dr. Scott Diamond, Dr. Jason Burdick, and Dr. Lewis Chodosh, I am grateful for your time, attention, ideas,

suggestions and interest. Furthermore, I thank you for your insight into the “world outside of graduate school”. Your career and life advice has proven very helpful.

To Dr. Kelly Yee and Dr. Risat Jannat, you have no idea how much your support, empathy, and friendship has meant to me throughout the growing pains of PhD research. Dr. Lauren Pepper, my gym buddy, without you, I’d be 40lbs heavier and insane!

I would like to thank all members of the Hammer Lab throughout my time at Penn for your support, friendship, and willingness to discuss ideas. In particular, Randi Saunders and Aaron Dominguez you guys simply brighten my morning and day, and my cells and I are forever indebted to you for always warming the media! Dr. Mathew Paszek thank you so much for teaching me the ins and outs of cell culture (…I don’t know if I should thank you or hate you for it...) and for always being ready to answer cell culture questions at all hours of the day or night! Olga Shebanova, I must thank you for always being there at the right time—you’ve listened to me, “yelled” at me, provided support, and kept me on track. A huge thank you goes to team polymersome— The Extrusion Kings: Nimil Sood and Nick Dang, The Synthesis Guru: Joshua Katz (primarily for your understanding with the extruder usage, and of course your synthesis and chemistry knowledge!) , Neha Kamat, Dr. Natalie Christian, Samuel Bernard, Ali Dhanaliwali, Shraddha Ranka, and Greg Robbins—and Brendon Ricart for all their help! Good luck in the future! I must further thank Nimil Sood for his invaluable help with my final *in vivo* study; his dedication, drive, perseverance, and good spirits were much appreciated. I wish him the best of luck in his future studies. Dr. Michael Beste: we

went through this from the beginning to the end and your friendship and support has been indispensible.

I have had the opportunity to collaborate with many outstanding scientists during my PhD whose assistance not only aided in completing my thesis work, but also to helped me grow as a researcher. Thank you to Dr. Ramacharan Murali, Dr. Michael Therien, Dr. Jaclyn Fruedenberg, Dr. Geng Zhang, and Dr. Hongtao Zhang. Thank you to Julie Czupryna and Lanlan Zhou for coming to the rescue with animal handling help.

Additional thanks to ULAR, in particular, Howard Gross, Michelle Turner and their staff, for assistance with animal husbandry. I must express my gratitude to Dr. David Wasserman for his assistance with *in vivo* imaging and analysis of the images. Furthermore, I appreciate all the suggestions and advice Dr. Brenton Hoffman provided with regards to cell culture and cellular assays.

A special thanks to the administrative staff of the CBE and BE Offices.

To my Philly Phriends and Phamily—in particular, MHB, JGSN, The Chevra, etc.- you have been my cheering squad and I thank you immensely.

I would be remiss if I did not thank those people that made it possible for me to embark on this journey long before I realized that I wanted to attend graduate school. While the list would be extraordinarily long if I mentioned everyone, thank you to my wonderful teachers in the Cold Spring Harbor Public School System and my amazing professors at The Cooper Union; you planted the seeds of curiosity that have led me to embark on this journey. To my Cooper Union ChemE's 2002, you guys rock!

I would like to express my unbound love for my family and gratitude for their unwavering support throughout my life. This body of work is a proof of your love, dedication, encouragement, and ideas. To my aunt and uncle, who have always treated me as their own, thank you so much for loving me. To my cousin Betty—thank you for always answering my why's and to her and Mark, her husband, for reading over all of my papers though the years. To my cousin Sammy, thank you for your endless advice on life, and to his wife Samara for her interest in my research and for great suggestions. To their kids, Arielle, Sophie, Dov, Boaz, and Shay, for the smiles they have provided me. (PS- these thanks are in AGE order on purpose!)

To my little sister Jill, you should know, I have always looked up to you… and not just because you are taller, but because of the amazing person you are. You are the person I strive to be and I have learned so much from you. Thank you for being you and for always being there for me. You have no idea how much your love, support, and friendship has meant to me. You have made my life so amazing and I am thankful you are a major part of it.

To my savta Yaffa, my grandmother, who thought, so many years ago, that'd I'd be a professor! Sorry to disappoint you, I'm going to industry! But, I can honestly say, it is because of you that I know my "fractions" today. Your patience to teach me everything from proper toilet usage, to math, to reading, to cooking, has been immeasurably important in my life. Even though you have lived far from me, you have always been a huge part of my life, and for that I am grateful.

They say it takes two to tango… it also takes two to make me! Thanks to my parents for bringing me into this world. It is an amazing place with many endless possibilities. To my dear mother, thank you for everything. It is because of *you*, that I am who I am. Your encouragement, love, support, help, and generosity, has been unconditional from the day I was born and for that I am forever grateful. Thank you for believing in me, even when I didn't believe in myself. Thank you for exposing me to scientific research even before I knew what it is. You are, and probably will always be, the smartest and most resourceful person I know and I thank you for sharing some of that wisdom with me. You are my inspiration.

To Joe, words cannot describe my love for you. I know without you, none of this would have been possible. Thank you.

ABSTRACT

POLYMERSOMES: MULTI-FUNCTIONAL TOOLS FOR *IN VIVO* CANCER THERANOSTIC APPLICATIONS

Dalia Hope Levine

Dr. Daniel A. Hammer

Nanoparticles are currently being developed as delivery vehicles for therapeutic and contrast imaging agents. Polymersomes (mesoscopic polymer vesicles) possess a number of attractive biomaterial properties, including greater biocompatibility, prolonged circulation times, and increased mechanical stability, that make them ideal for these applications. The polymersome architecture, with its large hydrophilic reservoir and thick hydrophobic lamellar membrane, provides significant storage capacity for water soluble and insoluble substances.

The primary thesis aims are to develop multi-functional polymersomes for combination therapeutic applications, as well as simultaneous therapeutic and diagnostic applications. These multi-functional vesicles are capable of simultaneously loading both therapeutic agents, such as doxorubicin and combretastatin, and optical imaging agents, such as porphyrin-based near infrared (NIR) fluorophores, into their hydrophobic and hydrophilic regions.

Doxorubicin, an anti-neoplastic agent, was encapsulated into PEO-b-PCL polymersomes and its release was characterized *in situ*. *In vitro* and *in vivo* studies confirmed the therapeutic potential of doxorubicin loaded polymersomes. Furthermore,

the *in vitro* therapeutic efficacy of polymersomes loaded with combretastatin, an anti-vascular agent, was established with and without co-doxorubicin loading. The co-encapsulation of DOX and combretastatin into polymeric vesicles, generates a multi-functional drug loaded polymersome with the potential to eliminate tumorigenic cells an endothelial cells, respectively.

The use of near infrared (NIR) emissive porphyrin polymersomes, loaded with porphyrin, for biodistribution studies, to non-invasively track the location of the polymersomes in tumor bearing mice was demonstrated using a noninvasive small animal optical imaging instrument which detects NIR fluorescence signal. Passive accumulation of drug loaded NIR-emissive polymersomes in tumor tissues of mice, as well as other organs, was observed. The study findings suggest the potential utility of NIR-emissive porphyrin polymersome in clinical diagnostic applications. Furthermore, preliminary results utilizing drug loaded porphyrin polymersomes to retard tumor growth and monitor vesicle location suggest these vesicles may have great future clinical utility.

The ability to load components into the polymersome membrane and core shows enormous promise for future dual modality polymersomes with potential to be nanostructured biomaterials for future theranostic applications which provide both therapy and diagnosis.

TABLE OF CONTENTS

LIST OF FIGURES

LIST OF SYMBOLS AND ABBREVEATIONS

Abbreviations

ACN	Acetonitrile
Cryo-TEM	Cryogenic transmission electron microscopy
DI	Deionized
DLS	Dynamic Light Scattering
DOX	Doxorubicin
E	Absorption extinction coefficient
ELISA	Enzyme-linked Immunosorbent Assay
λ	Wavelength
λ_{ex}	Excitation Wavelength
λ_{em}	Emission Wavelength
GFP	Green Fluorescent Protein
HBSS	Hepes Buffered Saline Solution
HUVECs	Human Umbilical Vein Endothelial Cells
mOsM	Milli-osmolar
NIR	Near-infrared
NIRF	Near-infrared fluorophore
PBD	Polybutadiene
PBF	Porphyrin Based Fluorophore
PBS	Phosphate buffered Saline
PCL	Poly(ε-caprolactone)

PDI	Polydispersity index
PEE	Polyethylehtylene
PEO-	Poly(ethylene oxide)
PmCL	Poly(γ-methyl ε-caprolactone)
PZn	Zinc porphyrin [(porphyrinato)zinc(II)]
THF	Tetrahyrofuran
VDA	Vasculature Disruptin Agent

Chapter 1

AN INTRODUCTION TO AMPHIPHILIC VESICLES AS DELIVERY VEHICLES AND IMAGING TOOLS AND SPECIFIC AIMS OF THE THESIS DISSERTATION

ADAPTED FROM

Dalia Hope Levine, P. Peter Ghoroghchian, Jaclyn Freudenberg, Geng Zhang, Michael J. Therien, Mark I. Greene, Daniel A. Hammer, and Ramachandran Murali, *Methods*, 2008, vol. 46, p. 25-32.

1.1 BACKGROUND: INTRODUCTION TO POLYMERSOMES

Nanosized carriers are prime candidates for the delivery of highly toxic or hydrophobic therapeutic agents. These delivery vehicles have the potential to augment the pharmacodynamic and pharmacokinetic profiles of drug molecules, thereby enhancing the therapeutic efficacy of the pharmaceutical agents [1]. Further, encapsulating the drug molecule in a delivery system can increase *in vivo* stability, extend its blood circulation time, and further provide a means for controlling the release of the agent [1]. Moreover, the delivery system can alter the biodistribution of the drug molecule by allowing the agent to accumulate at the tumor site, either passively or actively with targeting [1]. In addition to their role in therapeutic drug delivery, by serving as diagnostics tools, nanosized carriers can deliver imaging agents to detect and non-invasively diagnose disease. Combining these two ideas, the marriage of the drug delivery and imaging in one vehicle leads to the generation of a nanocarrier for theranostics—therapeutics and diagnostics.

Polymersomes, polymer vesicles self-assembled from a diverse array of synthetic amphiphilic block-copolymers containing hydrophilic and hydrophobic blocks [2-4], have been shown to possess superior biomaterial properties, including greater stability and storage capabilities [5-7], as well as prolonged circulation time, as compared to liposomes (vesicles derived from phospholipids) [8]. A particularly attractive storage feature, highlighted in Figure 1.1, is the large hydrophobic core of the polymersome membrane, which follows from the membrane-forming amphiphilic polymers being larger than conventional phospholipids [9]. Further, block copolymer chemistries can be

tuned through polymer synthesis to yield polymersomes with diverse functionality [10].

A vast majority of vesicles made of synthetic copolymers have dense polyethylene oxide (PEO) outer shells, which affords them “stealth” like character that may lead to increased circulation times and *in vivo* biocompatibility [5]. Thus, although liposomes are presently used in various biotechnological and pharmaceutical applications to improve therapeutic indices and enhance cellular uptake [4], it appears that polymersomes can offer superior advantages for future clinical therapeutic and diagnostic imaging applications.

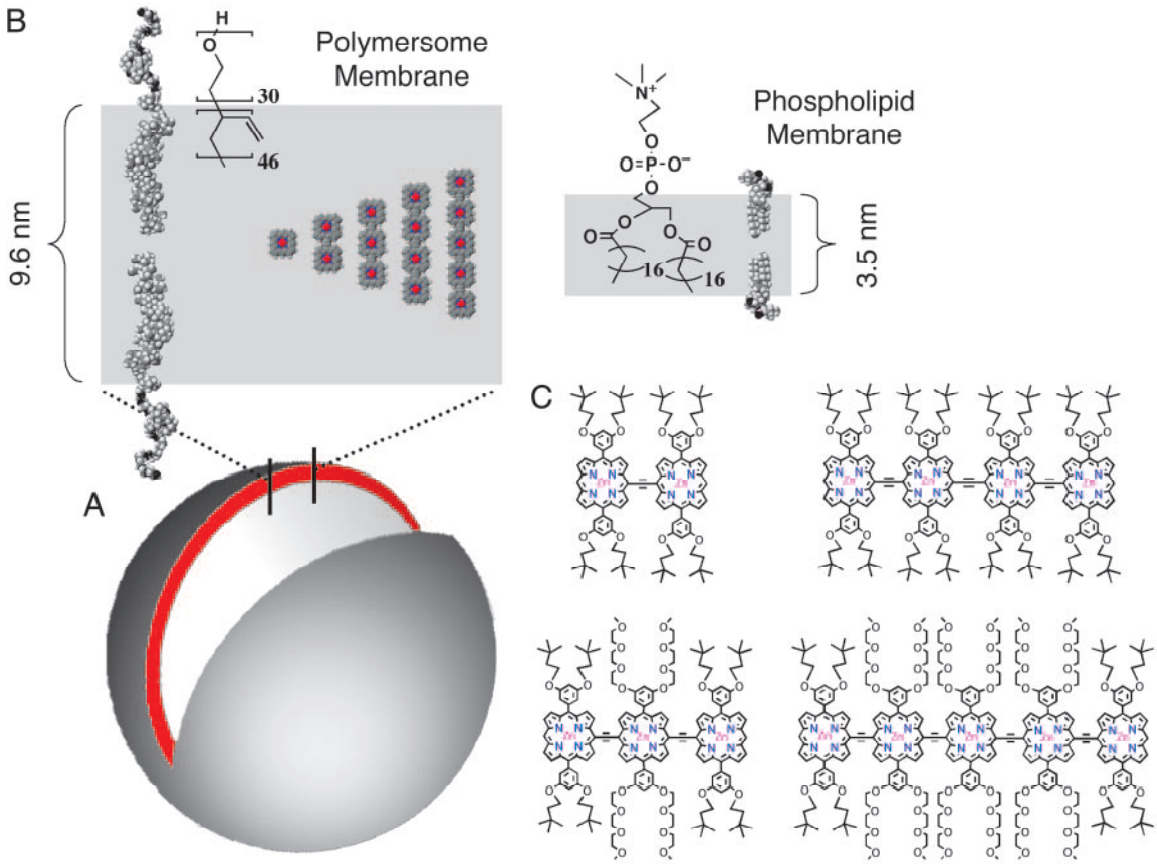

Figure 1.1- Schematic representations of NIR-emissive polymersomes.
(A) In aqueous solution, amphiphilic diblock copolymers of polyethyleneoxide-1,2 polybutadiene (PEO30-PBD46) self-assemble into polymer vesicles (polymersomes) with the hydrophobic PBD tails orienting end-to-end to form bilayer membranes. The depicted unilamellar polymersome displays an excised cross-sectional slice illustrating the bilayer PBD membrane (gray) containing the hydrophobic (porphinato)zinc(II) (PZn)-based near-IR fluorophores (NIRFs, red). (B) CAChe-generated sectional schematic of the NIR-emissive polymersome membrane indicating the molecular dimensions of: (i) the PBD component of the bilayer (9.6 nm); (ii) the large, dispersed PZn-based NIRFs (2.1-to-5.4 nm); and, (iii) a typical liposome membrane (3-4 nm) comprised of phospholipids (1-stearoyl-2-oleoyl-sn-Glycero-3-Phosopho-choline – SOPC). (C) Chemical structures of NIR fluorophores PZn2-PZn5. Copyright (2005) National Academy of Sciences, U.S.A. [9]

In aqueous solutions, amphiphilic block copolymers can self-assemble into mesoscopic structures (≤200nm-50μm in diameter) [3]. The ratio of hydrophilic to hydrophobic block volume fraction determines whether micelles (spherical, prolate, or oblate), or vesicles (polymersomes) will form [2, 11-13]. As a general rule, however, a

ratio of hydrophilic block to total polymer mass of approximately ≤ 35% ± 10% yields membrane structures, while copolymers with ratios greater than 45% generally form micelles; those with ratios less than 25% form inverted microstructures [14]. Micellar structures have been used as intracellular and systemic delivery systems [15-18] but present significant limitations when compared to polymersomes. In aqueous solutions, they can only encapsulate hydrophobic molecules unless strong binding or covalent linking strategies are incorporated for sequestering aqueous-soluble components.

In contrast to micelles, polymersomes can *simultaneously* encapsulate hydrophilic components in their aqueous interior and hydrophobic molecules within their thick lamellar membranes [10]. In addition, biologically active ligands, such as antibodies, can be readily conjugated to the exterior brush surface to target the vesicles or to provide a therapeutic response [19-22]. These properties of the vesicle architecture (Figure 1.2) effectively create a multimodal platform, which can be used for therapeutic (drug delivery) and/or diagnostic (imaging) applications.

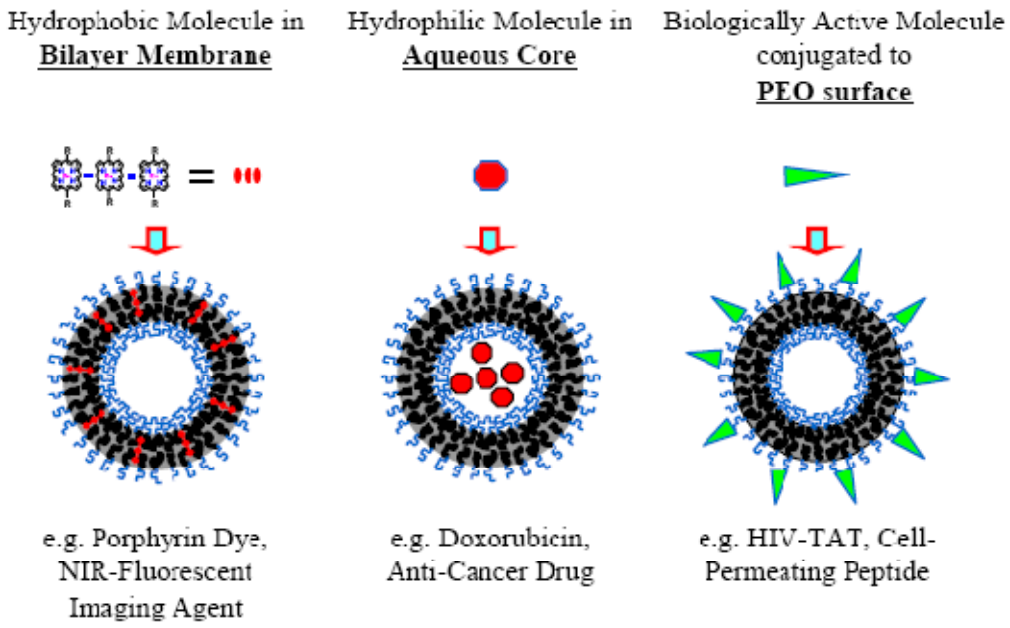

Figure 1.2- General application of polymersome architecture in theranostics. Schematic representation of polymersome assembly illustrating three possible applications, namely optical imaging, drug delivery, and targeted- therapy.

Although vesicles can be targeted to specific sites using biologically active ligands, the anatomical and pathophysiological abnormalities of tumor tissue alone can be utilized to aid in the localized delivery of macromolecules [23]. The tumor vasculature, characterized by irregularly shaped, dilated, defective, and/or leaky blood vessels, disorganized endothelial cells with fenestrations, as well as other abnormalities, allows for the passive accumulation of macromolecules at the tumor site [24]. Further, due to poor lymphatic drainage, nanoparticles can accumulate and remain at the tumor site even in the absence of a targeting moiety [25]. This phenomenon is known as the enhanced permeability and retention (EPR) effect and makes it possible to achieve high local concentrations of macromolecules at the tumor site without specific targeting [24]. However, a question that has yet to be addressed with polymersomes is how much

additional accumulation is possible with targeting.

1.2 Diblock Co-polymers and Amphiphilic Molecules Forming Vesicles and Release Mechanisms

In addition to yielding robust multi-compartment vesicles, some of block co-polymer formulations that have demonstrated promise for controlled release of pharmaceuticals.

Initial polymersome research by Hammer and Discher used poly(ethylene oxide)-block-poly(ethylethylene) (PEO-b-PEE) diblock copolymers to demonstrate the formation of polymersomes in aqueous solution, as well as to characterize the vesicle's material and physical properties [3]. Additional work in the field has led to the synthesis of a number of biocompatible PEO-based amphiphilic block copolymers that form aqueous vesicles dispersions, including poly(ethylene oxide)-block-poly(butadiene) (PEO-b-PBD) [7].

A significant limitation of these polymers for *in vivo* therapeutics is that they are not biodegradable and likely not fully biocompatible. In an effort to create vesicles that degrade and release their contents *in vivo,* PEO-b-PBD polymers have been blended with hydrolysable block copolymers, such as poly(ethylene oxide)-block-poly(lactic acid) (PEO-b-PLA) or poly(ethylene oxide)-block-poly(caprolactone) (PEO-b-PCL); these vesicles have been shown to undergo hydrolytic degradation intracellularly (in the acidic environment of the endolysosomal compartment), leading to release of the polymersomes' encapsulates [26-28]. Cryo-TEM images and dynamic light scattering measurements serve to demonstrate that nanoscale phase transitions occur in these blends

as the polyester backbone of the vesicles' hydrolytic components degrade over time; the intact vesicle begins to form pores, which leads to the transition to worm-like micelles and ultimately leads to the formation of spherical micelles [27]. Further, it has been shown that the release rate of encapsulates in blended polymersomes increases linearly with increasing mole ratio of hydrolysable polymer [26]. While these studies represent a reasonable first step in the development of polymersomes for therapy, it is critical to overcome the hurdle of *in vivo* toxicity presented by the residual PEO-b-PBD in these structures.

Recently, efforts in our group have focused on the development of self-assembled polymersomes from fully-biodegradable synthetic amphiphiles. The ability to generate self-assembled, fully-bioresorbable vesicles comprised of an amphiphilic diblock copolymer consisting of two previously FDA-approved building blocks, poly(ethylene oxide) (PEO) and poly(caprolactone) (PCL), has been demonstrated by Ghoroghchian and coworkers [10]. Unlike polymersomes formed from the blending of "bio-inert" and hydrolysable block copolymers [26], these fully-bioresorbable PEO-b-PCL vesicles undergo acid catalyzed hydrolysis of their ester linkages and degrade without leaving any potentially toxic byproducts [10, 29]. We have demonstrated the release of doxorubicin from these systems with time-constants of 18-24 hours, depending on pH; *in vivo* testing of these polymersomes for delivery is underway as further discussed in Chapter 2.

In contrast to acid catalyzed hydrolysis of the polymer backbone, which occurs on the order of hours to days, pH triggered contents release, using block copolymers whose solubility in aqueous solutions is dependent upon solution pH, can occur much more

rapidly [30]. Borchert and colleagues generated polymersomes comprised of poly(2-vinylpyridine)-block-poly(ethylene oxide) (P2VP-b-PEO) copolymers and showed that the resultant vesicles disassemble in acidic solutions and quickly and completely release their contents; this dissolution is due to the protonation of the P2VP block in acidic solutions (below pH 5) which converts the previously hydrophobic block into a water soluble polymer [30].

Cerritelli and colleagues have designed and characterized a diblock copolymer of poly(ethylene glycol) (PEG) and poly(propylene sulfide) (PPS) with a reduction sensitive disulfide link between the two blocks (PEG-SS-PSS); they demonstrated the ability of this block copolymer to form polymer vesicles which burst within a few minutes of endocytosis due to the reductive environment in the endosome [31]. In addition to diblock copolymers, various other polymeric amphiphiles can form vesicles in aqueous solutions. Napoli et al. synthesized a triblock copolymer of poly(ethylene glycol)-block-poly(propylene sulfur)-block-poly(ethylene glycol) (PEG-b-PPS-b-PEG) [32], which at dilute concentrations forms polymeric vesicles [33, 34]. Napoli and colleagues then demonstrated that vesicles comprised of this triblock copolymer could be destabilized by the oxidation of the hydrophobic PPS block; when oxidized, PPS is first converted to poly(propylene sulphoxide) and subsequently converted to poly(propylene sulfone), both of which are more hydrophilic than PPS [35]. This change in hydrophobicity of the "hydrophobic" block alters the ratio of hydrophobic block to total polymer mass, leading to changes in morphology of the self-assembled structures from vesicles, to worm-like micelles, to spherical micelles, and finally to unimolecular micelles [35]. These

polymers present the promise of biodegradability, due to oxidation of the hydrophobic chain into small molecules solutes that can be readily cleared [32].

Another possibility to generate fully biodegradable vesicles is to utilize polypeptides as their composite amphiphiles. Vesicles and micelles comprised of polypeptide block copolymers can mimic the shape and biological performance of natural vesicles and micelles [36]. Sun et al. synthesized various diblock copolypeptides of poly(L-lysine)-block-poly(L-phenylalanine) (PLL-b-PPA) which spontaneously self-assemble into giant vesicles in aqueous solutions [36].

In addition to vesicle generation using block co-polymers, amphiphilic Janus-dendrimers have demonstrated the ability to self-assembly into regular structures ranging from dendritic spherical vesicles to cubosomes. The mechanical stability of the dendrosomes suggest they may be useful for *in vivo* applications.

1.3 THERAPEUTIC APPLICATIONS OF POLYMERSOMES

Currently, many compounds with toxic side effects or low bioavailability hold extraordinary promise as potential therapeutic agents. However, limited bioavailability of hydrophobic compounds and/or toxic side effects of these molecules can render their therapeutic value ineffective. Further, the ability of the therapeutic agents to reach the target site can be limited by the body's clearance. Thus, the development of a polymeric delivery vehicle with specifically tuned pharmacokinetics, which can encapsulate and release highly toxic therapeutic agents for concentrated local delivery, should greatly increase therapeutic efficacy.

Doxorubicin (DOX) is an amphipathic anti-neoplastic agent that shows much

promise in cancer therapy, both alone and in conjunction with antibodies and peptides [37] and other chemotherapeutics [27] and pharmaceuticals [38]. One of the major limitations associated with administration of this chemotherapeutic agent is cardiac myocyte toxicity [39]. However, utilizing drug carriers to deliver doxorubicin can alleviate some of the associated cardio-toxicity by altering the pharmacodistribution of the drug, thereby reducing the drug concentration in the heart [39]. Delivery of doxorubicin in liposomes has been shown to extend the circulation time and alter the pharmacodynamics of doxorubicin in such a way as to decrease its toxicity while still maintaining its anticancer activity [39]. Using active loading methods originally developed for liposomes, doxorubicin can be efficiently loaded into the aqueous center [10, 26, 40] of polymer vesicles.

Paclitaxel (taxol), an anticancer agent, whose therapeutic efficacy is limited by its poor aqueous solubility [41] is currently administered in a mixture of Cremophor EL (polyoxyethylated castor oil) and dehydrated ethanol [42] to increase bioavailability. Systemic administration of taxol is associated with several negative side effects in patients including dyspnea, hypotension, bronchospasm, urticaria, and erythematous rashes [42]. In addition, the formulation agent (Cremophor EL) used to solubilize the hydrophobic taxol is believed to be responsible for inducing the hypersensitivity reactions observed in patients [42]. As a result, various aqueous formulations of taxol have been examined to decrease toxic side effects and increase water solubility. Li et al. demonstrated the ability to load taxol into the hydrophobic bilayer of PEO-b-PBD polymer vesicles and thus increase the water solubility of this drug while maintaining its cytotoxic properties [43].

Combination therapy involves the administration of different classes of chemotherapeutics to a patient in order to treat the disease; this approach has been shown to be generally effective and many cancer treatment regimes employ such multi-drug therapy. A combination regime of DOX and TAX has been shown clinically to retard tumor growth more effectively in comparison to the administration of a single agent alone [44]. A reasonable hypothesis is that the synergistic effect of these two drugs would be increased when both drugs are administered in the same delivery vehicle, as this would ensure delivery of the drug molecules in prescribed ratios to a given target at the same time; Ahmed et al. demonstrated the ability to co-encapsulate DOX and TAX into polymer vesicles and showed the increased synergistic effect when DOX and TAX are in the same polymersome [27, 28]. PEG-b-PLA/PEG-b-PBD blended polymer vesicles were loaded with DOX in their hydrophilic reservoir and TAX in their hydrophobic bilayer, and were administered *in vivo*; the results demonstrate a higher maximum tolerated dose (MTD), as well as increased tumor shrinkage and maintenance, when both agents are administered in vesicles rather than as free drugs [27]. Since there are a wide variety of both hydrophilic and hydrophobic pharmaceuticals, this paradigm is generally applicable to creating other polymersome-formulations for combination therapy. Ultimately, as mentioned before, further work to combine these pharmaceuticals within a safe and fully biodegradable formulation is necessary.

In addition to small molecules, peptides, proteins, and nucleic acids have been encapsulated in block copolymer assemblies. Lee et al. successfully encapsulated myoglobin, hemoglobin, and albumin in PEO-b-PBD based polymer vesicles at varying degrees of encapsulation efficiency [5]. Arifin and Palmer further demonstrated that

bovine hemoglobin (Hb) could be encapsulated inside PEO-b-PBD polymer vesicles with oxygen affinities similar to those of human red blood cells; they demonstrated that these "polymersomes-encapuslated hemoglobin" (PEH) dispersions could store and transport Hb and potentially act as *in vivo* oxygen therapeutics [45]. The ability to encapsulate proteins within polymersomes provides a promise for future protein therapies, which are currently facing delivery obstacles.

1.4 DIANGNOSTIC APPLICATIONS FOR POLYMERSOMES

The ability to non-invasively image nanoparticles *in vivo* is a major advantage in determining their biodistribution and developing these delivery vehicles for both therapeutic and diagnostic applications. Biodistribution studies with polymersomes, in particular, would be greatly aided by the encapsulation of an imaging agent in the vesicles; this would enable non-invasive monitoring of the location of vesicles during drug delivery without the need to sacrifice the animal. Although nanoparticles have been used with a spectrum of different imaging modalities including PET [46, 47] and MRI [48-50], here we will focus on polymersomes that encapsulate fluorescent agents for optical imaging. Because light scattering decreases with increasing wavelength, and hemoglobin and water absorption spectra have their nadir in the near infrared (NIR) spectral region, much work has been focused on developing NIR contrast agents for *in vivo* imaging studies [9]. To this end, Ghoroghchian et al. have successfully loaded porphyrin-based near infrared fluorophores (NIRFs) into the hydrophobic bilayer membranes of PEO-b-PBD [9, 10, 51, 52], PEO-b-PCL [52], PEO-b-PEE [52], and poly(ethylene oxide)-block-poly(methylcaprolactone) (PEO-b-PmCL) [52]

polymersomes.

Studies using PEO-b-PBD polymersomes have shown that porphyrin-based NIRFs, when encapsulated in polymersomes, are able to generate a signal with enough intensity to penetrate through 1 cm of a solid tumor [9]. Further, when these NIR-emissive nanopolymersomes are injected into the tail-vein of mice, the biodistribution of the nanoparticles can be tracked *in vivo* via non-invasive NIR fluorescence-based optical imaging [53]. Combining drug delivery with imaging will allow for the continuous non-invasive monitoring of drug-loaded nanopolymersomes *in vivo*, obviating the need to sacrifice animals at each time point to determine basic pharmacokinetic and biodistribution profiles, thereby greatly reducing animal load.

In addition to developing drug delivery applications, NIR-emissive polymersomes have also been shown to be useful for *ex vivo* cellular labeling and *in vivo* cellular tracking. Dendritic cells (DCs) play an important role in the immune response and have shown potent anticancer activity, leading to DC-based vaccines research [54]. Current progress in DC-based vaccines has been, however, limited by various factors [54], some of which could be overcome by the development of imaging methods for *in vivo* DC tracking [19]. Christian et al. have demonstrated the ability to label DCs *ex vivo* with polymersomes encapsulating porphyrin-based NIRFs; the TAT peptide, as will be discussed in greater detail below, was conjugated to these NIR-emissive polymersome to facilitate efficient uptake of polymer vesicles by DCs [19]. Christian and colleagues determined that DC surface-associated polymersomes shed over the first 24 to 48 hours; but polymer vesicles that were fully internalized by the DCs remained stably incorporated

over 3 days [19]. They further showed that the NIR-emissive-polymersome-labeled DCs, when administered into the foot pad of mice, traffic to the nearest lymph node (popliteal lymph node) and could be tracked *in vivo* via optical imaging over 33 days [55]. They further showed that dendritic cells are sequestered in the liver when the cells are delivered intravenously (42), indicating that the mode of dendritic cell delivery will be critical for the effectiveness of cancer immunotherapy. These results suggest that polymer vesicles can be employed for cell tracking in longitudinal studies and could thus assist in the further development of cell-based vaccines. Overall, the results in this section demonstrate that the loading of imaging agents, such as porphyrin-based NIRFs, into the polymersome bilayer creates soft matter optical imaging agents suitable for *in vitro* diagnosis and deep-tissue imaging, non-invasive biodistribution and pharmacokinetic studies, as well as *in vivo* cellular tracking.

An alternative imaging modality that can be used to image polymer vesicles is diagnostic ultrasound. Zhou et al. prepared air-encapsulated polymersomes via lyophilization and rehydration of previously formed polymer vesicles [56]. The polymer bubbles were imaged using a Pie Medical Scanner 350 and were visualized as bright spots, validating the acoustic activity of air-encapsulated polymersomes [56]. These results show that polymer vesicles hold promise in the realm of ultrasound imaging as well as optical imaging.

1.5 Polymersome Surface Modifications For Enhanced Delivery and Therapy

Biologically-active molecules conjugated to the surfaces of polymersomes can be

used to direct these nanoparticles to sites of disease and inflammation. Modifying polymer vesicles with biological ligands enables targeting of upregulated receptors and molecules on affected cells *in vitro* and *in vivo*, thereby enhancing the nanoparticles' EPR effect and further mitigating the potential toxic side effects of systemic delivery. Additionally, chemotherapeutics, when used in conjunction with molecular targeting agents, can have a synergistic effect [57]. In addition to therapeutic applications, over the past two decades the use of anticancer antibodies against molecular targets has been developed for tumor imaging applications [37]. Polymer vesicles can be directed to specific sites *in vivo* by conjugation of targeting moieties to the end group of their hydrophilic polymer block (usually PEO). It is important to recognize that the conjugation of ligands to the polymersome surfaces can alter the composite polymer amphiphiles' hydrophilic-block-to-total-mass ratio leading to a change in structural morphology (e.g. from vesicles to micelles).

Using a modular biotin-avidin chemistry, Lin and colleagues functionalized polymer vesicles with anti-ICAM-1 antibody to target ICAM-1 (intercellular adhesion molecule-1) [21], a molecule that is upregulated on endothelial cells during inflammation. Using micropipette aspiration, they measured the adhesiveness of these functionalized polymer vesicles to ICAM-1 immobilized on the surface of polystyrene beads and determined that the adhesion strength is linearly proportional to the surface density of the anti-ICAM-1 molecules on the polymersome [21]. This finding is in contrast to their earlier adhesion experiments carried out with functionalized biotinylated polymersomes and avidin coated beads [22], suggesting that the adhesiveness of functionalized vesicles is not only dependent on surface density, but also upon the

presentation/orientation of the targeting molecules on the vesicle surface [21].

Additionally, sialyl lewis^X (sLe^X), a selectin ligand, has been conjugated to polymer vesicles using similar biotin-avidin modular chemistry as previously described (Hammer et al., in press, Faraday-Discussions 139). In addition to ICAM-1 molecules, selectins are also upregulated at sites of inflammation [21]. In an effort to create "leukopolymersomes," i.e. polymersomes that mimic the adhesive properties of leukocytes, dual functionalized vesicles of sLe^x and anti-ICAM-1 have been made by the Hammer lab. The investigators were able to measure firm and rolling adhesion of anti-ICAM-1-, sLe^x-, and anti-ICAM-1/sLe^x conjugated polymersomes under flow along ICAM-1, P-selectin, and ICAM-1/Pselectin coated surfaces, respectively, at venous shear rates. It is believed that dual functionalized leukopolymersomes will be able to serve as targeting agents to bring both therapeutics (drugs) and diagnostics (imaging agents) to sites of inflammation [21].

Meng and co-workers functionalized polymersomes comprised of PEG-block-poly(ester) and PEG-block-poly(carbonate) diblock copolymers with anti-human IgG (a-HIgG) or anti-human serum albumin (a-HSA) [6]. a-HIgG and a-HSA were either conjugated to the polymersome through covalent attachment to carboxyl groups on the vesicle surface or by attachment to protein G, which was covalently attached to the polymersome surface via the carboxyl groups; using imaging surface plasmon resonance (iSPR), they determined that immobilization of antibodies on the vesicle surface through protein G is preferred for targeting [6]. iSPR was further used to demonstrate the potential of antibody functionalized vesicles for targeting antigens [6].

In addition to targeting, these biologically active ligands can aid in cellular uptake

[58]. As previously mentioned, Christian et al. demonstrated that the highly cationic HIV-derived TAT peptide, when coupled to NIR-emissive polymersomes, enhances cellular delivery of polymer vesicles to dendritic cells while moderately affecting cell viability [19]. Intracellular uptake of polymersomes was dependent upon their concentration and incubation time in solution; viability was affected by these factors as well [19].

We have recently attempted to conjugate small anti-HER2/neu peptidomimetics, designed by Murali and coworkers [57], to polymersomes in order to further develop these nanoparticles for both clinical breast cancer diagnosis (NIR-emissive polymersomes) and therapy (e.g. with and without doxorubicin incorporation). In comparison to normal epithelial tissues, over-expression of the HER2 protein, a member of the epidermal growth factor (EGFR) or HER family, has been seen in approximately 30% of breast, ovarian, and colon cancers [37, 57]. A family of anti-HER2/neu peptides (AHNPs) designed by Murali et al. has a potency on par with that of the full-length monoclonal antibody (Herceptin®; Genentech, San Francisco, CA) and demonstrates biochemical and biological properties predictive of clinical therapeutic response [57]. It has been demonstrated that AHNP prevents tumor growth of transformed T6-17 cells, in which HER2/neu is over-expressed, *in vivo* and *in vitro* [57]. However, the relatively short half-life of peptides and proteins *in vivo* is one challenge that still remains to be overcome when using such agents for therapeutic applications [59]. To overcome the challenge of rapid clearance, “stealth” or “sterically stabilized” nanoparticles, such as pegylated liposomes, have been employed to deliver peptides [60]. Thus, linking AHNP to a nanoparticle surface can greatly improve the pharmacokinetics of the small peptide

and allow for targeting as well as improved therapeutic efficacy.

Ghoroghchian et al. observed changes in polymersome morphology from vesicles to micelles post-conjugation of the AHNP peptides to PEO-b-PBD vesicles [53]. Vesicles, as well as small spherical micelles, not present in aqueous suspensions of the functionalized and unfunctionalized diblock copolymer without peptide, were observed in the polymersome suspension post AHNP conjugation [53]. Since these micelles were not seen in cryoTEM images of the pure or unfunctionalized polymer, it is probable that they are comprised of peptide-conjugated polymer; furthermore, it is hypothesized that the vesicles in the suspension consist of polymer not conjugated to AHNP peptide [53]. Peptide-conjugated vesicle generation with less hydrophobic AHNP peptide family members were also attempted and again resulted in phase separation of the diblock copolymer-peptide "triblock" from the diblocks [53]. Our interpretation of these results is that the underlying polymer material needs to be redesigned to accommodate peptides and preserve vesicular structure in order to develop AHNP polymersomes fit for clinical diagnostic and therapeutic applications.

1.6 FUTURE DIRECTIONS

Polymersomes are new and valuable tools for both disease diagnosis and therapy. Our view is that the enhanced stability and tunability of polymersomes will ultimately lead to the development of effective carriers for *in vivo* drug delivery, molecular imaging, and cellular mimicry that extend well beyond what has thus far been achieved with phospholipid vesicles.

In pharmacodelivery, the potential to co-encapsulate two drug molecules in the

same polymersome enables combination therapies and eliminates the need to individually administer two separate drug formulations. As such, polymersome may not only be more effective in treating recurrent, resistant, or residual tumors, but may also be more convenient for patient administration and treatment tolerance. It is also possible to make separate polymersome formulations, each with different drugs or with different dosing that deliver drugs in a sequence, as needed for the particular type of disease that is being treated. Additionally, localizing therapeutics to the site of intent, either through passive accumulation (EPR effect) or with targeting ligands, can enable administration of higher doses of drug while minimizing the toxic side effects of systemic delivery. Further, the ability to image polymer vesicles during delivery will offer numerous advantages for understanding the mechanisms of therapy as well as efficiently designing drug delivery regimens in small animal models. Aside from the demonstration of the activity of multi-modal polymersomes with existing block copolymers, we believe that further developments in polymer design will extend the applicability of polymersomes to different drugs and imaging modalities.

In addition to targeted therapeutic drug delivery, targeting ligands can be used to direct diagnostic agents to tumors sites, assisting in *in vivo* diagnostic imaging. Air-encapsulated polymeric vesicles facilitate nanodiagnostics using ultrasound. Further, the encapsulation of both porphyrin-based near-infrared fluorophores and air into the same vesicle should yield a multi-modal polymersome, where both ultrasound and optical imaging can be performed concurrently thereby enhancing tumor imaging. Finally, we have presented evidence that ultrasonics can be used as a delivery tool; and, thus, we see promise for simultaneous clinical diagnostic imaging and *in vivo* therapeutic drug

delivery with the correct polymer formulations.

1.7 SPECIFIC AIMS

1.7.1 Aim 1: To load physiologically relevant therapeutic molecules and imaging agents into the fully bioresorbable polymersome center and thick lamellar membrane and characterize the kinetics of drug release from the polymersome

- Aim 1.a) Load clinically relevant anti-cancer therapeutic into the hydrophilic interior of the polymersome and characterize the kinetics of drug release from the core.
- Aim 1.b) Load clinically relevant anti-angiogenic therapeutic/vascular disrupting agent (VDA) into the hydrophobic bilayer.
- Aim 1.c) Co-load both therapeutic agents into one polymersome for the simultaneous delivery of a vascular disrupting agent and chemotherapeutic.
- Aim 1.d) Co-encapsulate a therapeutic agent, doxorubicin, into the vesicle core and a near infrared imaging agent, porphyrin into the bilayer of the same polymersome for biodistribution studies.

1.7.2 Aim 2: To demonstrate the potential use of amphiphilic Janus-dendrimers for in vivo drug delivery applications

- Aim 2.a) Load doxorubicin, an anti-neoplastic agent, into the aqueous core of dendrosomes, vesicles self assembled from dendrimers and characterize the release.
- Aim 2.b) Determine the dendrosome effects on cell viability using Human Vein Endothelial Cells (HUVECs).

1.7.3 Aim 3. To use the drug loaded polymersome and porphyrin incorporated polymersomes to study the in vitro effects of polymersomes using HUVECs and SK-BR-3 tumorigenic cells

- Aim 3.a) Determine the effects of unloaded polymersome on cell viability.
- Aim 3.b) Determine the cellular uptake of polymersome by HUVECs and SK-BR-3 Cells.
- Aim 3.c) Determine the effects of drug loaded polymersomes on cell viability when cultured separately and in co-culture.

1.7.4. Aim 4. To demonstrate the in vivo potential of polymersome for imaging and drug delivery applications using athymic nude mice with xenograft tumors

- Aim 4.a) Determine the biodistribution of polymersome and establish their *in vivo* potential as imaging agents for *in vivo* deep tissue optical imaging.
- Aim 4.b) Demonstrate the anti-tumor effect of drug loaded polymersomes on tumor suppression *in vivo*.
- Aim 4.c) Highlight the potential of drug and imaging agent loaded vesicles for theranostic applications.

1.8 ORGANIZATION OF THE THESIS

1.8.1 Chapter 1

This chapter provides a brief introduction into the various vesicles self assembled from diblock copolymers and other amphiphilic building blocks, such as dendrimers. Particular detail is given to polymersomes self assembled from diblock copolymers. The motivation for development and characterization of these vesicles is elaborated upon by describing their potential for therapeutic applications through delivery of pharmaceutical

agents within the core and bilayer and attachment of biologically active ligands to the brush surface. Furthermore, the use of vesicles for diagnostic applications is discussed and provides additional motivation for their development as biological tools. Lastly, the potential for these vesicles to combine both therapy and diagnosis into one vesicles is briefly discussed. These ideas will be further explored throughout the body of this thesis.

1.8.2 Chapter 2

The generation of a fully bioresorbable polymersome capable of simultaneously delivering a vascular disrupting agent, combretastatin, and a chemotherapeutic, doxorubicin, is described. Furthermore, the method of loading doxorubicin into vesicles self-assembled from a variety of diblock copolymers and its release are discussed. The ability to encapsulate each pharmaceutical agent separately as well as in concert is highlights the enormous promise for using polymersomes as multi-drug delivery agents for the eradication of tumorigenic cells and endothelial cells.

1.8.3 Chapter 3

The formation of self-assembled monodispersed vesicles from amphiphilic Janus-dendrimers, dendrosomes, is introduced. In addition, the ability to load doxorubicin into these vesicles is demonstrated and the release kinetics of the drug at various pHs is established. Furthermore, the viability effects of these dendrosomes on HUVECs were investigated and viability results demonstrate that the uptake of dendrosomes is well tolerated by the HUVECs at short times.

1.8.4 Chapter 4

This chapter discusses the generation of a near infrared (NIR) emissive polymersome, a self-assembled polymer vesicles loaded with porphyrin in its

hydrophobic compartment and highlights the special properties of these fluorophores that render them useful for *in vivo* deep tissue optical imaging applications. Furthermore, the loading of doxorubicin into porphyrin incorporated polymersomes is demonstrated and its release is characterized. Subsequent chapters will demonstrate the significance of loading both an imaging agent and chemotherapeutic into one vesicles for *in vivo* applications.

1.8.5.Chapter 5

Cellular studies carried out using Human Umbilical Vein Endothelial Cells (HUVECs) and SK-BR-3 tumorigenic cells to determine the cytotoxic potential of drug loaded vesicles are discussed in this chapter. In addition, the effects of unloaded vesicles on cellular viability were investigated and results are presented. Furthermore, the cellular uptake of vesicles was explored using porphyrin loaded polymersomes and the findings are noted in this chapter.

1.8.6 Chapter 6

The use of porphyrin polymersome for biodistribution and diagnostic studies is demonstrated using biocompatible and bioresorbable polymersomes. Initial studies over 12 hours to 9 days utilized the biocompatible polymersome comprised of PEO-b-PBD due to its *in vivo* stability (i.e. does not degrade *in vivo*). More recent work showed the ability to use bioresorbable polymersomes generated from PEO-b-PCL diblock copolymer for imaging purposes. Furthermore, the use of drug loaded vesicles for *in vivo* applications was investigated using doxorubicin loaded PEO-b-PCL polymersomes and is described. Lastly, this chapter closes by marrying the two concepts—imaging and drug delivery highlighting the promise for polymersomes as theranostic agents.

1.8.7 Chapter 7

This final chapter summarizes and highlights many of the findings discussed throughout the work presented in the previous chapters. Preliminary and promising results presented are presented in further detail. Finally, this chapter offers suggestions for improving and expanding upon the utility of polymersomes *in vivo* as drug delivery vehicles and imaging agents with the final goal of obtaining *multi-functional* vesicles for *in vivo* dual therapeutic and theranostic applications.

1.9 REFERENCES

1. Cegnar, M., J. Kristl, and J. Kos, *Nanoscale polymer carriers to deliver chemotherapeutic agents to tumours.* Expert Opinion on Biological Therapy, 2005. **5**(12): p. 1557-1569.

2. Antonietti, M. and S. Forster, *Vesicles and liposomes: A self-assembly principle beyond lipids.* Advanced Materials, 2003. **15**(16): p. 1323-1333.

3. Discher, B.M., et al., Polymersomes: Tough vesicles made from diblock copolymers. Science, 1999. **284**(5417): p. 1143-1146.

4. Discher, D.E. and A. Eisenberg, Polymer vesicles. Science, 2002. **297**(5583): p. 967-973.

5. Lee, J.C.M., et al., Preparation, stability, and *in vitro* performance of vesicles made with diblock copolymers. Biotechnology and Bioengineering, 2001. **73**(2): p. 135-145.

6. Meng, F., G.H.M. Engbers, and J. Feijen, Biodegradable polymersomes as a basis for artificial cells: encapsulation, release and targeting. Journal of Controlled Release, 2005. **101**(1-3): p. 187-198.

7. Bermudez, H., et al., Molecular weight dependence of polymersome membrane structure, elasticity, and stability. Macromolecules, 2002. **35**(21): p. 8203-8208.

8. Photos, P.J., et al., Polymer vesicles *in vivo*: correlations with PEG molecular weight. Journal of Controlled Release, 2003. **90**(3): p. 323-334.

9. Ghoroghchian, P.P., et al., Near-infrared-emissive polymersomes: Self-assembled soft matter for *in vivo* optical imaging. Proceedings of the National Academy of Sciences of the United States of America, 2005. **102**(8): p. 2922-2927.

10. Ghoroghchian, P.P., et al., Bioresorbable vesicles formed through spontaneous self-assembly of amphiphilic poly(ethylene oxide)-block-polycaprolactone. Macromolecules, 2006. **39**(5): p. 1673-1675.

11. Zupancich, J.A., F.S. Bates, and M.A. Hillmyer, Aqueous dispersions of poly(ethylene oxide)-b-poly(gamma-methyl-epsilon-caprolactone) block copolymers. Macromolecules, 2006. **39**(13): p. 4286-4288.

12. Hillmyer, M.A., et al., Complex phase behavior in solvent-free nonionic surfactants. Science, 1996. **271**(5251): p. 976-978.

13. Hillmyer, M.A. and F.S. Bates, Synthesis and characterization of model polyalkane-poly(ethylene oxide) block copolymers. Macromolecules, 1996. **29**(22): p. 6994-7002.

14. Discher, D.E. and F. Ahmed, Polymersomes. Annual Review of Biomedical Engineering, 2006. **8**: p. 323-341.

15. Savic, R., et al., Micellar nanocontainers distribute to defined cytoplasmic organelles. Science, 2003. **300**(5619): p. 615-618.

16. O'Reilly, R.K., C.J. Hawker, and K.L. Wooley, Cross-linked block copolymer micelles: functional nanostructures of great potential and versatility. Chemical Society Reviews, 2006. **35**(11): p. 1068-1083.

17. O'Reilly, R.K., et al., Facile syntheses of surface-functionalized micelles and shell cross-linked nanoparticles. Journal of Polymer Science Part a-Polymer Chemistry, 2006. **44**(17): p. 5203-5217.

18. Sun, X.K., et al., An assessment of the effects of shell cross-linked nanoparticle size, core composition, and surface PEGylation on *in vivo* biodistribution. Biomacromolecules, 2005. **6**(5): p. 2541-2554.

19. Christian, N.A., et al., Tat-functionalized near-infrared emissive polymersomes for dendritic cell labeling. Bioconjugate Chemistry, 2007. **18**(1): p. 31-40.

20. Lin, J.J., et al., Adhesion of polymer vesicles. Physical Review Letters, 2005. **95**(2).

21. Lin, J.J., et al., Adhesion of antibody-functionalized polymersomes. Langmuir, 2006. **22**(9): p. 3975-3979.

22. Lin, J.J., et al., The effect of polymer chain length and surface density on the adhesiveness of functionalized polymersomes. Langmuir, 2004. **20**(13): p. 5493-5500.

23. Matsumura, Y. and H. Maeda, A New Concept for Macromolecular Therapeutics in Cancer-Chemotherapy - Mechanism of Tumoritropic Accumulation of Proteins and the Antitumor Agent Smancs. Cancer Research, 1986. **46**(12): p. 6387-6392.

24. Iyer, A.K., et al., Exploiting the enhanced permeability and retention effect for tumor targeting. Drug Discovery Today, 2006. **11**(17-18): p. 812-818.

25. Duncan, R., Polymer-Drug Conjugates: Targeting Cancer, in Biomedical Aspects of Drug Targeting, V.R. Muzykantov and V.P. Torchlin, Editors. 2002, Kluwer Academic Publishers: Boston. p. 197-199.

26. Ahmed, F. and D.E. Discher, Self-porating polymersomes of PEG-PLA and PEG-PCL: hydrolysis-triggered controlled release vesicles. Journal of Controlled Release, 2004. **96**(1): p. 37-53.

27. Ahmed, F., et al., Biodegradable polymersomes loaded with both paclitaxel and doxorubicin permeate and shrink tumors, inducing apoptosis in proportion to accumulated drug. Journal of Controlled Release, 2006. **116**(2): p. 150-158.

28. Ahmed, F., et al., Shrinkage of a rapidly growing tumor by drug-loaded polymersome: pH-triggered release through copolymer degradation. Molecular Pharmaceutics 2006. **3**(3): p. 340-250.

29. Bei, J.Z., et al., Polycaprolactone-poly(ethylene-glycol) block copolymer .4. Biodegradation behavior *in vitro* and *in vivo*. Polymers for Advanced Technologies, 1997. **8**(11): p. 693-696.

30. Borchert, U., et al., pH-induced release from P2VP-PEO block copolymer vesicles. Langmuir, 2006. **22**(13): p. 5843-5847.

31. Cerritelli, S., D. Velluto, and J.A. Hubbell, PEG-SS-PPS: Reduction-sensitive disulfide block copolymer vesicles for intracellular drug delivery. Biomacromolecules, 2007. **8**(6): p. 1966-1972.

32. Napoli, A., et al., New synthetic methodologies for amphiphilic multiblock copolymers of ethylene glycol and propylene sulfide. Macromolecules, 2001. **34**(26): p. 8913-8917.

33. Valentini, M., et al., Precise determination of the hydrophobic/hydrophilic junction in polymeric vesicles. Langmuir, 2003. **19**(11): p. 4852-4855.

34. Napoli, A., et al., Lyotropic behavior in water of amphiphilic ABA triblock copolymers based on poly(propylene sulfide) and poly(ethylene glycol). Langmuir, 2002. **18**(22): p. 8324-8329.

35. Napoli, A., et al., Oxidation-responsive polymeric vesicles. Nature Materials, 2004. **3**(3): p. 183-189.

36. Sun, J., et al., Direct formation of giant vesicles from synthetic polypeptides. Langmuir, 2007. **23**(16): p. 8308-8315.

37. Berezov, A., et al., Disabling ErbB receptors with rationally designed exocyclic mimetics of antibodies: Structure-function analysis. Journal of Medicinal Chemistry, 2001. **44**(16): p. 2565-2574.

38. Sengupta, S., et al., Temporal targeting of tumour cells and neovasculature with a nanoscale delivery system. Nature, 2005. **436**(7050): p. 568-572.

39. Waterhouse, D.N., et al., Drug Safety, 2001. **24**: p. 903-920.

40. Choucair, A., P.L. Soo, and A. Eisenberg, Active loading and tunable release of doxorubicin from block copolymer vesicles. Langmuir, 2005. **21**(20): p. 9308-9313.

41. de Menezes, D.E.L., L.M. Pilarski, and T.M. Allen, *In vitro* and *in vivo* targeting of immunoliposomal doxorubicin to human B-cell lymphoma. Cancer Research, 1998. **58**(15): p. 3320-3330.

42. Haran, G., et al., Transmembrane Ammonium-Sulfate Gradients in Liposomes Produce Efficient and Stable Entrapment of Amphipathic Weak Bases. Biochimica Et Biophysica Acta, 1993. **1151**(2): p. 201-215.

43. Bolotin, E.M., et al., Ammonium Sulfate Gradients for Efficient and Stable Remote Loading of Amphiphathic Weak Bases into Liposomes and Ligandoliposomes. Journal of Liposome Research, 1994. **4**(1): p. 455-479.

44. Sharma, U.S., S.V. Balasubramanian, and R.M. Straubinger, Pharmaceutical and Physical-Properties of Paclitaxel (Taxol) Complexes with Cyclodextrins. Journal of Pharmaceutical Sciences, 1995. **84**(10): p. 1223-1230.

45. Weiss, R.B., et al., Hypersensitivity Reactions from Taxol. Journal of Clinical Oncology, 1990. **8**(7): p. 1263-1268.

46. Li, S.L., et al., Self-assembled poly(butadiene)-b-poly(ethylene oxide) polymersomes as paclitaxel carriers. Biotechnology Progress, 2007. **23**(1): p. 278-285.

47. Gustafson, D.L., A.L. Merz, and M.E. Long, Pharmacokinetics of combined doxorubicin and paclitaxel in mice. Cancer Letters, 2005. **220**(2): p. 161-169.

48. Arifin, D.R. and A.F. Palmer, Polymersome encapsulated hemoglobin: A novel type of oxygen carrier. Biomacromolecules, 2005. **6**(4): p. 2172-2181.

49. Pressly, E.D., et al., Structural effects on the biodistribution and positron emission tomography (PET) imaging of well-defined Cu-64-labeled nanoparticles comprised of amphiphilic block graft copolymers. Biomacromolecules, 2007. **8**(10): p. 3126-3134.

50. Sun, G., et al., Strategies for optimized radiolabeling of nanoparticles for *in vivo* PET Imaging. Advanced Materials, 2007. **19**(20): p. 3157-+.

51. Kelly, K.A., et al., Detection of vascular adhesion molecule-1 expression using a novel multimodal nanoparticle. Circulation Research, 2005. **96**(3): p. 327-336.

52. Perez, J.M., et al., Peroxidase substrate nanosensors for MR imaging. Nano Letters, 2004. **4**(1): p. 119-122.

53. Tsourkas, A., et al., *In vivo* imaging of activated endothelium using an anti-VCAM-1 magnetooptical probe. Bioconjugate Chemistry, 2005. **16**(3): p. 576-581.

54. Ghoroghchian, P.P., et al., Broad spectral domain fluorescence wavelength modulation of visible and near-infrared emissive polymersomes. Journal of the American Chemical Society, 2005. **127**(44): p. 15388-15390.

55. Ghoroghchian, P.P., et al., Controlling bulk optical properties of emissive polymersomes through intramembranous polymer-fluorophore interactions. Chemistry of Materials, 2007. **19**(6): p. 1309-1318.

56. Ghoroghchian, P.P., Emissive Polymer Vesicles: Soft Nanoscale Probes for *In vivo* Optical Imaging, in Bioengineering. 2006, University of Pennsylvania: Philadelphia. p. 364.

57. Figdor, C.G., et al., *Dendritic cell immunotherapy: mapping the way.* Nature Medicine, 2004. **10**(5): p. 475-480.

58. Christian, N.A., *Development and Application of Tat-Near-Infrared-Emissive Polymersomes for In vivo Optical Imaging of Dendritic Cells*, in *Bioengineering*. 2007, University of Pennsylvania: Philadelphia.

59. Zhou, W., et al., *Biodegradable polymersomes for targeted ultrasound imaging.* Journal of Controlled Release, 2006. **116**(2): p. e62-e64.

60. Park, B.W., et al., *Rationally designed anti-HER2/neu peptide mimetic disables p185(HER2/neu) tyrosine kinases in vitro and in vivo.* Nature Biotechnology, 2000. **18**(2): p. 194-198.

61. Brooks, H., B. Lebleu, and E. Vives, *Tat peptide-mediated cellular delivery: back to basics.* Advanced Drug Delivery Reviews, 2005. **57**(4): p. 559-577.

62. Lee, K.Y. and S.H. Yuk, *Polymeric protein delivery systems.* Progress in Polymer Science, 2007. **32**(7): p. 669-697.

63. Nobs, L., et al., *Current methods for attaching targeting ligands to liposomes and nanoparticles.* Journal of Pharmaceutical Sciences, 2004. **93**(8): p. 1980-1992.

Chapter 2

POLYMERSOMES: SELF-ASSEMBLED VESICLES FOR DRUG DELIVERY

ADAPTED FROM

P. Peter Ghoroghchian, Guizhi Li, **Dalia H. Levine**, Kevin P. Davis, Frank S. Bates, Daniel A. Hammer, and Michael J. Therien, *Macromolecules*, 2006, vol. 36, no. 6, p. 1673-1675.

Dalia Hope Levine, P. Peter Ghoroghchian, Jaclyn Freudenberg, Geng Zhang, Michael J. Therien, Mark I. Greene, Daniel A. Hammer, and Ramachandran Murali, *Methods*, 2008, vol. 46, p. 25-32.

Joshua S. Katz, **Dalia H. Levine**, Kevin P. Davis, Frank S. Bates, Daniel A. Hammer, and Jason A. Burdick, *Langmuir*, 2009, vol. 28, no. 8, p. 4429-4434.

D. H Levine, J. S. Katz, N. Dang, J. A. Burdick, J. Hadfield, and D. A. Hammer, Manuscript in Preparation

D.H. Levine, N. Sood, F. Bates, D.A. Hammer, Experiments Underway for Manuscript Preparation

2.1 SUMMARY

Polymersomes (polymer vesicles) have attractive biomaterial properties compared to phospholipid vesicles, including prolonged circulation times, increased mechanical stability, and the unique ability to incorporate hydrophobic molecules within their thick lamellar membranes and hydrophilic molecules within their core [5-8]. The generation of self-assembled nano-sized vesicles from various diblock copolymers has been demonstrated. The attractive biomaterial properties of these vesicles make the polymersome a prime vehicle for the delivery of pharmaceutical agents to tumors.

Currently, new thought into cancer treatment suggests the use of combination therapy as a method to improve the anti-tumor effects of chemotherapeutics. Such combinations can include multiple chemotherapeutics, chemotherapeutics and peptides or antibodies, or chemotherapeutics and anti-angiogenesis agents or vascular disrupting agents (VDA).

Doxorubicin, an anthracycline antibiotic, is currently used in the treatment of a variety of cancers ranging from solid tumor to leukemias. However, one of the major therapeutic limitations of doxorubicin is its associated cardiotoxicity at cumulative doses. Encapsulating doxorubicin in the aqueous core of vesicles, however, may decrease the toxicity. The ability to load doxorubicin into biocompatible, bioresorbable, as well as stabilized vesicles is demonstrated.

Combretastatin A4, a VDA, has been shown to cause vascular failure in new vasculature around solid tumors, while not affecting healthy vasculatures. But, this molecule is hydrophobic, limiting its bioavailability and creating challenges to delivery.

The incorporation of combretastatin in the hydrophobic vesicle bilayer, however, can assist with delivery. Its incorporation into bioresorbable vesicles with and without doxorubicin will be explored in this chapter.

Here, we demonstrate the ability to encapsulate each pharmaceutical agent separately as well as in combination, thereby highlighting the enormous promise for using polymersomes as multi-drug delivery agents for the eradication of tumorigenic cells and endothelial cells.

2.2 INTRODUCTION

Currently, many compounds with toxic side effects or low bioavailability hold extraordinary promise as potential therapeutic agents. However, limited bioavailability of hydrophobic compounds and/or toxic side effects of these molecules can render their therapeutic value ineffective. Further, the ability of the therapeutic agents to reach the target site can be limited by the body's clearance. Thus, the development of a polymeric delivery vehicle with specifically tuned pharmacokinetics, which can encapsulate and release highly toxic therapeutic agents for concentrated local delivery, should greatly increase therapeutic efficacy.

As discussed in Chapter 1, presently liposomes, vesicles derived from phospholipids, are used in a limited number of biotechnological and pharmaceutical applications to improve therapeutic indices and enhance cellular uptake [4]. However, in contrast to liposomes, polymersomes, polymer vesicles self-assembled from synthetic amphiphilies, have been shown to possess superior biomaterial properties [5, 6, 8]. Self-assembled from amphiphilic polymers, with hydrophilic and hydrophobic blocks,

polymersomes can encapsulate aqueous components in their interior and hydrophobic molecules within their thick lamellar membranes.

The ability to load components into the membrane and interior of polymersomes shows enormous promise for dual modality polymersomes that enable delivery of two therapeutic agents as will be discussed in this chapter or a therapeutic agent and imaging agent as will be discussed in Chapter 4. As a proof of concept, we have successfully loaded various hydrophobic molecules, i.e. Nile Red, into the bilayer as well as various hydrophilic molecules, i.e. Calcein, into the aqueous core[10]. Additionally, we have successfully loaded both hydrophilic and hydrophobic molecules simultaneously into the same polymersomes [10].

While the ability to load therapeutics into biocompatible polymeric vesicles, such as those generated from PEO-b-PBD, is crucial for understanding and comparing the loading and release kinetics of the drug from vesicles, the ability to load pharmaceutical agents into bioresorbable polymers is paramount if these vesicles are to be used for *in vivo* drug delivery. Recently, much attention has been focused on developing polymersomes composed of fully-bioresorbable polymers. The ability to generate self-assembled, fully-bioresorbable vesicles comprised of an amphiphilic diblock copolymer consisting of two previously FDA-approved building blocks: poly(ethylene oxide) (PEO) and polycaprolatone (PCL) has been demonstrated [10]. Unlike polymersomes formed from the blending of "bio-inert" and hydrolysable block copolymers [26], these fully-bioresorbable vesicles leave no potentially toxic byproducts upon degradation [29].

In addition to generating vesicles that are biocompatible and biodegradable, the ability to stabilize the membrane and control the release of the vesicles contents, is imperative for the controlled release of many chemotherapeutics with a narrow therapeutic window. While previous work has demonstrated the stabilization of polymersome membranes [61-66] we aimed to design stabilized polymersomes that are also biodegradable. To that end, a functional group (i.e. acrylate) was incorporated at the PCL terminal end of PEO-b-PCL diblock polymers.

Doxorubicin (DOX) is an amphipathic anti-neoplastic agent that shows much promise in cancer therapy, both alone and in conjunction with antibodies and peptides [37]. Currently, DOX is widely administered for the treatment of various types of cancer ranging from solid tumors to leukemias [67-70]. One of the major limitations associated with administration of this chemotherapeutic agent, however, is cardiac myocyte toxicity [39]. However, utilizing drug carriers to deliver doxorubicin can alleviate some of the associated cardio-toxicity; drug carriers alter the pharmacodistribution of the drug and thus reduce the drug's concentration in the heart [39]. Delivery of doxorubicin in liposomes has been shown to extend the circulation time and alter the pharmacodynamics of doxorubicin in such a way as to decrease its toxicity while still maintaining its anticancer activity [39]. Using active loading methods originally developed for liposomes, doxorubicin can be efficiently loaded into the aqueous center [10, 26, 40] of polymer vesicles.

Combination therapies, involving the combination of various chemotherapeutics for cancer treatment, have proven very effective and in fact many cancer therapies now

include a multi-drug regimen. However, therapies that use a Maximum Tolerated Dose (MTD) approach, whereby the highest tolerated dose of chemotherapeutic is administered as a single dose or over a short period followed by drug free periods, are aimed at eliminating as many tumor cells as possible [71]. In addition to the toxic systemic side effects associated with the MTD approach, during drug free cycles where the normal tissue is allowed to recover, non-tumorigenic endothelial cells composing the vasculature can continue to supply the small number of remaining tumor cells with the nutrients and oxygen required for survival and remove waste products. Thus, although the initial administration may be efficacious, these "drug free" periods can allow tumors to relapse [71]. A new approach to administer chemotherapeutics over longer periods of time with small doses is being considered as a way to reduce systemic toxicity and possibly improve anti-tumor effects [71]; this slower more controlled dosing, termed 'metronomic chemotherapy' has been shown to have an anti-angiogenesis effect as well [71]. This bodes well for the polymersome as a potential delivery system, where the drug release kinetics can be specifically tuned to release drug on both short time scales (hours) to longer time scales (days). The ability to vary release kinetics using different polymer backbones will be illustrated here; however the potential to vary the backbone and ultimately the release kinetics is much greater than the limited number of examples which are presented in this chapter.

In addition to administering chemotherapy in a slower more controlled manner as a method of creating an anti-angiogenic effect, the combination of chemotherapeutics with anti-angiogenic drugs has been examined. Studies have demonstrated the potential of anti-angiogenic drugs to improve the cytotoxic chemotherapeutic effects which both

drugs are administered in combination [71]. Since tumors require a network of blood vessels to survive and grow, angiogenesis, the growth of new blood vessels is crucial for tumor survival and metastasis. These newly formed blood vessels are required to provide oxygen and nutrients to the tumor cells and remove carbon dioxide and waste. In fact, a crucial step in tumor growth and subsequent invasion and metastasis of tumor cells is the switch to the "angiogenic phenotype" [72].

These nascent blood vessels are immature and their walls are poorly developed [73], distinguishing them from normal vasculature. Furthermore, while angiogenesis occurs rapidly in tumor tissues, in normal healthy tissues the rate of angiogenesis is minimal [74]. For these reasons, as well as others, targeting tumor endothelium is advantageous in the treatment of cancer. As a result, the combination of chemotherapeutics with anti-angiogenesis agents, which suppress neovascularization, or vascular disrupting agents (VDA), which result in rapid and selective disruption of the tumor vasculature has emerged as a promising therapy [71, 73]. These agents target genetically stable endothelial cells that constitute the blood vessels around tumors, rather than the transformed tumor cells themselves [75].

However, this combination therapy is not without challenges which must be overcome. First, if the tumor vasculature is destroyed by the VDA prior to administering the chemotherapeutic, it can prevent the tumor from receiving the necessary amount of chemotherapeutic required to destroy the tumor cells [38]. Furthermore, inhibiting blood supply can lead to the upregulation of various cellular markers, for example, hypoxia inducible factor (HIF1-α) which has been linked to increased tumor invasiveness and

resistance to chemotherapy [38]. However, the use of polymer vesicles may solve some of the challenges associated with anti-angiogenic drug/VDA delivery by simultaneously delivering both chemotherapeutic and anti-angiogenic agent/VDA directly to the tumor site. As discussed in Chapter 1, the polymersome architecture lends itself nicely to dual drug loading.

Thus the addition of a VDA into the hydrophobic bilayer of doxorubicin loaded vesicles can potentially create a multi-drug polymersome capable of destroying cancerous tumors cells and their vasculature. Combretastatin A4, a hydrophobic vascular disrupting agent, inhibits the polymerization of tubulin and causes "irreversible vascular shutdown within solid tumors" while leaving the healthy vasculature intact [76]. Hence, combretastatin A4, is a key candidate to incorporate into the bilayer of doxorubicin loaded vesicles. Thus, the combination of combretastatin A4 and doxorubicin into one vesicle will create a multi-modal platform for the eradication of tumor cells and the endothelial cells which support them.

This chapter explores the challenges associated with loading DOX into the aqueous core of polymersomes generated from biocompatible diblock copolymer, poly(ethylene oxide)-b-polybutatdiene (PEO-b-PBD) as well as the bioresorbable diblock copolymers, poly(ethylene oxide)-b-polycaprolactone (PEO-b-PCL) and poly(ethylene oxide)-b-poly(methyl caprolactone) (PEO-b-PmCL). In addition, it discusses the release of the drug from these vesicles. Furthermore, the ability to load doxorubicin into combretastatin incorporated vesicles is demonstrated, confirming the generation of a *multi-functional* multidrug vesicles for the eradication of tumor cells and the endothelial

cells which support them.

2.3 EXPERIMENTAL METHODS

2.3.1 Preparation of PEO-b-PCL Polymersomes for Doxorubicin Loading and Release Studies

Self-assembly via thin-film hydration was employed in order to form the PEO (2k)-b-PCL (12k) copolymers into their equilibrium morphologies. Film hydration has been extensively utilized for preparing non-degradable polymersomes comprised of PEO-b-PBD and PEO-b-PEE diblock copolymers [4, 9]. Briefly, 200 microliters of a 70 mg/ml (or 35mg/ml for development studies) PEO-b-PCL copolymer solution in methylene chloride were uniformly deposited on the surface of a roughened Teflon plate followed by evaporation of the solvent for >12h. Addition of aqueous solution, (~290 milliosmolar ammonium sulfate solution, pH ~5.4) and sonication for approximately 60 minutes at 65°C led to spontaneous budding of biodegradable polymersomes off the Teflon-deposited thin-film, into the aqueous solution. The sonication procedure involved placing the sample vial containing the aqueous based solution and dried thin-film formulation (of polymer uniformly deposited on Teflon) into a sonicator bath (Branson; Model 3510) at 60-65°C for 30 minutes followed by constant agitation for 60 minutes at 60-65°C. Subsequently, five cycles of freeze-thaw extraction followed by placing the sample vials in liquid N_2 and subsequently thawing in a water bath at ~55~65°C. Extrusion using a pressure driven Lipex Thermobarrel Extruder (1.5 mL capacity) at 65°C was performed to yield small (<300-nm diameter) unilamellar polymersomes that possess appropriately narrow size distributions. The size distribution of the PEO-b-PCL suspension was determined by dynamic light scattering (Figure 2.5).

Once vesicles of the appropriate size were formed, extruded samples were dialyzed in iso-osmotic Sodium Acetate Solutions (50 mM Sodium Acetate, 100mM Sodium Chloride, pH~5.5). Dialysis solutions were changed 3 times over approximately 30 hours. Post-dialysis, doxorubicin was actively loaded into the polymersomes through an ammonium sulfate gradient. The polymersomes were incubated with doxorubicin in a ratio of 1:0.2 polymer:drug (w/w) for 7 hours at a temperature above their main gel to liquid-crystalline phase transition temperature [77-79]. Aggregation of DOX within the polymersome core led to quenching of its fluorescence emission. For loading studies, to demonstrate loading, fluorescence data was obtained at various time points over the seven hour incubation (using a SPEX Fluorolog-3 fluorimeter; λex = 480nm, λem = 590nm). This incubation time was later extended to 9 hours.

Non-entrapped DOX was removed from the solution (using an Acta Basic 10 HPLC with Frac 950; the solution was passed through a C-1640 column with Sephacryl S500-HR media. Subsequent studies employed a HiTrap desalting column instead of the C-1640 column. The collected DOX-loaded polymersome suspension was centrifuged and concentrated into an approximately 1 mL volume. The vesicles were then aliquoted into various (290 mOsM) solutions buffered at pH ~5 (50 mM sodium acetate and 100 mM sodium chloride) and pH ~ 7.4 (PBS), with N = 4 samples for each buffer. Release studies of DOX from the loaded polymersomes were initiated immediately following aliquoting; DOX fluorescence was measured fluorometrically (using a SPEX Fluorolog-3 fluorimeter; λex = 480nm, λem = 590nm) at various intervals up to fourteen days. As DOX was released from the polymersome core, and diluted into the surrounding solution, its fluorescence emission increased over time. At the culmination of the study, the

samples were solubilized using Triton X-100. The percent release over time was calculated by comparing the measured fluorescence at each time point to final DOX fluorescence, as determined upon solubilization of remaining intact polymersomes with Triton X-100, at the completion of the study, as per Equation 2.1. Release rates were calculated by comparing the fluorescence at two time points over the time period between the time points as per Equation 2.2.

Equation 2.1:

$$cumulative\ \%\ release_t = \frac{|fl_i - fl_t|}{|fl_i - fl_{ps}|}$$

$$where, fl_i = initial\ fluorescence$$

$$fl_t = fluorescence\ at\ time\ t$$

$$fl_{ps} = fluorescence\ post\ solubilization\ with\ triton\ x-100\ and\ heat$$

Equation 2.2:

$$release\ rate = \frac{(fl_2 - fl_1)}{(t_2 - t_1)}$$

$$where, fl_i\ is\ the\ fluorescence\ at\ time\ i$$

$$t_i = the\ time\ at\ i$$

2.3.2 Preparation of PEO-b-PmCL Polymersomes for Doxorubicin Loading and Release Studies

Similar to PEO-b-PCL and PEO-b-PCL-Ac doxorubicin loaded vesicles, PEO-b-PmCL vesicles were prepared via thin film hydration. Briefly, a thin film of polymer was deposited on a Teflon film, and the organic was allowed to dry. Following this step, the film was hydrated with ammonium sulfate solution and sonicated at 65□C. Vesicles spontaneously self-assembled and budded off the Teflon as a result of the energy provided via sonication. Subsequent to sonication, vesicles were further processed as

noted in Section 2.3.1and dialysis was performed. Samples were dialyzed however, into iso-osmotic Sodium Chloride (NaCl) solution acidified with 12.1N HCl to yield a solution with pH~5.5, osmolarity~290mOsM. Dialysis into sodium acetate buffer at pH 5.5, as performed with PEO-b-PCL vesicles, discussed in Section 2.3.1did not yield stable loading as determined via fluorescence measurements; hence dialysis in various buffers was attempted, as will be discussed in Section 2.4.2, and it was determined that stable fluorescence counts were obtained for loading when acidified NaCl was used as the dialysis media. Three exchanges were made over approximately 30 hours. Post DOX loading, DOX was removed on two HiTrap desalting columns in series (GE Healthcare)

The vesicles were then aliquoted into various (290 mOsM) solutions buffered at pH ~5 (50 mM sodium acetate and 100 mM sodium chloride) and pH ~ 7.4 (PBS), with N = 4 samples for each buffer. Release studies of DOX from the loaded polymersomes were initiated immediately following aliquoting; DOX fluorescence was measured fluorometrically (using a SPEX Fluorolog-3 fluorimeter; λ_{ex} = 480nm, λ_{em} = 590nm) at various intervals up to fourteen days. As DOX was released from the polymersome core, and diluted into the surrounding solution, its fluorescence emission increased over time. At the culmination of the study, the samples were solubilized using Triton X-100. The percent release and release rate over time was calculated by comparing the measured fluorescence at each time point to final DOX fluorescence, as determined upon solubilization of remaining intact polymersomes with Triton X-100, at the completion of the study (Equation 2.1and Equation 2.2).

2.3.3 Preparation of PEO-b-PBD Polymersomes for Doxorubicin Loading and Release Studies

Doxorubicin loaded PEO-b-PBD vesicles were prepared via thin film hydration as described above. Briefly, a thin film of polymer (35-70mg/ml in organic) was deposited on a Teflon film, and the organic was allowed to dry. Following this step, the film was hydrated with ammonium sulfate solution (pH ~5.3~5.5, ~290mOsM) and sonicated at 65□C. Vesicles spontaneously self-assembled and budded off the Teflon as a result of the energy provided via sonication. Subsequent to sonication, vesicles were further processed as noted in Section 2.3.1and dialysis was performed.

In order to determine the loading buffer which yields the most stable loading, for development, samples were initially dialyzed, into either iso-osmotic Sodium Chloride (NaCl) solution acidified with 12.1N HCl to yield a solution with pH~5.5 or iso-osmotic Sodium Acetate/Sodium Chloride Buffer at a pH of 5.5. (Following this, studies were carried out using Acidified NaCl Solution for the dialysis exchange.) Three exchanges were made over approximately 30 hours.

The vesicles were then aliquoted into various (290 mOsM) solutions buffered at pH ~5 (50 mM sodium acetate and 100 mM sodium chloride) and pH ~ 7.4 (PBS), with N = 4 samples for each buffer. Release studies of DOX from the loaded polymersomes were initiated immediately following aliquoting; DOX fluorescence was measured fluorometrically (using a SPEX Fluorolog-3 fluorimeter; λex = 480nm, λem = 590nm) at various intervals up to fourteen days. As DOX was released from the polymersome core, and diluted into the surrounding solution, its fluorescence emission increased over time. At the culmination of the study, the samples were solubilized using Triton X-100. The

percent release over time was calculated by comparing the measured fluorescence at each time point to final DOX fluorescence, as determined upon solubilization of remaining intact polymersomes with Triton X-100, at the completion of the study.

2.3.4 Doxorubicin Release from Doxil (lipid vesicles)

Doxil®, the commercially available liposomal formulation of doxorubicin, was obtained from the Hospital of the University of Pennsylvania Pharmacy for research purposes only. Similar to the release studies performed on PEO-b-PCL and PEO-b-PmCL vesicles, the 10ul of the concentrated Doxil (20mg/10ml) solution was placed in 2.95 mL of either phosphate buffered saline (PBS) (pH 7.4, 290mOsM), or sodium acetate buffered solution (pH 5, 290mOsM) at a concentration below the quenching concentration of the encapsulated doxorubicin as determined by absorbance measurement. The final concentration of doxorubicin was .0068mg/ml in buffer. Release studies of DOX from the loaded liposomes were initiated immediately following aliquoting; fluorescent measurements (using a SPEX Fluorolog-3 fluorimeter; λ_{ex} = 480nm, λ_{em} = 590nm) were made at various intervals up to fourteen days post aliquoting. As noted, as DOX was released from the polymersome core, and diluted into the surrounding solution, its fluorescence emission increased over time. At the culmination of the study, the samples were solubilized using Triton X-100 and heat. The percent release over time was calculated by comparing the measured fluorescence at each time point to final DOX fluorescence, as determined upon solubilization of remaining intact polymersomes with Triton X-100, at the completion of the study.

2.3.5 Preparation of PEO-b-PCL-Ac Polymersomes for Doxorubicin Loading and Release Studies

Prior to polymersome formation, the functionalize block copolymer was synthesized by Joshua S. Katz via a two step process, as shown in Figure 2.1. Briefly, the diblock copolymer was synthesized via a ring opening polymerization of the ε-caprolactone using monomethoxy PEG as a macroinitiator and stannous octoate as the catalyst. Once the block copolymer was synthesized, the terminal hydroxyl group on the caprolactone block was acrylated using acryloyl chloride and dichloromethane.

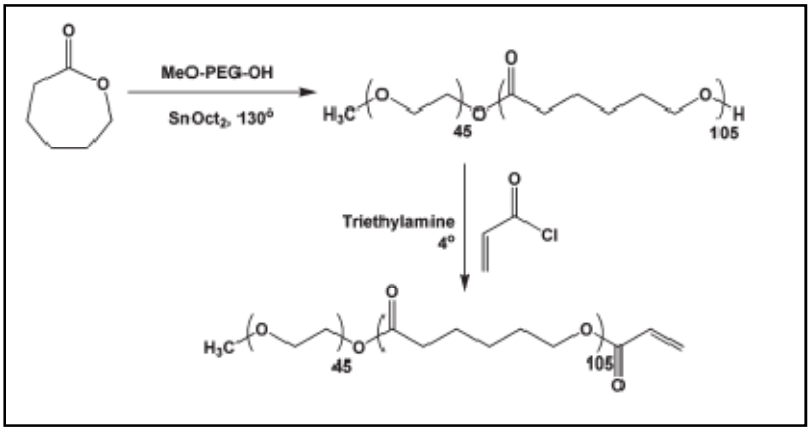

Figure 2.1- Synthesis of Acrylate-Terminated PEO-b-PCL Copolymer

Polymersomes were generated by the self-assembly of polymer thin films on roughened Teflon into aqueous medium (70-100 mg/mL solution of polymer in methylene chloride, drying, immersion in aqueous solution), followed by sonication at 65□C, freeze-thaw cycling (five cycles liquid nitrogen to 65□C), and heated, automated extrusion (400 and 200 nm membranes) [4, 9]. The photoinitiator DMPA (18 μg/mg polymer for 1:1 mol polymer: mol photoinitiator, as determined by J.S. Katz) was co-cast with the polymer on the Teflon for inclusion into the membrane prior to hydration. DOX was encapsulated utilizing an ammonium sulfate gradient [77-79] (a 10 mg/mL DOX in

water was added to the polymersome suspension at a ratio of 1:0.2 polymer: drug and incubated at 65□C for 7-9 hours) [77], and free DOX was removed on two HiTrap desalting columns in series (GE Healthcare). Post DOX loading and removal of free DOX, UV light exposure was completed with an OmniCure Series 1000 spot-curing lamp with a collimating lens (Exfo, Ontario, Canada; 365 nm, 55 mW/cm2). Release into phosphate-buffered saline (PBS) was monitored by recording the fluorescence of polymersome suspensions over time (SPEX Fluorolog-3 fluorimeter, λ_{ex} = 480 nm, λ_{em} = 590 nm). The amount of DOX encapsulated was determined by polymersome dissociation with addition of 100 μL of 30% TritonX-100 and incubation for 60 min at 37□C.

2.3.6 Preparation of PEO-b-PCL Polymersomes for Combretastatin Incorporation Studies

Self-assembly via thin-film hydration was used to assemble the PEO-b-PCL copolymers into their equilibrium morphologies. Film hydration has been extensively utilized for preparing non-degradable polymersomes comprised of PEO-b-PBD and PEO-b-PEE diblock copolymers [4, 9]. Briefly, a 70mg/mL PEO-b-PCL copolymer solution in methylene chloride was prepared and added to combretastatin at a 0.9:1 drug:polymer molar ratio. Two hundred microliters of the polymer-drug solution were uniformly deposited on the surface of a roughened Teflon plate followed by evaporation of the solvent for >12h. Addition of aqueous solution, (~290mOsM Phosphate Buffered Saline, PBS) and sonication at 65°C led to spontaneous budding of biodegradable polymersomes, off the Teflon-deposited thin-film, into the aqueous solution. The sonication procedure involved placing the sample vial containing the aqueous based

solution and dried thin-film formulation (of polymer-drug uniformly deposited on Teflon) into a sonicator bath (Branson; Model 3510) @ 60-65°C for 30 minutes followed by constant agitation for 60 minutes at 60-65°C. Subsequently, five cycles of freeze-thaw extraction followed by placing the sample vials in liquid N_2 and then thawing in a water bath at 50-60°C. Extrusion using a pressure driven Lipex Thermobarrel Extruder (1.5 mL capacity) at 65°C was performed to yield small (<300-nm diameter) unilamellar polymersomes that possess appropriately narrow size distributions. The size distribution of the PEO-b-PCL suspension was determined by dynamic light scattering. Post extrusion, non-entrapped combretastatin was removed from the sample by concentrating using a Centricon centrifugal device. The sample was centrifuged, filtrate removed, and additional PBS buffer was added to the concentrated sample for a total of nine times. The collected polymersome solution was centrifuged to concentrate the sample.

To determine the concentration, one hundred microliter sample aliquots were removed and the combretastatin was extracted from the vesicles by adding the aliquot to 400 microliters of PBS and 500 microliters of methylene chloride, and subsequently vortexing and centrifuging the sample. The resulting aqueous layer was carefully removed, and the remaining organic layer with drug was placed in a vacuum. The dried powder resulting from evaporation of the methylene chloride was reconstituted in 1 milliliter of acetonitrile. The concentration of combretastatin was determined by measuring the absorbance (molar extinction coefficient $12{,}579 M^{-1}cm^{-1}$ in acetonitrile at 300nm). Polymer concentration was determined by a mathematical calculation.

2.3.7 Preparation of Dual Drug PEO-b-PCL Polymersomes for Combretastatin Incorporation and Doxorubicin Loading

Self-assembly via thin-film hydration was used to assemble the PEO-b-PCL copolymers into their equilibrium morphologies. Film hydration has been extensively utilized for preparing non-degradable polymersomes comprised of PEO-b-PBD and PEO-b-PEE diblock copolymers [4, 9]. As described in section 2.3.670 mg/ml (or 35mg/ml or for development studies) PEO-b-PCL copolymer solution in methylene chloride was prepared and added to combretastatin at a 0.9:1 drug:polymer molar ratio and a thin film of the polymer-drug solution was uniformly deposited on the surface of a roughened Teflon plate. The addition of aqueous solution, (~290mOsM Ammonium Sulfate Solution, pH~5.4) and sonication for approximately 60 minutes at 65°C led to spontaneous budding of biodegradable polymersomes, off the Teflon-deposited thin-film, into the aqueous solution. As described, the sonication procedure involved placing the sample vial into a sonicator bath (Branson; Model 3510) @ 60-65°C for 30 minutes to equilibrate the sampled followed by constant agitation for 60 minutes at 60-65°C. Post sonication, five cycles of freeze-thaw extraction followed by placing the sample vials in liquid N_2 and subsequently thawing in a water bath at 50-60°C. Extrusion using a pressure driven Lipex Thermobarrel Extruder (1.5 mL capacity) at 65°C was performed to yield small (<300-nm diameter) unilamellar polymersomes that possess appropriately narrow size distributions. The size distribution of the combretastatin PEO-b-PCL suspension was determined by dynamic light scattering.

Once vesicles of the appropriate size were formed, samples were dialyzed in iso-osmotic Sodium Acetate Solutions (50 mM Sodium Acetate, 100mM Sodium Chloride,

and pH ~ 5.5). Dialysis solutions were changed 3 times over approximately 30 hours. Post-dialysis, doxorubicin was actively loaded into the combretastatin incorporated polymersomes through an ammonium sulfate gradient. The polymersomes were incubated with doxorubicin in a ratio of 1:0.2 polymer:drug (w/w) for 9 hours at a temperature above their main gel to liquid-crystalline phase transition temperature [77-79]. Aggregation of DOX within the polymersome core led to quenching of its fluorescence emission. For loading studies, to demonstrate loading, fluorescence data was obtained at various time points over the nine hour incubation (using a SPEX Fluorolog-3 fluorimeter; λ_{ex} = 480nm, λ_{em} = 590nm).

Non-entrapped DOX and combretastatin were removed from the solution (using an Acta Basic 10 HPLC with Frac 950; the solution was passed through a HiTrap desalting column. The collected dual drug polymersome suspension was centrifuged and concentrated. Samples were aliquoted and an absorbance spectrum of the resulting vesicles was obtained from 190nm to 700nm. Furthermore, vesicles were solubilized using Triton X-100 to demonstrate doxorubicin loading into the aqueous core. Once the vesicles are solubilized, if DOX is in encapsulated in the aqueous core, there should be a marked increase in fluorescence from the sample as DOX from aqueous core is freed into the external media.

2.4 RESULTS AND DISCUSSION

2.4.1 Loading and Release of Doxorubicin in PEO-b-PCL Polymersomes

To assess the mechanism by which the PEO-b-PCL vesicles load a physiologically relevant, the loading of Doxorubicin (DOX) was monitored

spectrofluorometrically (λ_{ex}=480nm, λ_{em}=590nm) over the course of 7 hours; this was later followed through 9 hours. Since the aggregation of doxorubicin inside the core, when loaded actively via ammonium sulfate gradient, results in quenching of the fluorophore, a decrease in fluorescence over time was generally observed as drug molecules load into the vesicles. However, it should be noted, this decrease in fluorescence was concentration dependent, and hence if the concentration outside the vesicles was initially high (i.e. above the quenching concentration), loading was actually seen as an increase in fluorescence as the DOX concentration in the external solution decreased below the quenching concentration with loading. As such, in all loading studies, the final determination of loading was thus made based on stabilization of the fluorescence output over time.

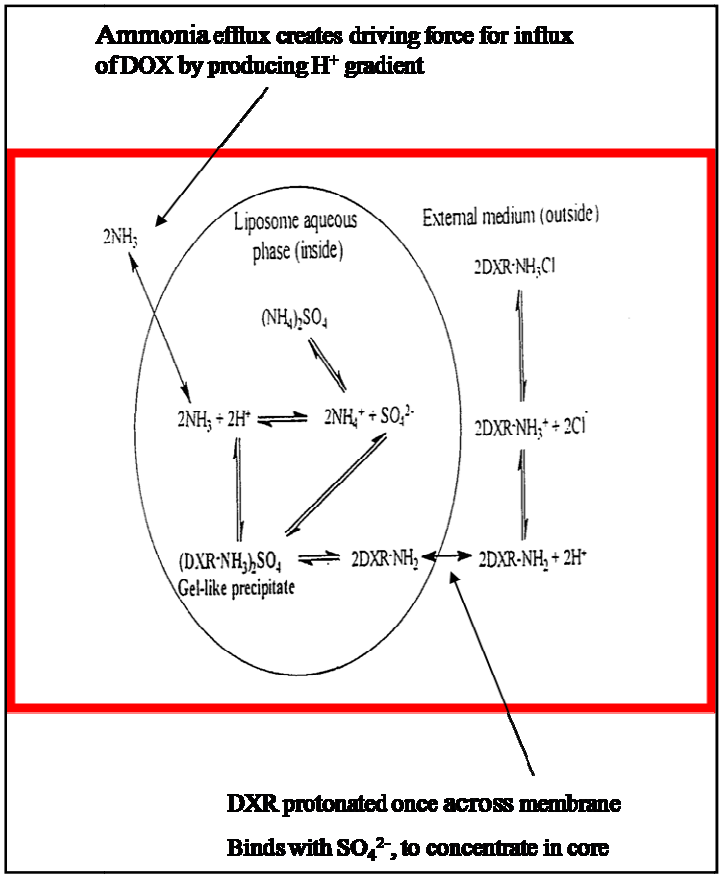

Figure 2.2- Schematic of remote DOX loading in vesicles by an ammonium sulfate gradient created between the intravesicle aqueous phase and the external solution [79].

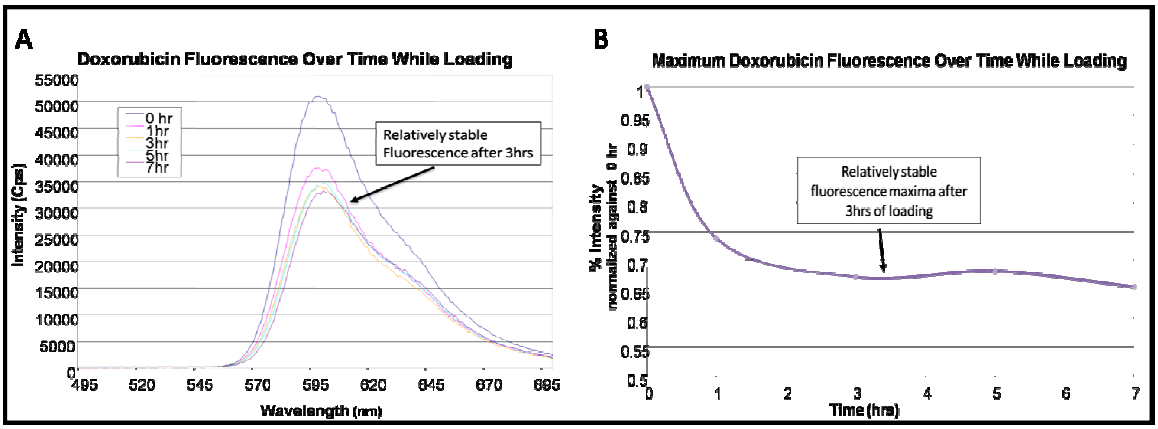

Figure 2.3- Characterizing the loading of doxorubicin into PEO-b-PCL polymersomes.
A) Doxorubicin fluorescence spectra over time while loading into vesicles. B) The normalized maximum fluorescence of doxorubicin over time, where all values are normalized back to the 0h fluorescence maxima. In both graphs, A) and b) he decrease in fluorescence and the stabilization of the fluorescent signal after 3 hours is clearly demonstrated

Using Cryotransmission electron microscopy (cryo-TEM) we confirmed that the remote loading of DOX did not adversely affect the structure of the membrane or vesicular structure of the polymersome. DOX loaded polymersomes were observed via cryo-TEM (Figure 2.1) and demonstrate the vesicle like morphology seen with unloaded polymersomes. However, in contrast to unloaded polymersomes, images of DOX loaded vesicles have an electron-opaque band in the aqueous core [79] (Figure 2.1, A-C) resulting from the fibrous-bundle aggregates formed when doxorubicin precipitates when encapsulated in the presence of a pH gradient [80].

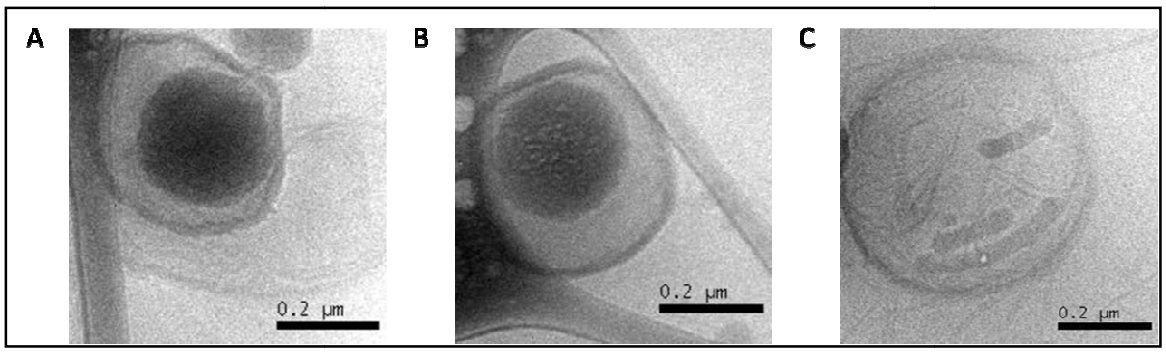

Figure 2.4- Cryo-TEM Images of Doxorubicin loaded PEO-b-PCL vesicles. Note the solid like aggregates in both circular and rod like form in the vesicle center; this is the solgel

We assessed the mechanism by which PEO-b-PCL vesicles load (See Section 2.4.1) and release a physiologically relevant encapsulant. As a model system, Doxorubicin, an anti neoplastic agent which inhibits DNA replication, was actively encapsulated into the aqueous compartment of 200nm PEO-b-PCL vesicles (Figure 2.5) though an ammonium sulfate gradient [77, 79, 81] (See Section 2.3.1). *in situ* release

C)

where doxorubicin release was monitored fluorometrically (λ_{ex}=480nm, λ_{em}=590nm) over 14 days. Cumulative release and release rate were calculated according to equations Equation 2.1and Equation 2.2, respectively.

While the kinetics of the release varied at the two pHs, an initial burst release phase (where approximately 20% of the initial payload within the first 8 hrs) was observed for both pH's followed by a more controlled pH dependent release over the 14 day release study (Figure 2.6A). However, the dynamics of release varied at each condition (Figure 2.6B). At a pH of 5, one single release phase (β') is observed over the entire 14 days; it appears that the dominant mechanism of release at both short and long

times at this pH is acid catalyzed hydrolysis of the PCL membrane (Figure 2.6C). In contrast, at a pH of 7.4, two distinct phases (α, β) are observed. Kinetic release studies suggest that initially (days 1-5, α phase) doxorubicin release from the polymersome core is primarily dependent upon passive diffusion of the drug across the PCL membrane. At subsequent times, (days 5-14, β phase) drug release is predominantly facilitated by hydrolytic matrix degradation of the caprolactone backbone Figure 2.6C). The rate constants of the β (pH 7.4) and β' (pH 5) phases are similar further suggesting a similar mechanism of release. Since acid catalyzed hydrolysis of the membrane occurs at both short and long times at pH 5, DOX release at pH 5 is more rapid that at pH 7.4

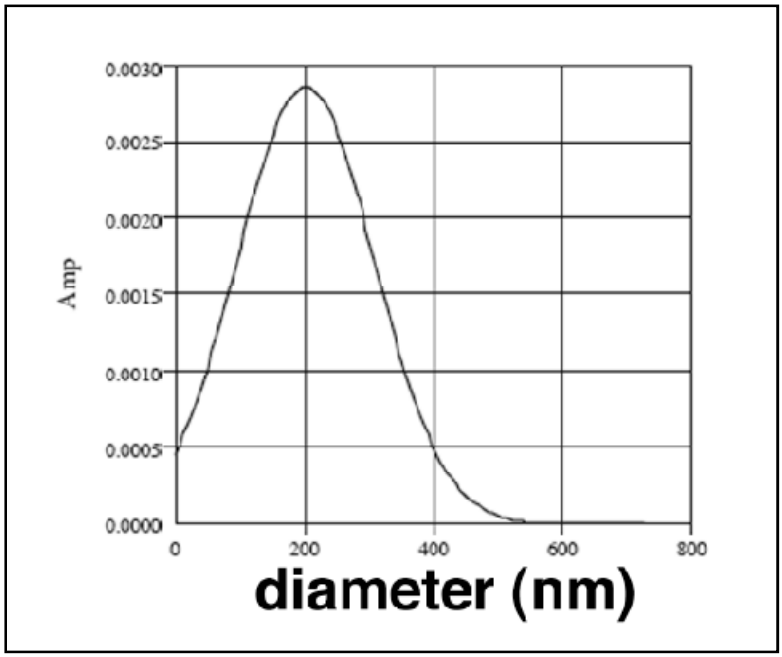

Figure 2.5- Cumulative histogram of the size distribution of PEO(2k)-b-PCL(12k)-based polymersomes as obtained via dynamic light scattering (DLS) at 25°C.
Vesicles were formed via thin film self- assembly upon aqueous hydration and heating at 65°C for 1 hr. A mono-dispersed distribution of 200 nm diameter polymersomes was subsequently obtained upon 5 cycles of freeze-thaw extraction followed by extrusion through a thermo-barrel supported (5 passes at 65°C) 200 nm pore cutoff membrane.

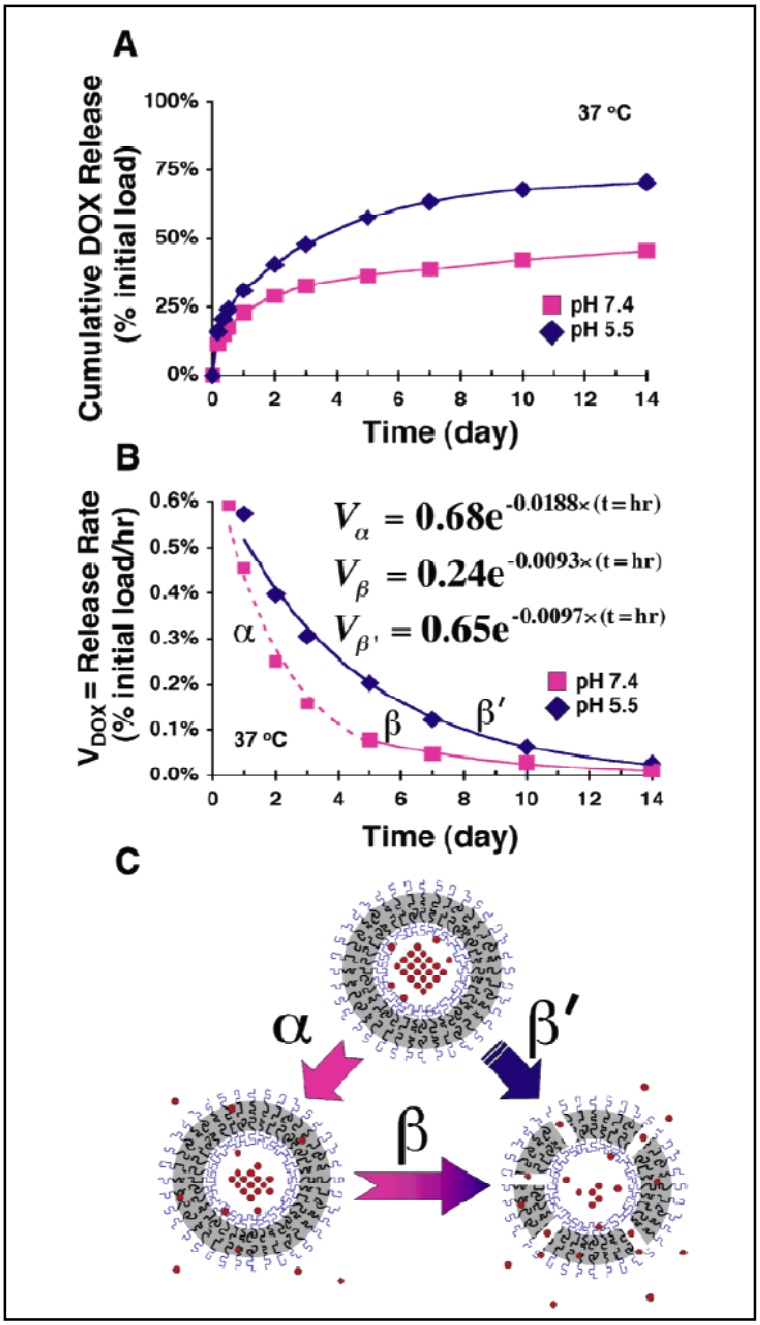

Figure 2.6- *in situ* release of doxorubicin from PEO-b-PCL polymersomes
(A) Cumulative *in situ* release of doxorubicin, loaded within 200 nm diameter PEO(2K)-*b*-PCL(12K)-based polymersomes, under various physiological conditions (pH 5 and 7.4; *T* = 37 °C) as measured fluorometrically over 14 days. *N* = 4 samples at each data point; individual data points for each sample varied by less than 10% of the value displayed at each time interval. (B) Release rates of DOX (V_{dox}) from 200 nm diameter PEO(2K)-*b*-PCL(12K)-based polymersomes vs time. Dotted and solid lines represent exponential fits obtained by regression analysis R^2 = 0.99 for

each curve), and the displayed equations correspond to the respective release regimes (α, β, β',). (C) Schematic illustrating differing regimes of DOX release via (α) intrinsic drug permeation through intact vesicle membranes vs (β, β′) release predominantly by PCL matrix degradation.

2.4.2 Loading and Release of Doxorubicin into PEO-b-PmCL Vesicles

To determine whether the addition of a methyl group on the γ-carbon of the caprolactone back bone alters the loading or release rate of doxorubicin from the vesicle interior, Doxorubicin was actively encapsulated into the aqueous compartment of 200nm PEO-b-PmCL vesicles (Figure 2.1) though an ammonium sulfate and pH gradient [77, 79, 81] (See Section 2.3.2). Figure 2.7A demonstrates that an increase in DOX fluorescence occurs post vesicle destruction with Triton X-100; as explained above, releasing the DOX from the vesicle core results in an increase in DOX fluorescence. Figure 2.7B-D are cryo-TEM images of DOX loaded PEO-b-PmCL vesicles; the areas in the center of the vesicle are due to the DOX-SO_4^{-2} gel-like precipitate, and further demonstrate encapsulation of DOX into the aqueous core; however, loading into each vesicle appears variable and it appears that some vesicles may have loaded more or less DOX than other vesicles.

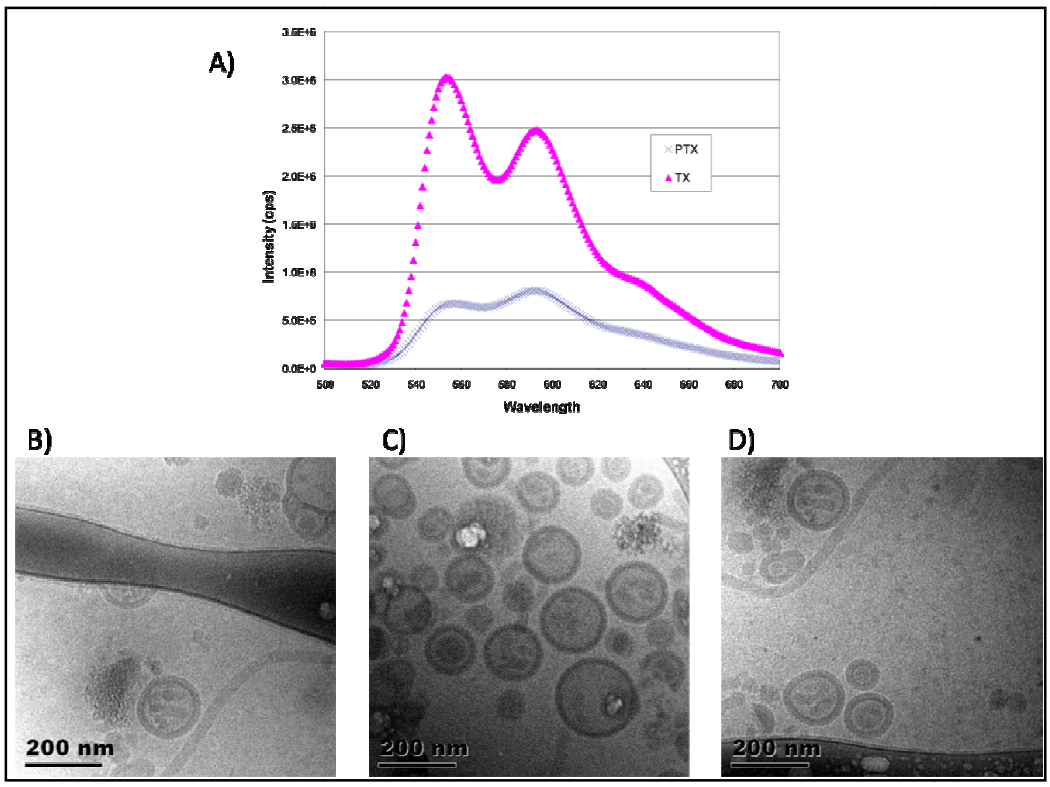

Figure 2.7- Doxorubicin loading in PEO-b-PmCL vesicles
A) Doxorubicin Fluorescence pre (PTX) and post (TX) treatment with Triton X-100. The increase in fluorescence upon vesicle rupture due to Triton X-100 confirms the loading of doxorubicin into the aqueous core of the vesicles. B-D) CyroTEM images of DOX loaded PEO-b-PmCL vesicles where the DOX aggregates, circular and rod-like in form, appear as dark areas in the aqueous core.

In contrast to PEO-b-PCL vesicles, samples were dialyzed into unbuffered iso-osmotic Sodium Chloride (NaCl) solution (pH~5.5, osmolarity~290mOsM). While dialysis into sodium acetate buffer at pH 5.5 yielded stable DOX loading for PEO-b-PCL vesicles (Figure 2.3), dialysis in this buffer did not yield stable loading (as determined via fluorescence measurements) for PEO-b-PmCL vesicles (Figure 2.8). The pH of the spent acetate buffer, when loading PEO-b-PCL vesicles showed an increased in pH from acidic conditions (starting) to basic conditions after dialysis, demonstrating the efflux of ammonia and the establishment of an H^+ gradient (Figure 2.2). This was not observed for

the loading of DOX in PEO-b-PmCL vesicles, where the pH of the spent dialysis solutions remained acidic. It was surmised that the methyl group in the PmCL block may have increased the hydrophobicity of the block in comparison to PCL, hindering the ammonia from crossing the bilayer and establishing the pH gradient. As such, dialysis in various buffered and unbuffered solutions was attempted, and it was determined that stable fluorescence counts (correlating to stable loading) were obtained for loading when acidified NaCl was used as the dialysis media (Figure 2.8). Furthermore, when examined, the pH of the spent acidified NaCl also increased from acidic to basic conditions, suggesting that NH_3 crossed the vesicle membrane and established a pH gradient across the PmCL membrane.

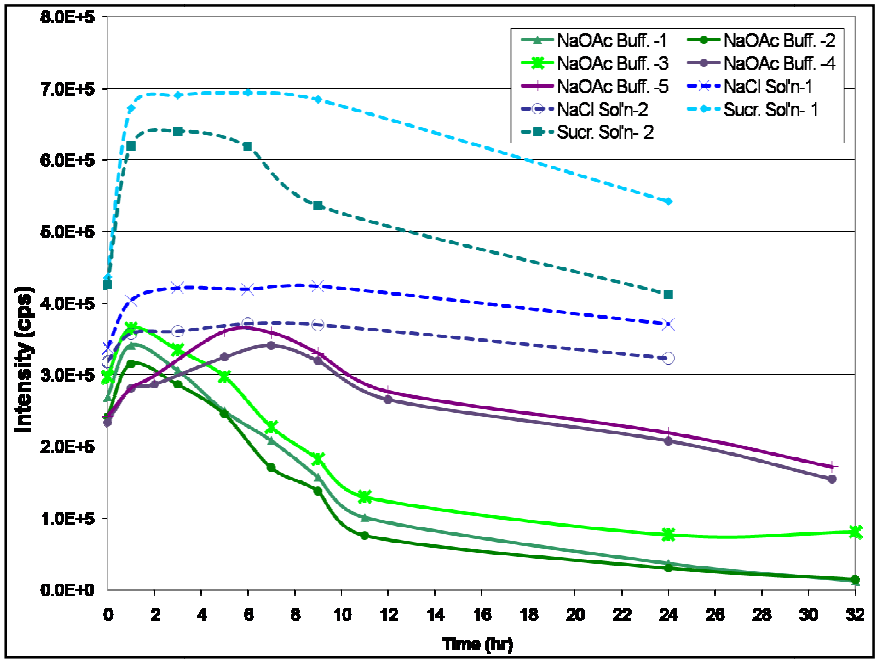

Figure 2.8- Doxorubicin fluorescence over time while loading into PEO-b-PmCL vesicles after dialysis in various iso-osmotic buffered and unbuffered solutions.

-

C. Note the fluorescence remains relatively stable after three hours of loading for either of the samples dialyzed in sodium chloride solution. NaOAc

Buff.=Sodium Acetate/Sodium Chloride Buffered Solution at pH 5.5 (samples 1-3, not stirred while loading, samples 4- 5- stirred while loading); NaCl Sol'n=Sodium Chloride Solution, pH 5.5 (unbuffered); Sucr. Sol'n=Sucrose Solution, pH 5.5 (unbuffered)

in situ release studies were conducted at various physiological conditions (pH 5.5 and pH 7.4,@T=37□C) where doxorubicin release was monitored fluorometrically as described above (λ_{ex}=480nm, λ_{em}=590nm) over 14 days. Cumulative release and release rate were calculated according to equations Equation 2.1and Equation 2.2, respectively. Similar to release from PEO-b-PCL, we observed an initial burst phase release where over 50% of the total amount of drug released was released during the first 12 hours. This correlates well with the release rate where the initial release rate during the burst phase is significantly higher than the release rate during the subsequent days. The dip observed in the cumulative release of the drug in the pH 7.4 buffer could be the result of drug degradation in pH 7.4 buffer at 37□C or the drug "reloading" in the vesicles post release to establish an equilibrium across the non-hydrolyzed vesicle membrane. As is evident from the cyro-TEM images in Figure 2.7, not all vesicles are loaded with the same amount of DOX and hence some of the DOX may be redistributed upon release. In both the pH 5.5 and the pH 7.4 buffers, the percent cumulative release of drug from the vesicles is significantly less than observed for the PEO-b-PmCL vesicles (Figure 2.6).

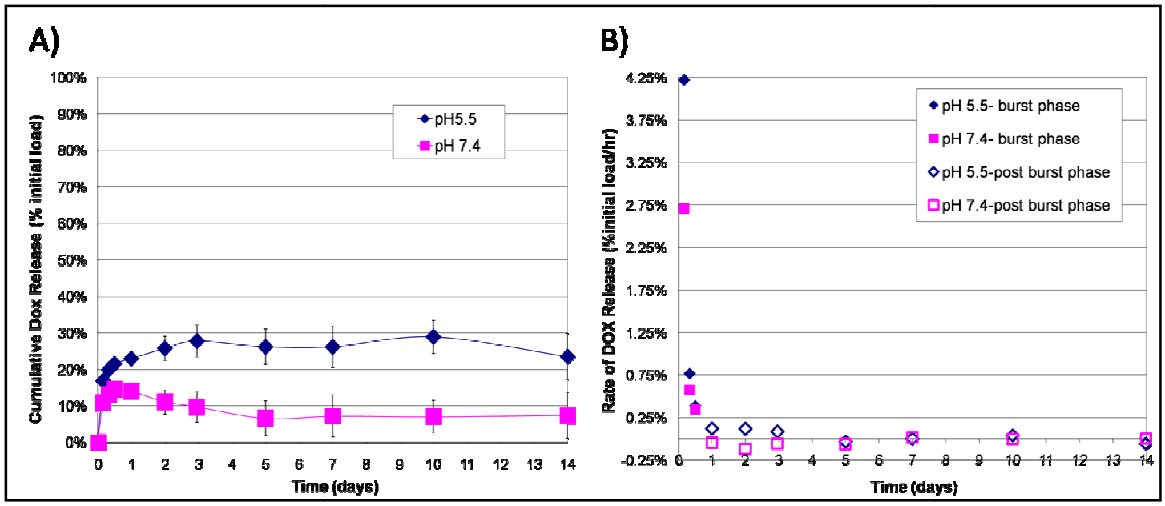

Figure 2.9- *in situ* release of doxorubicin from PEO-b-PmCL polymersomes A) Doxorubicin Cumulative Release and B) Release Rate from PEO-b-PmCL vesicles at physiological pH's

2.4.3 Loading and Release of Doxorubicin in PEO-b-PBD Polymersomes

To examine the release of Doxorubicin from biocompatible but non-biodegradable vesicles, DOX was loaded actively into PEO-b-PBD vesicles through a gradient. Similar to DOX loading in PEO-b-PmCL vesicles, various dialysis media were tested, and it was determined that the optimal dialysis solution which leads to a stable fluorescence within 7-9 hours was iso-osmotic acidified NaCl (pH 5.5). Successful loading was confirmed by cryo-TEM microscopy and bursting of the vesicles using Triton X-100 and heat.

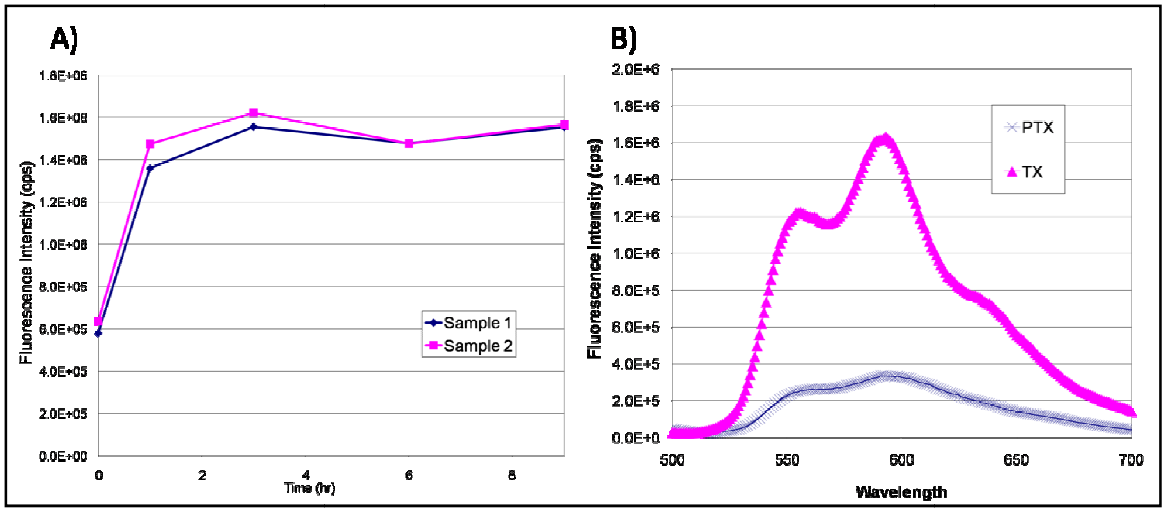

Figure 2.10- Doxorubicin loading into PEO-b-PBD polymersomes
A)Loading of doxorubicin into PEO-b-PBD vesicles over time and B) the confirmation of doxorubicin loading in PEO-b-PBD vesicles.

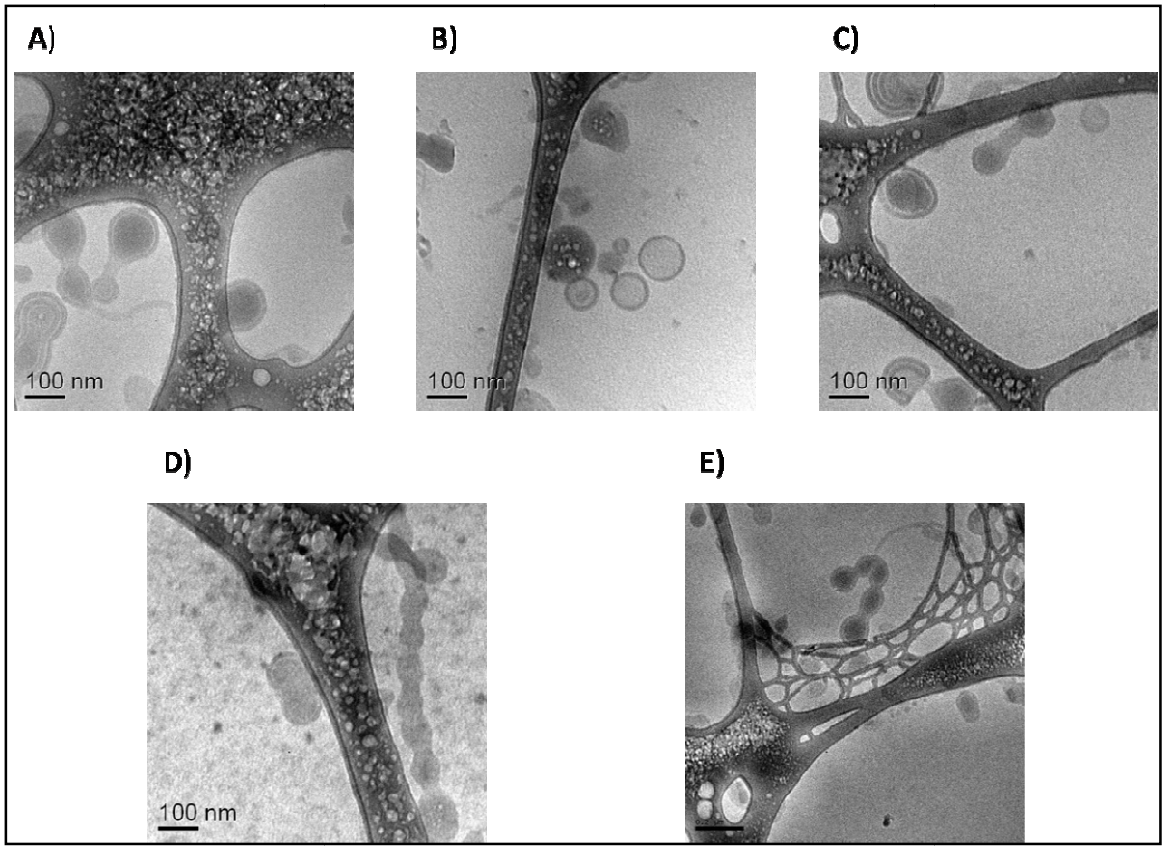

Figure 2.11- Cryo-TEM Images of DOX loaded PEO-b-PBD vesicles
A) Budding vesicles are observed, B) Not all vesicles are loaded with DOX, C) Fully loaded DOX vesicle with not much space between the DOX aggregate and the vesicle wall, D-E) Pearlized structures resulting from DOX loading.

From Figure 2.11 it is evident that not every vesicle has DOX encapsulated within it; furthermore, at times there is very little (if any) separation between the DOX aggregate and the bilayered membrane. Additionally, some of the vesicles have a cause of the appearance of "stringed vesicles" but they are prevalent in the images.

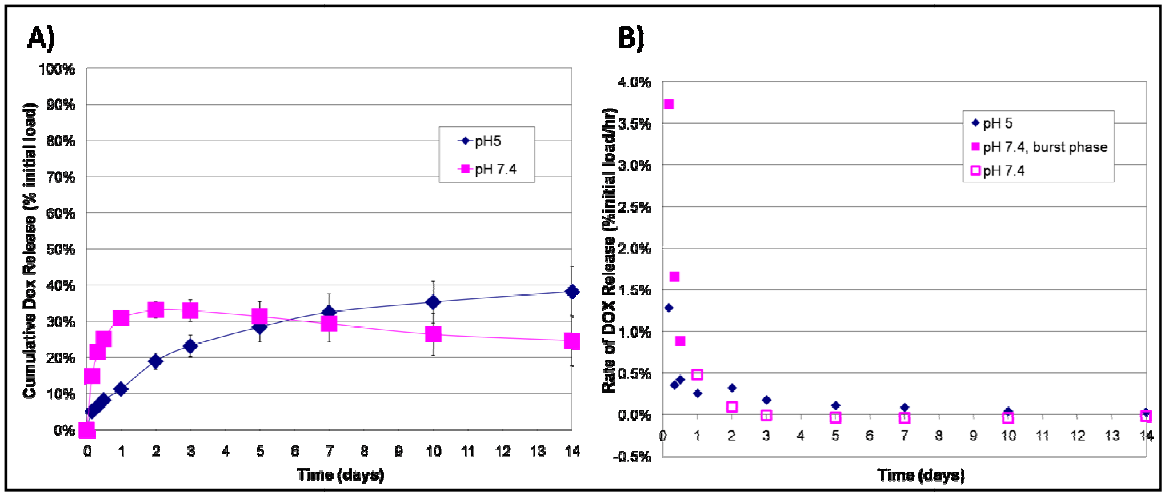

Figure 2.12- *in situ* release of DOX from PEO-b-PBD vesicles
A) Cumulative DOX release and B) DOX Release Rate from PEO-b-PBD vesicles at pH 5 and pH 7.4

In situ DOX release studies were carried out fluorometrically for DOX loaded PEO-b-PBD vesicles in physiologically simulated conditions. Vesicles in pH 7.4 undergo a burst phase release where over 20% of the total DOX is released within the first 12 to 24 hours (Figure 2.12A); this burst phase at pH 7.4 is further evidenced by the quick rate of DOX release over the first 24 hours (Figure 2.12B, closed boxes) which quickly tapers off over the subsequent 13 days (Figure 2.12B, open boxes). It is surmised that the drug released during this early time period is drug which was adhered to the PEO brush or localized to the membrane, but not locked into the core. Following the burst phase release, a more controlled release is observed. It is interesting to note that, as in the case of DOX loaded PEO-b-PmCL vesicles, the cumulate DOX release decreases at later time points; again, this may be the result of DOX degradation in the pH 7.4 solution as DOX is known to degrade more rapidly in non-acidic solutions [82, 83]. Since not every vesicle has DOX inside (Figure 2.11B-D) another possibility for the decrease in

cumulative DOX release at later times is that DOX is reentering unloaded vesicles (Figure 2.11) which are initially still intact at pH 7.4.

At a pH of 5.5, less than 10% of the drug is released from the PEO-b-PBD vesicles within the first 24 hours, and it appears that the vesicles do not go through the burst phase release, as evidenced by the slow and controlled cumulative release and slower release rate, Figure 2.12A and B, respectively. Release rates do not reach over 1.5% initial load/ hr even at early time points. Since it is unlikely that the PBD backbone is degraded over the 14 days, in both conditions, it is believed that the drug release at both pHs is due to permeation of DOX across the membrane and not vesicles destruction.

2.4.4 Release of Doxorubicin from Doxil ® (Doxorubicin liposomal formulation)

Doxorubicin loaded liposomes were obtained and diluted to yield a .0068mg/ml concentration of DOX in iso-osmotic pH 7.4 PBS buffer or iso-osmotic pH 5.5 Sodium Acetate Buffer.

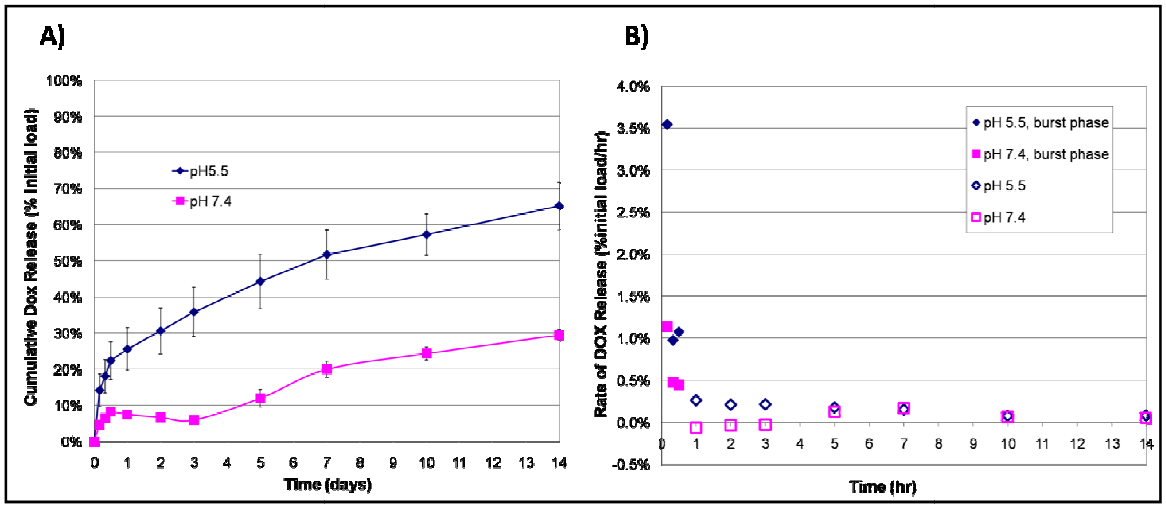

Figure 2.13-Release of Doxorubicin from the clinically administered liposomal formulation of doxorubicin

A)Cumulative doxorubicin release from liposomes (Doxil ®) and (B) Doxorubicin release rate from liposomes

Similar to the above release experiments, the release of DOX from lipid vesicles, (DOXIL ®) was measured fluorometrically. Cumulative release and release rate were calculated according to equations Equation 2.1and Equation 2.2, respectively. Release at both pH's demonstrates a characteristic burst phase over the first 12 hours followed by a more controlled release over the subsequent days. However, the burst release is more pronounced in the acid buffer as over 20% of the drug is released in the first 12 hours at a pH of 5.5, whereas in PBS buffer (pH 7.4) only 10% of the total is released over the first 12 hours (Figure 2.13A). The burst phase is further demonstrated by examining the release rate of the drug (%initial load/hr) which is greater than 1.0% initial load/hr for the first 12 hour for the pH 5.5 condition, but quickly decreases post burst phase release to less than 0.5% initial load/hr after the first day (B). At a pH of 7.4, it appears the DOX fluorescence decreases over days 1-3; this may be due to a redistribution of drug back into the vesicles, or the result of DOX degradation at pH 7.4 as discussed above; during these days, the rate of degradation or re distribution is greater than the rate of release. However, as the vesicles begin to breakdown due to hydrolysis of the lipid, the rate of release surpasses the rate of degradation and/or drug redistribution, and the cumulative release of drug slowly increases over the next 11 days (Figure 2.13A). The release rate correlates with this observed cumulative release, as initially the %initial load/hr is 0.5-1.0, but decreases after the burst phase to approximately 0.1% (Figure 2.13B).

2.4.5 Loading and Release of Doxorubicin into PEO-b-PCL-Ac Membrane Stabilized Vesicles

As mentioned, one of the benefits of polymersomes over liposomes is the unique ability to tune to degradation and release kinetics of the polymer backbone for enhanced control of drug delivery rates. To that end, we sought to stabilize the membrane structure and decrease the permeation of drug across the membrane prior to membrane hydrolysis by forming biodegradable membrane stabilized vesicles through the use of a acryl group on the terminal hydroxyl end of the PCL block, a photoiniator, and a light source. Once assembled into polymersomes and in the presence of a photoinitiator, UV light exposure induces a radical polymerization through the functional groups (Figure 2.14). This approach does not hinder hydrolysis of the PCL chain and yields oligo-caprolactone units, PEG, and kinetic chains of poly(acrylic acid) as the degradation products [84].

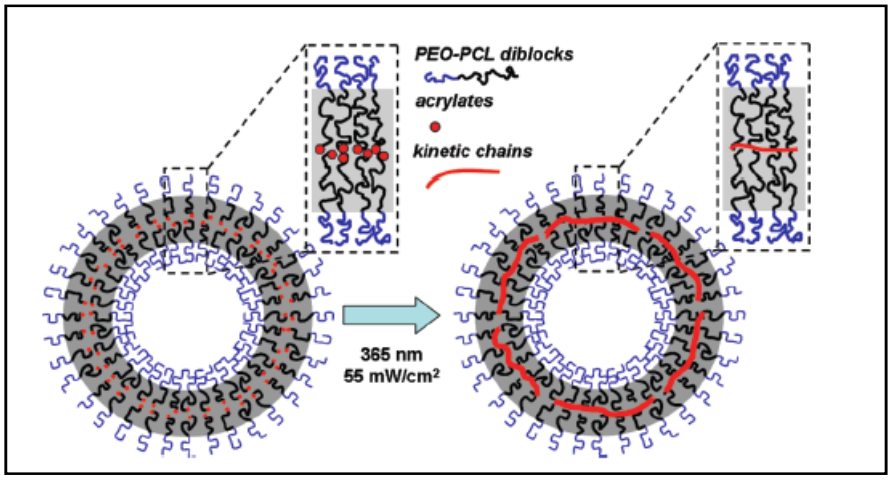

Figure 2.14- Schematic of Hydrophobic End Group Polymerization for Stabilization of Polymersome Membranes

Joshua S. Katz determined that only in the case where DMPA, the photoinitiator was loaded into the bilayer and the polymersomes were exposed to UV irradiation was

polymerization of the acrylate groups observed (i.e., disappearance of acrylate peaks in NMR spectra, Figure 2.15A). Additionally, significant peak broadening can be seen in the NMR spectrum of the UV exposed polymersomes containing DMPA, indicative of an increase in molecular weight that would be expected to accompany acrylate polymerization. UV light alone or simply the presence of DMPA were both insufficient to induce polymerization. Furthermore, the amount of DMPA necessary for complete conversion of the acrylate groups was also investigated (Figure 2.14, Figure 2.15B). A 1:1 mol/mol ratio of DMPA to polymer was necessary for complete conversion of acrylates.

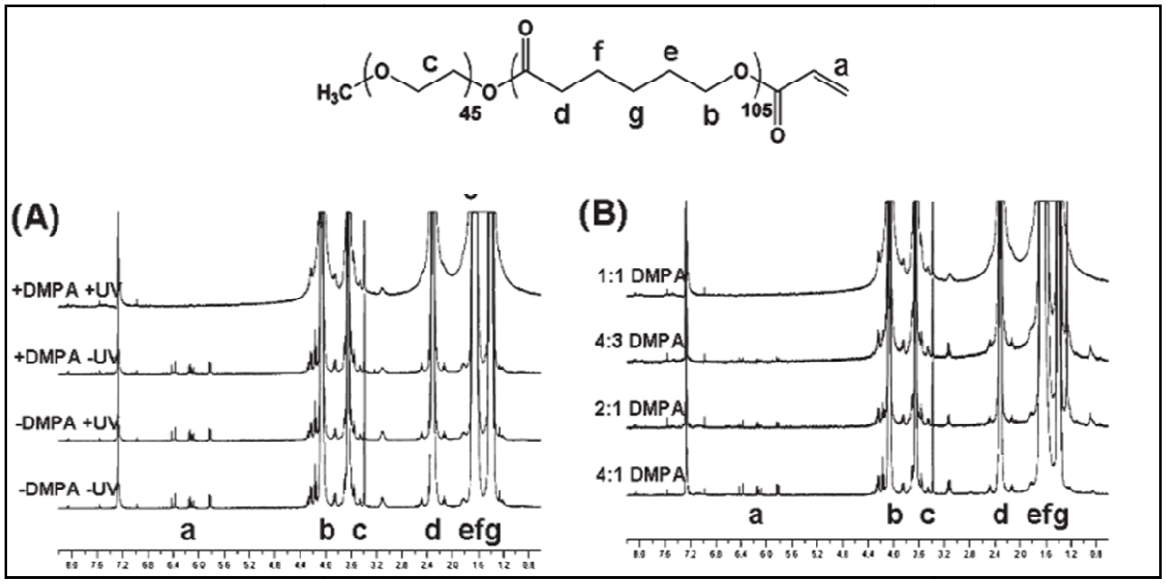

Figure 2.15- (A) NMR spectra of dehydrated polymersomes of AcPCL-b-PEG with or without DMPA loaded into the membrane before and after UV light exposure as indicated. The -DMPA+UV sample received a 30min dose of UVlight, while the +DMPA+UV sample received a 5 min dose. (B) NMR spectra of AcPCL-b-PEG polymersomes with varying amounts of DMPA loaded into the membrane (reported as molar ratio of polymer:DMPA). All samples received a 10 min dose of UV light. Lowercase letters indicate assignment of peaks to the chemical structure shown.

To demonstrate membrane stabilization as a method of controlling the release of drug from the polymersome, doxorubicin was encapsulated in PEO-b-PCL-Ac polymersomes loaded with DMPA in the membrane and the release was monitored via fluorescence dequenching of the drug as discussed in Section 2.3 EXPERIMENTAL METHODS. We compared formulations with and without 15 min exposure to UV light (Figure 2.16A). As mentioned, as DOX releases from the polymersome and is diluted into the surrounding solution, its fluorescence increases over a baseline level [85], enabling tracking of the release from the polymersomes. Results are normalized to the initial amount of DOX encapsulated (determined by membrane disruption through Triton exposure to an additional sample for each group) less the baseline fluorescence. Formulations were also highly stable, exhibiting negligible release (<1%) when stored at 4□C over the same period of time. The characteristic initial burst phase release, seen with PEO-b-PCL vesicles, was seen for both stabilized and non-stabilized polymersomes; however, the amount of drug released was slightly more when encapsulated in the non-stabilized polymersomes. The drug molecules released during this burst phase are likely from the DOX that partitioned into the membrane prior to stabilization (DOX is amphiphilic). However, following the burst phase release, the rate of release was much slower for stabilized polymersomes compared to the non-stabilized polymersomes (Figure 2.16B). By 7 days, only an additional ~5% more of the drug from that released during the burst phase was observed to be released for the stabilized vesicles, compared to the additional ~25% more being released for the non-stabilized samples, similar to what was observed with PEO-b-PCL vesicles in Section 2.4.1. Due to degradation of

DOX in aqueous solutions [82, 83], exact release profiles cannot be determined by this method. However, from the two observed profiles (Figure 2.16), it is evident that drug release is significantly retarded by stabilization of the membrane.

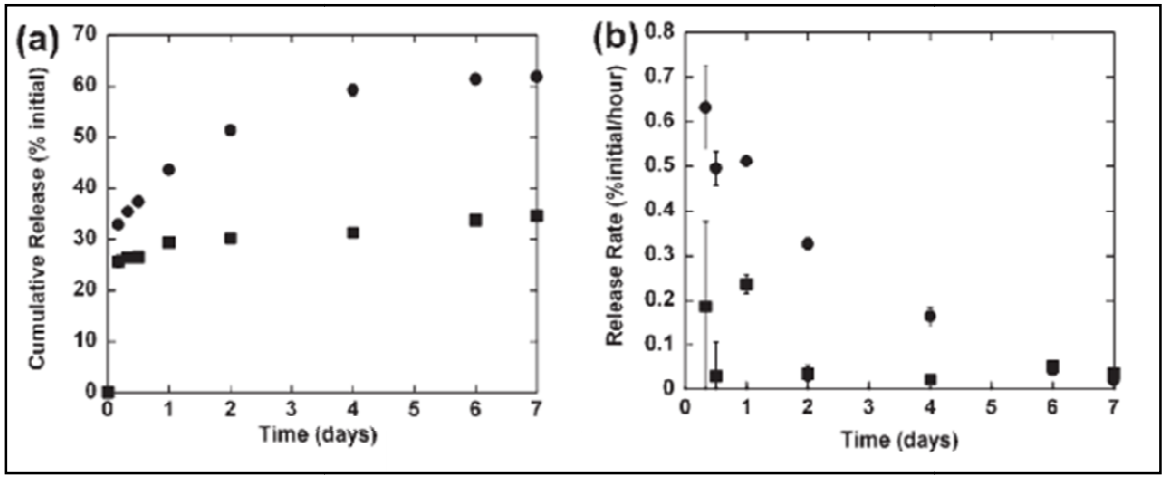

Figure 2.16- Doxorubicin Release from PEO-b-PCL-Ac vesicles
(a) Percent cumulative released and (b) release rates of DOX encapsulated in PEO-b-PCL-Ac polymersomes with 1:1 DMPA either without exposure (circles) or with exposure to 15 min UV light (squares). The amount released was normalized to the initial amount encapsulated and is reported as means (n=3) and standard deviations.

2.4.6 Incorporation of Combretastatin into PEO-b-PCL Vesicles

Combretastatin, an anti-angiogenesis drug, was incorporated into the hydrophobic membrane of the PEO-b-PCL vesicles by dissolving it as well as the polymer in methylene chloride prior to thin-film hydration and vesicle formation. A relatively monodispersed vesicle population of approximately 200nm drug incorporated vesicles was obtained post vesicle formation and extrusion as determined by DLS. Incorporation of combretastatin was determined by spectroscopy; absorbance spectra were obtained and compared for vesicles with and without drug as well as free drug Figure 2.17. These spectra demonstrate that the combretastatin was incorporated into the vesicles as a peak

at approximately 345nm was observed for vesicles containing combretastatin, but not for drug free vesicles. The red shift in the combretastatin spectra for combretastatin vesicles in comparison to spectra of free combretastatin in ACN is probably due to the altered environment inside the vesicle membrane.

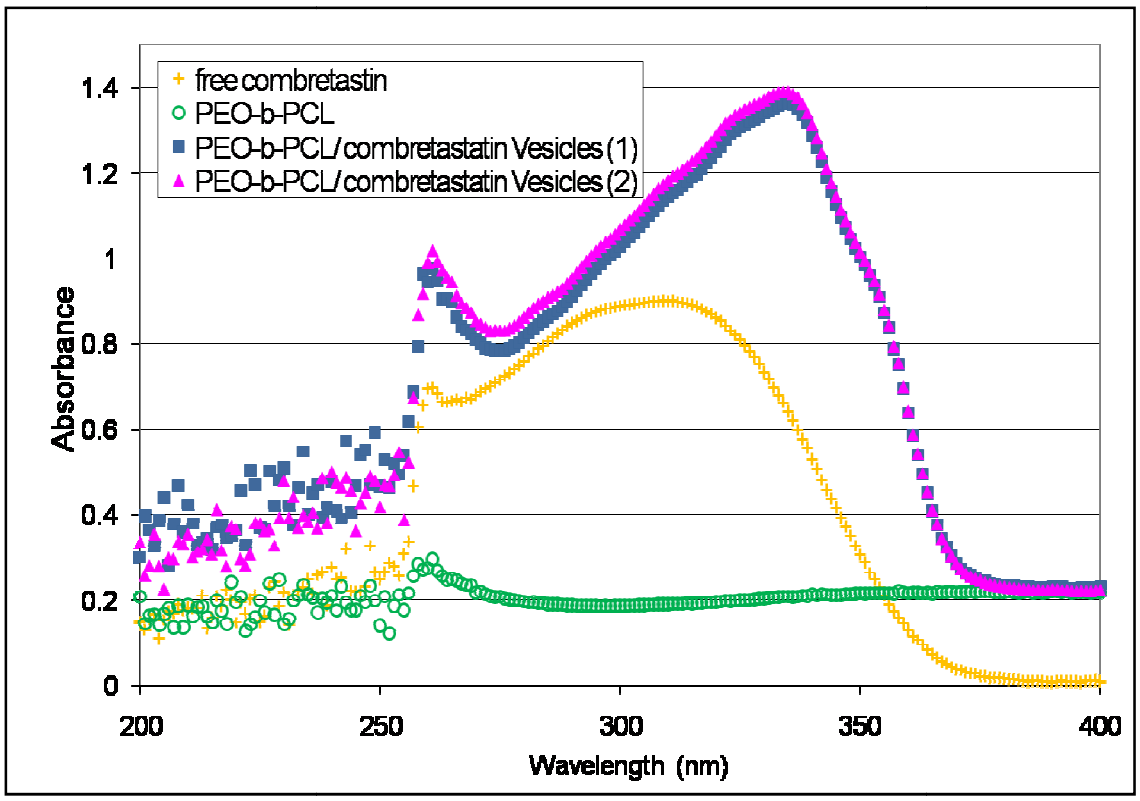

Figure 2.17- Absorbance spectra of 1) combretastatin incorporated PEO-b-PCL vesicles (closed triangle, closed square), 2)PEO-b-PCL vesicles (circles), and 3) free combretastatin in ACN (plus sign).

2.4.7 Dual Drug Vesicles: The Incorporation of Combretastatin and Loading of Doxorubicin in PEO-b-PCL Vesicles

As described, dual drug loaded polymersomes were generated by forming a thin film of combretastatin and PEO-b-PCL and hydrating to form vesicles. Post vesicle formation, vesicles were dialyzed to establish an ammonium sulfate gradient and subsequently loaded with doxorubicin. Doxorubicin loading was tracked

fluorometrically as described in sections 2.3.1and 2.4.1. Figure 2.18A shows fluorescence changes over time while loading DOX into combretastatin incorporated vesicles. Again, fluorescence intensity stabilizes after the first three hours and remains constant over the entire loading study. In order to demonstrate both the incorporation of combretastatin and the encapsulation of doxorubicin, absorbance spectra of the vesicles were obtained. In Figure 2.19, the peaks for both DOX (~480nm) and combretastatin (~280nm) are clearly visible demonstrating the incorporation of both drugs into one vesicle. Figure 2.18B clears shows an increase in fluorescence post treatment of Triton X-100 and heat demonstrating release of doxorubicin into the external solution from its initially quenched state inside vesicle aqueous core.

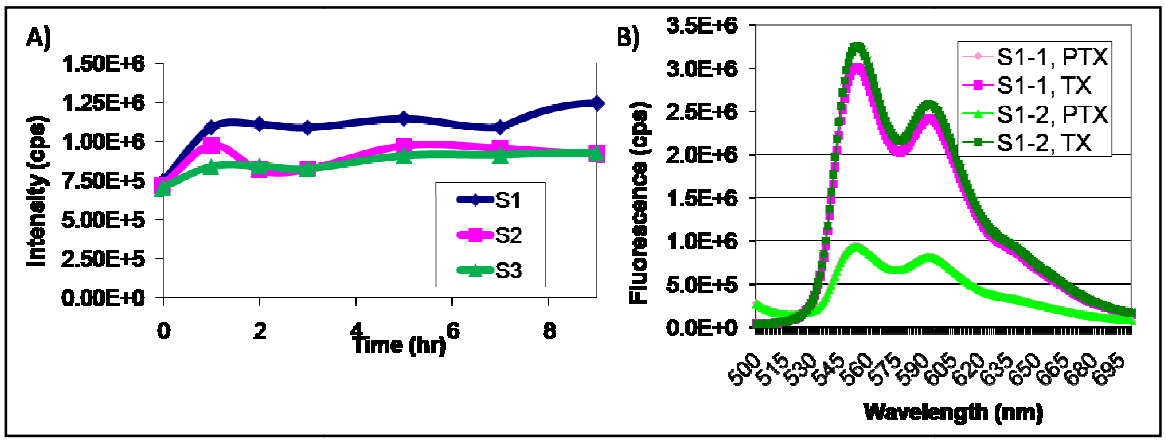

Figure 2.18- Doxorubicin loading in Combretastatin vesicles
A) Fluorescence intensity while loading over time B) Bursting of Sample 1 of DOX loaded combretastatin vesicles; S1= Sample 1, etc.; PTX- prior to treatment with Triton X; TX- after treatment with Triton X

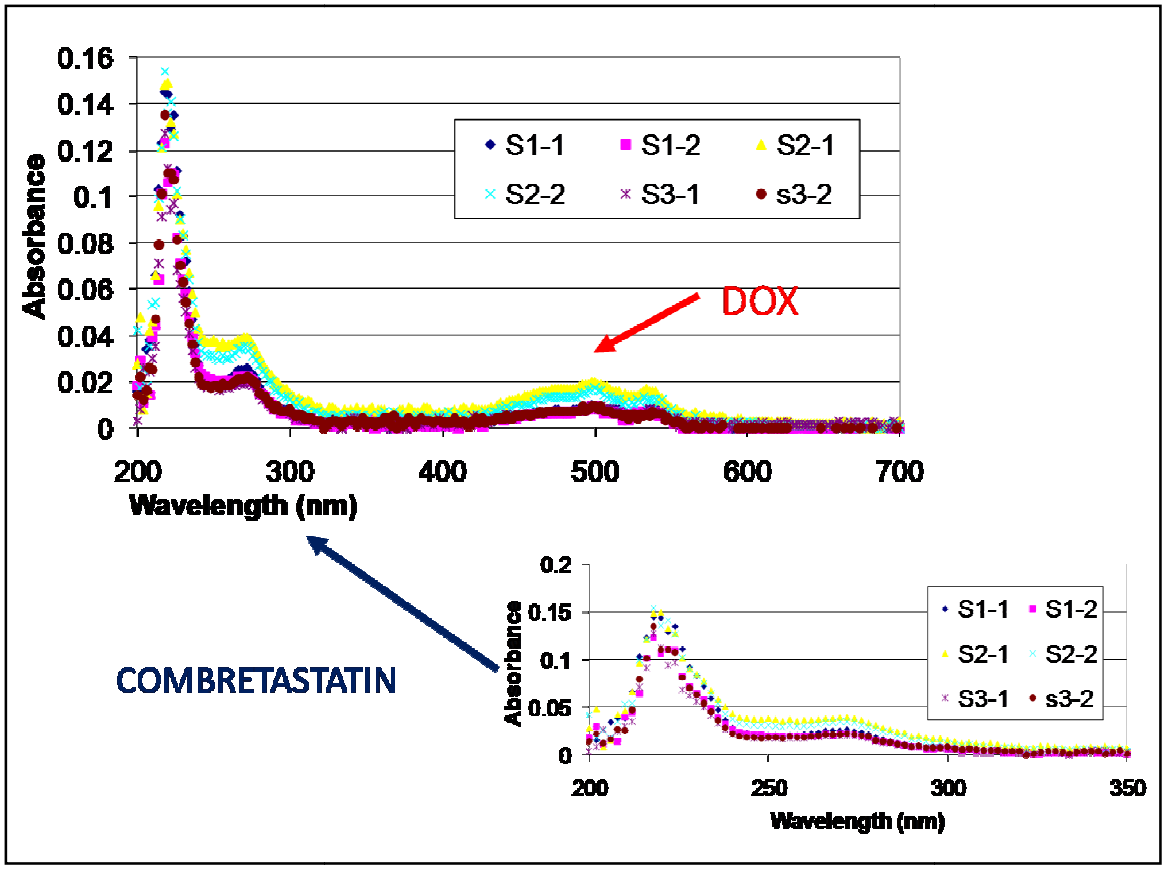

Figure 2.19- Absorbance Spectra of DOX loaded combretastatin incorporated polymeric vesicles.
The top image shows the entire spectra with peaks for both DOX and combretastatin, while the bottom image shows the spectra for combretastatin alone. S1= sample 1, etc.; -1 is the first part of the sample, etc.

2.5 CONCLUSIONS

This study highlights the enormous potential of polymersomes as vehicles for both single drug and combination drug cancer therapy. Doxorubicin, an amphipathic anti-neoplastic agent, was loaded into the aqueous core of both biocompatible (PEO-b-PBD) and bioresorbable (PEO-b-PCL and PEO-b-PmCL) nano-polymersomes and the release was characterized in physiologically relevant buffers. Furthermore, doxorubicin was loaded into the aqueous core of fully biodegradable stabilized polymersomes, and a

decreased release rate was observed in comparison to non-stabilized vesicles. This reduced release rate is beneficial for high local delivery of chemotherapeutics over an extended period.

Combretastatin, a VDA which binds tubulin and leads to vascular disruption in tumors, was incorporated into the hydrophobic bilayer of PEO-b-PCL vesicles with and without doxorubicin. Because of the enhanced permeation and retention (EPR) effect, discussed in Chapter 1, vesicles naturally accumulate at the tumor site to do the leaky and abnormal vasculature. Hence, vesicles loaded with combretastatin traffic to the tumor site, even without targeting moieties, thereby further assisting with the elimination of endothelial cells lining the tumor vasculature.

The ability to load both chemotherapeutics and vascular disrupting agents from bioresorbable vesicles in a controlled fashion suggests that these vesicles may be useful for clinical applications.

2.6 ACKNOWLEDGEMENTS

This work was supported by grants from the National Institutes of Health (EB003457-01 and CA115229), the National Cancer Institute (R33-NO1-CO-29008), Commonwealth Funds, Pennsylvania and Abramson Cancer Center, University of Pennsylvania, and infrastructural support was provided by a grant from the MRSEC Program of the National Science Foundation (DMR05-20020 and DMR-00-79909). A portion of the work discussed in this chapter was performed in the University of Minnesota I.T. Characterization Facility, which receives partial support from the NSF through the NNIN program.

2.7 REFERENCES

1. Bermudez, H., et al., *Molecular weight dependence of polymersome membrane structure, elasticity, and stability.* Macromolecules, 2002. **35**(21): p. 8203-8208.
2. Lee, J.C.M., et al., *Preparation, stability, and in vitro performance of vesicles made with diblock copolymers.* Biotechnology and Bioengineering, 2001. **73**(2): p. 135-145.
3. Meng, F., G.H.M. Engbers, and J. Feijen, *Biodegradable polymersomes as a basis for artificial cells: encapsulation, release and targeting.* Journal of Controlled Release, 2005. **101**(1-3): p. 187-198.
4. Photos, P.J., et al., *Polymer vesicles in vivo: correlations with PEG molecular weight.* Journal of Controlled Release, 2003. **90**(3): p. 323-334.
5. Discher, D.E. and A. Eisenberg, *Polymer vesicles.* Science, 2002. **297**(5583): p. 967-973.
6. Ghoroghchian, P.P., et al., *Bioresorbable vesicles formed through spontaneous self-assembly of amphiphilic poly(ethylene oxide)-block-polycaprolactone.* Macromolecules, 2006. **39**(5): p. 1673-1675.
7. Ahmed, F. and D.E. Discher, *Self-porating polymersomes of PEG-PLA and PEG-PCL: hydrolysis-triggered controlled release vesicles.* Journal of Controlled Release, 2004. **96**(1): p. 37-53.
8. Bei, J.Z., et al., *Polycaprolactone-poly(ethylene-glycol) block copolymer .4. Biodegradation behavior in vitro and in vivo.* Polymers for Advanced Technologies, 1997. **8**(11): p. 693-696.
9. Ahmed, F., et al., *Block copolymer assemblies with cross-link stabilization: From single-component monolayers to bilayer blends with PEO-PLA.* Langmuir, 2003. **19**(16): p. 6505-6511.
10. Discher, B.M., et al., *Cross-linked polymersome membranes: Vesicles with broadly adjustable properties.* Journal of Physical Chemistry B, 2002. **106**(11): p. 2848-2854.
11. Dudia, A., et al., *Biofunctionalized lipid-polymer hybrid nanocontainers with controlled permeability.* Nano Letters, 2008. **8**(4): p. 1105-1110.
12. Jofre, A., et al., *Amphiphilic block copolymer nanotubes and vesicles stabilized by photopolymerization.* Journal of Physical Chemistry B, 2007. **111**(19): p. 5162-5166.
13. Lee, S.M., et al., *Polymer-caged lipsomes: A pH-Responsive delivery system with high stability.* Journal of the American Chemical Society, 2007. **129**(49): p. 15096-+.
14. Li, F., et al., *Stabilization of polymersome vesicles by an interpenetrating polymer network.* Macromolecules, 2007. **40**(2): p. 329-333.
15. Berezov, A., et al., *Disabling ErbB receptors with rationally designed exocyclic mimetics of antibodies: Structure-function analysis.* Journal of Medicinal Chemistry, 2001. **44**(16): p. 2565-2574.
16. Carter, S.K., *ADRIAMYCIN (NSC-123127) - THOUGHTS FOR FUTURE.* Cancer Chemotherapy Reports Part 3 Program Information-Supplement, 1975. **6**(2): p. 389-397.

17. Young, R.C., R.F. Ozols, and C.E. Myers, *THE ANTHRACYCLINE ANTI-NEOPLASTIC DRUGS.* New England Journal of Medicine, 1981. **305**(3): p. 139-153.
18. Barenholz, Y., et al., *STABILITY OF LIPOSOMAL DOXORUBICIN FORMULATIONS - PROBLEMS AND PROSPECTS.* Medicinal Research Reviews, 1993. **13**(4): p. 449-491.
19. Gabizon, A.A., *SELECTIVE TUMOR-LOCALIZATION AND IMPROVED THERAPEUTIC INDEX OF ANTHRACYCLINES ENCAPSULATED IN LONG-CIRCULATING LIPOSOMES.* Cancer Research, 1992. **52**(4): p. 891-896.
20. Waterhouse, D.N., et al., Drug Safety, 2001. **24**: p. 903-920.
21. Choucair, A., P.L. Soo, and A. Eisenberg, *Active loading and tunable release of doxorubicin from block copolymer vesicles.* Langmuir, 2005. **21**(20): p. 9308-9313.
22. Kerbel, R.S. and B.A. Kamen, *The anti-angiogenic basis of metronomic chemotherapy.* Nature Rev. Cancer, 2004. **4**: p. 423-436.
23. Weinberg, r.A., *The Biology of Cancer*. 2007: Garland Science, Taylor & Francis Group.
24. Tozer, G., C. Kanthou, and B. Baguley, *Disrupting Tumor Blood Vessels.* Nature Rev. Cancer, 2005. **5**: p. 423-435.
25. Okaji, Y., et al., *Vaccines targeting tumour angiogenesis - a novel strategy for cancer immunotherapy.* Ejso, 2006. **32**(4): p. 363-370.
26. Hanahan, D., G. Bergers, and E. Bergsland, *Less is more, regularly: metronomic dosing of cytotoxic drugs can target tumor angiogenesis in mice.* The Journal of Clinical Investigation, 2000. **105**: p. 1045-1047.
27. Sengupta, S., et al., *Temporal targeting of tumour cells and neovasculature with a nanoscale delivery system.* Nature, 2005. **436**(7050): p. 568-572.
28. Gaukroger, K., et al., *Novel syntheses of cis and trans isomers of combretastatin A-4.* Journal of Organic Chemistry, 2001. **66**(24): p. 8135-8138.
29. Ghoroghchian, P.P., et al., *Near-infrared-emissive polymersomes: Self-assembled soft matter for in vivo optical imaging.* Proceedings of the National Academy of Sciences of the United States of America, 2005. **102**(8): p. 2922-2927.
30. Haran, G., et al., *Transmembrane Ammonium-Sulfate Gradients in Liposomes Produce Efficient and Stable Entrapment of Amphipathic Weak Bases.* Biochimica Et Biophysica Acta, 1993. **1151**(2): p. 201-215.
31. Lopes de Menezes, D.E., Pilarski, L.M., Allen, T.M., , Cancer Research, 1998. **58**: p. 3320-3330.
32. Bolotin, E.M., et al., *Ammonium Sulfate Gradients for Efficient and Stable Remote Loading of Amphiphathic Weak Bases into Liposomes and Ligandoliposomes.* Journal of Liposome Research, 1994. **4**(1): p. 455-479.
33. Abraham, S.A., et al., *The liposomal formulation of doxorubicin,* in *Liposomes, Pt E*. 2005. p. 71-97.
34. de Menezes, D.E.L., L.M. Pilarski, and T.M. Allen, *In vitro and in vivo targeting of immunoliposomal doxorubicin to human B-cell lymphoma.* Cancer Research, 1998. **58**(15): p. 3320-3330.

35. Beijnen, J.H., O. Vanderhouwen, and W.J.M. Underberg, *ASPECTS OF THE DEGRADATION KINETICS OF DOXORUBICIN IN AQUEOUS-SOLUTION.* International Journal of Pharmaceutics, 1986. **32**(2-3): p. 123-131.
36. Janssen, M.J.H., et al., *DOXORUBICIN DECOMPOSITION ON STORAGE - EFFECT OF PH, TYPE OF BUFFER AND LIPOSOME ENCAPSULATION.* International Journal of Pharmaceutics, 1985. **23**(1): p. 1-11.
37. Ifkovits, J.L. and J.A. Burdick, *Review: Photopolymerizable and degradable biomaterials for tissue engineering applications.* Tissue Engineering, 2007. **13**(10): p. 2369-2385.
38. Kwon, G.S., et al., *PHYSICAL ENTRAPMENT OF ADRIAMYCIN IN AB BLOCK-COPOLYMER MICELLES.* Pharmaceutical Research, 1995. **12**(2): p. 192-195.

Chapter 3

DENDROSOMES: SELF-ASSEMBLED VESICLES FOR DRUG DELIVERY

ADAPTED FROM

Virgil Percec, Daniela A. Wilson, Pawaret Leowanawat, Christopher Wilson, Andrew D. Hughes, Mark S. Kaucher, Daniel A. Hammer, **Dalia H. Levine**, Anthony J. Kim, Frank S. Bates, Kevin P. Davis, Timothy P. Lodge, Michael L. Klein, Russell DeVane, Emad Aqad, Brad M. Rosen, Andrea O. Argintaru, Monika J. Sienkowska, Kari Rissanen, Sami Nummelin, Jarmo Ropponen, *Nature*, Manuscript Submitted

3.1 SUMMARY

Biological membranes are complex molecular assemblies of phospholipids and stabilized by cholesterol, proteins and carbohydrates [86]. Liposomes, vesicles self-assembled from natural or synthetic phospholipid amphiphiles [87], can mimic biological membranes [88, 89], probe cell machinery[90], and be used to develop bio-inspired materials for medical applications [91, 92]. The design of synthetic lipid amphiphiles for vesicle self-assembly represents a formidable challenge since both natural and synthetic amphiphiles generated by traditional methods can produce unstable liposomes that require tedious separation and stabilization [91, 93-97].

Here we show that libraries of amphiphilic Janus-dendrimers self-assemble, by simple injection of their ethanol solution into water, into monodisperse and stable vesicles with excellent mechanical properties; these dendrimeric vesicles have been termed dendrosomes. In contrast to polymersomes, polymeric vesicles self-assembled from polydisperse block co-polymer amphiphiles[3, 4, 98, 99] with limited bioresorbability, stable and monodisperse dendrosomes exhibit, in addition to the classic spherical shape, the less encountered tubular[100], multilamellar vesicles[101], polygonal[102], cubosome[103] and other complex architectures such as disc-like, torroidal, rod-like, polygonal, spherical, ribbon-like and helical ribbon-like micelles[104].

Preliminary experiments demonstrate that dendrosomes are non-toxic to cells at short times, and many produce pH-sensitive membranes that deliver cancer drugs, such as doxorubicin, and incorporate pore forming proteins. Therefore, dendrosomes expand the precise and monodisperse primary structure of dendritic building blocks into new

functions[105-108]. Amphiphilic Janus-dendrimers self-assemble also in bulk and can be used to elucidate the mechanism of self-assembly of amhiphiles in the absence and presence of water[12]. We anticipate that dendrosomes will extend the capabilities of synthetic amphiphiles, generating responsive membranes with permeability controllable for desirable technological applications including novel pathways for targeted drug and gene delivery, *in vivo* imaging, and mediation of the efficiency of enzymes[109] and nucleic acids.

3.2 INTRODUCTION

The Perec Laboratory has designed twelve libraries containing 107 uncharged and positively charged amphiphilic Janus-dendrimers (Figure 3.1). These Janus-dendrimers were designed from natural AB3 and constitutional isomeric AB2 building blocks containing both hydrophilic and hydrophobic segments that can be rapidly combined to produce a large array of exact and monodispersed primary structures (Figure 3.1). These dendrimeric structures were synthesized by a combination of convergent, for the hydrophobic portion, and divergent or convergent methods for the hydrophilic portion. Two hydrophobic segments (one aliphatic and one mixed aliphatic-aromatic) and six hydrophilic segments (derived from oligoethylene oxide, dimethylolpropionic acid, glycerol, thioglycerol, *tert*-butylcarbamate and quaternary ammonium salts) were synthesized to generate the libraries of dendrimeric structures (Figure 3.1). This modular concept allowed the weight fraction of hydrophilic to hydrophobic blocks to be systematically varied.

The monodispersity of the dendrimers sets them apart from polymers and block copolymers which are polydisperse [3, 4, 98, 99]. Furthermore, while polymer chains have only limited scope for additional functionalization since they contain only two chain ends, the design of amphiphilic Janus-dendrimers, with their branched ends, allows a higher concentration and larger diversity of functionalities to be incorporated at both the hydrophilic and hydrophobic fragments of the molecule.

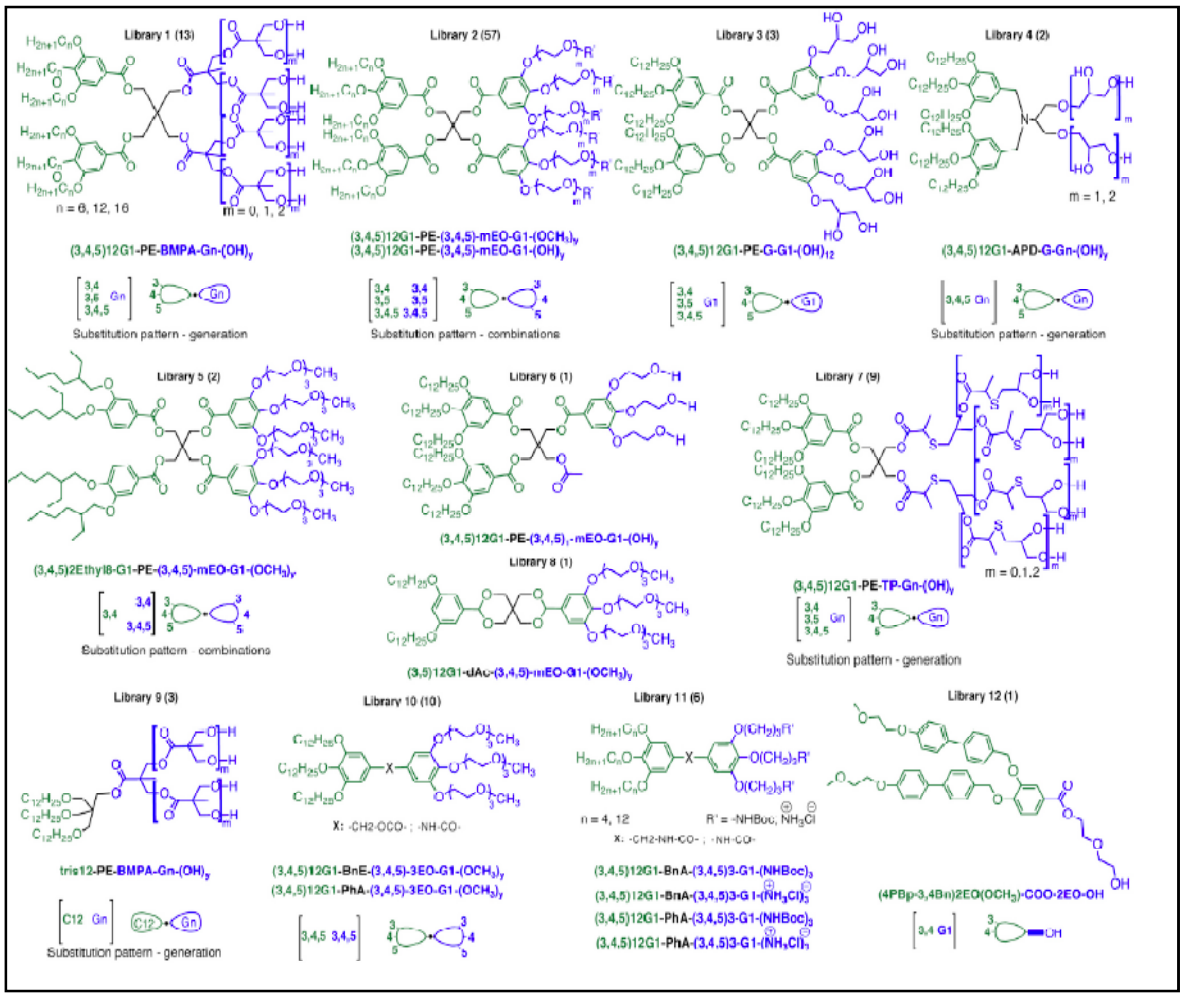

Figure 3.1- Library of Janus Dendrimers synthesized by the Perec Laboratory at the University of Pennsylvania

All amphiphilic Janus-dendrimers from Figure 3.1 self-assemble in both bulk and in aqueous based solutions to form regular structures (Figure 3.2 and Figure 3.3). Vesicle formation via injection of ethanol solutions of Janus-dendrimers into water (solvent injection method) was monitored by dynamic light scattering (DLS) as a function of concentration, temperature, and time. Formation of vesicles by injection of dendrimer in ethanol and in a variety of other protic and polar aprotic solutions into water was investigated as a function of temperature at a concentration of 0.5 mg/mL. Assemblies with sizes from 55 nm to 732 nm with polydispersity ranging from 0.021 to 0.530 were observed for the various concentrations, temperature, and time. These assemblies were stable in aqueous solutions up to at least 300 days from 25□C-80□C. Surprisingly most of the assemblies have low polydispersities of 0.021 to 0.200 via the solvent injection method alone (i.e. no further processing); in the field of self-assembled vesicles, these low values are considered monodisperse. For dendrimers from library 1, the size and polydispersity depend on concentration. For example, the dendrimer (3,5)12G1-PE-BMPA-G2$(OH)_8$ exhibited polydispersities ranging from 0.106 to 0.44 and Z-average sizes ranging from 84nm to 206 nm for concentrations ranging from 0.5 mg/mL to 4 mg/mL. In contrast, for dendrimers containing oligoethyleneoxide in the hydrophlic portion, polydispersity and size are minimally dependent on concentration.

Small assemblies fabricated by injection of ethanol solutions of the amphiphilic Janus-dendrimers into water were analyzed by cryo-TEM. 80 of these assemblies are unilamelar spherical dendrosomes and 55 have a polydispersity lower than 0.2 (Figure 3a). In addition, dendrosomes within dendrosomes [101, 110], polygonal [102] and tubular [100] dendrosomes, bicontinuous cubic particles (cubosomes [103]) and other

complex architectures such as disc-like, toroidal, rod-like, polygonal, spherical, ribbon-like and helical ribbon-like micelles[104] were also observed by the analysis of the 3-D intensity profiles of the optical micrographs and cryo-TEM images (Figures 2, 3). To our knowledge this is the first example of dendrocubosome obtained in a two-phase non-ionic surfactant system. The bilayer thickness of the dendrosomes was measured from cryo-TEM and found to range from 5 to 8 nm. Liposomes from phospholipids exhibit membrane thicknesses of 3 to 5 nm while the membrane thickness of polymersomes can be varied between 8 to 20 nm or even greater. The mechanical properties in combination with the measured thicknesses suggest that dendrosomes are excellent candidates for models of biological membranes.

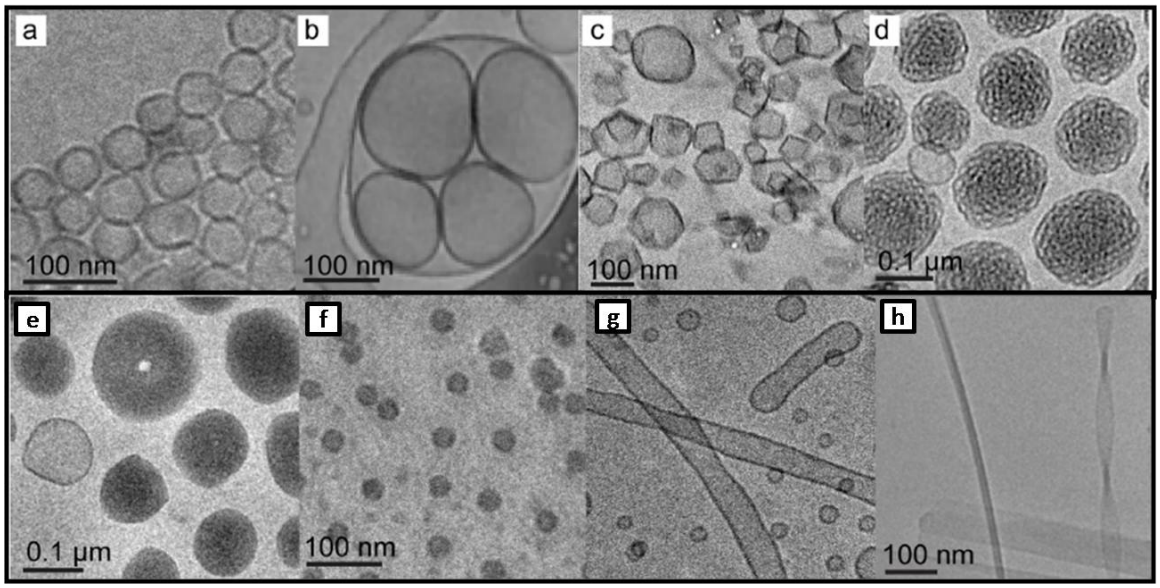

Figure 3.2- CryoTEM of dendritic assmeblies in aqueous solutions
(a) Monodisperse dendrosomes from (3,4)12G1-PE-(3,5)-3EO-G1-(OCH3)4 in ultrapure water (b) Dendrosomes contained inside a dendrosome bag from (3,4,5)12G1-PE- (3,4,5)-3EO-G-(OH)6 in PBS (c) Polygonal dendrosomes from (3,4)12G1-PE-(3,4)-3EO-G1-(OMe)4 (d) Bicontinuous cubic particles co-existing with low concentration of spherical dendrosomes from (3,5)12G1-PE-(3,4,5)-2EO-(OMe)6 (e) Disc-like micelles and toroids from (3,4,5)12G1-PE-(3,5)-3EO-(OMe)4 (f) Micelles from (3,4,5)12G1-PE-BMPA-G2-(OH)8 (g) Dendrosomes from (3,5)12G1-PE-(3,4,5)-3EO-(OMe)6 (h) Rod-like, ribbon and helical micelles from tris12-PE-BMPA-G2-(OH)8.

In addition to solvent injection method which yielded vesicles with little polydispersity, dendrosomes were also prepared by thin film hydration. In brief, hydration experiments were performed on films drop cast onto a roughened Teflon surface at a concentration of 2 mg dendrimer (in 200 μL solvent) per ~1 cm^2. Samples were dried under vacuum prior to hydration with 2 mL of ultra pure water or phosphate buffered saline at 50°C. This method was used to generate giant dendrosomes ranging in size from 2 to 50 μm in diameter, which were analyzed by either phase contrast or bright field microscopy. Visualization of both vesicle wall and cavity was carried out using fluorescence microscopy and a combination of hydrophobic (Nile Red) and hydrophilic

(Calcein) dyes. The hydrophobic dye was mixed with the Janus-dendrimer by adding 10 μM Nile Red to a solution of amphiphile in dichloromethane or diethyl ether. Films were prepared as described above and hydrated with 10 μM Calcein solution in saturated sucrose. Following hydration, Calcein containing dendrosomes were isolated from the free dye by repeated centrifugation washing cycles. Giant unilamellar dendrosomes were visualized by fluorescence microscopy where the hydrophobic dye was observed to concentrate exclusively in the wall whereas the hydrophilic dye was observed only in the aqueous interior (Figure 3.3).

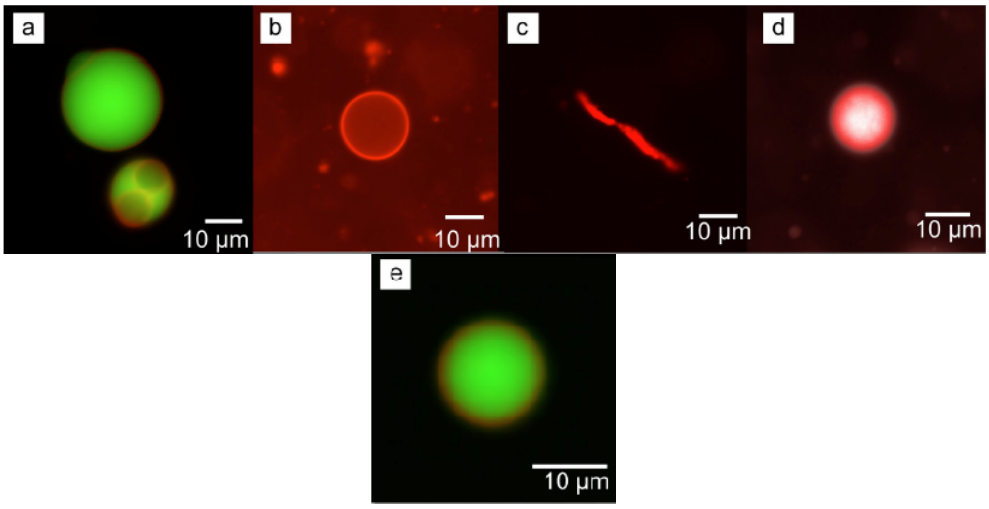

Figure 3.3- Optical Microscopy of giant dendrosomes
(a) Fluorescence microscopy image of dendrosome from (3,5)12G1-PE-(3,4)3EO-(OH)4 encapsulating both hydrophobic Nile Red and hydrophilic Calcein dyes (b)Dendrosome from (3,4)12G1-PE-BMPA-G2-(OH)8 visualized with Nile Red. (c) Worm-like micelle from (3,4,5)12G1-PE-BMPA-G2-(OH)8 encapsulating Nile Red (d) Spherical micelle from (3,4)12G1-PE-(3,4,5)3EO-(OH)6 encapsulating Nile Red. (e), Dendrosome from (3,4,5)12G1-PE-(3,4,5)3EO-G1-(OH)6 visualized with Nile Red and Calcein. Copyright (2009) Nature.

Micromanipulation experiments revealed that dendrosomes are more mechanically stable than liposomes, possessing higher areal expansion moduli, Ka than

phospholipids, yet displaying lipid-like critical areal strains (Figure 3.4). For example, dendrosomal materials 35-12-8 and 34-12-8 have area expansion moduli of approximately 950 mN/m, well in excess of the 781 mN/m measured for a 50% SOPC/50% cholesterol mixture [111].

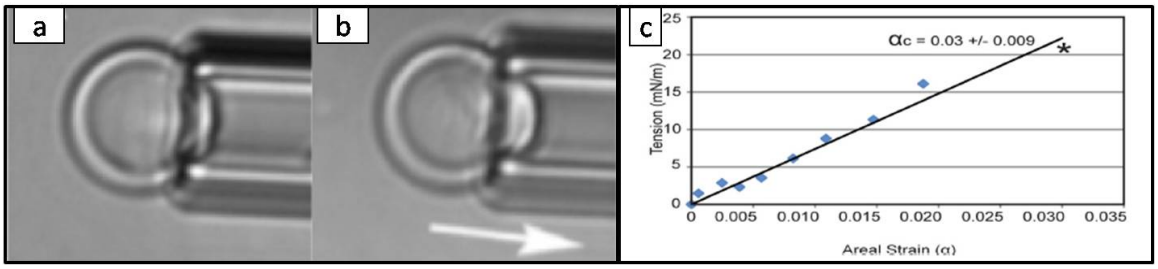

Figure 3.4-Micropipette aspiration experiments on dendrosomes
(a) Micropipette aspiration assessment of mechanical strength by micro deformation undernegative pressure of (3,5)12G1-PE-BMPA-G2(OH)$_8$. f, The same dendrosome under negative pressures howing small deformation of membrane. k, Areal strain ($\langle_c$) determined from micropipette aspiration upon rupture. Copyright (2009) Nature.

The stability of dendrosomes was investigated in biologically relevant media by formation of membranes via ethanol injection into both phosphate buffered saline and citrate buffer. Dendrosomes formed from compounds in library 1 showed poor stability in phosphate buffered saline. However, stability in citrate buffer was maintained over a period of two weeks. Dendrosomes formed from compounds from library 2 exhibited excellent stability in ultrapure water as well as in phosphate and citrate buffers. Selected dendrosomes were loaded with the anthracyclin drug, Doxorubicin, [92] used extensively in the treatment of Hodgkins lymphoma, stomach, lung and breast cancers. This drug shows activity as a DNA intercalator. As mentioned, one major limitation of Doxorubicin is cardiotoxicity at the therapeutic dosage. However, it is believed that cardiotoxicity is mitigated though encapsulation of the drug in nanoparticles;

encapsulated doxorubicin is commercially available in the liposomal preparation as Doxil [92, 96]. However, synthetic liposomal drug formulations suffer from higher leakage and reduced *in vivo* stability when compared to their natural counterparts.

Rapid growth and higher metabolic turnover exhibited by neoplastic cells result in both leaky vasculature and a lower than physiological pH (~5.2). As a consequence of the leaky vasculature and poor lymphatic drainage, nanoparticles, such as dendrosomes, tend to aggregate at tumor sites rather than healthy tissue; this is know as the EPR effect [24, 25]. As a consequence, dendrosomes tend to passively target tumor cells rather than healthy tissue. Janus-amphiphiles contain cleavable bonds which breakdown under acidic conditions and destabilize the vesicle structure. Without special design, NMR analysis showed that the cleavable bond in the Janus-dendrimer structure under identical pH conditions is the aromatic-aliphatic ester bond. Engineering the dendrosome with alternative pH-sensitive groups [92] is in progress in the Perec Laboratory. Selected Janus-dendrimers tagged with Texas Red dye were shown to co-assemble into fluorescent giant unilamelar liposomes with unlabelled Janus-dendrimers, block-copolymers and phospholipids which demonstrate the potential utility of tagged Janus-dendrimers, suggesting their use in theranotics (for detection and treatment of disease).

In order to determine their biocompatibility, unloaded dendrosomes were incubated with HUVECs for a predetermined period and then subsequently Cell Titer Blue assay was performed to determine the toxicity of the material on endothelial cells. It was determined that the dendrosomes are relatively nontoxic to endothelial cells and thus provide great promise as drug carriers.

Several examples of liposomes assembled from positively charged polymer-dendrimer block copolymers[112] and from charged amphiphilic dendrimers[108, 113] are available. Nevertheless, the results demonstrate a simple and general strategy to the design and synthesis of amphiphilic Janus-dendrimers that self-assemble into stable and monodisperse dendrosomes and other complex architectures. Dendrosomes expand the field of supramolecular dendrimer chemistry into new functions with possible technological applications.

3.3 EXPERIMENTAL METHODS

3.3.1 Preparation of Doxorubicin Loaded Dendrisomes (dendrimeric vesicles) for Loading and Release Studies

Self-assembly via thin-film hydration was used to assemble the dendrimers into their equilibrium morphologies. Film hydration has been extensively utilized for preparing non-degradable polymer vesicles comprised of PEO-b-PBD and PEO-b-PEE diblock copolymers [4, 9]. Briefly, 200 microliters of a 10mg/mL dendrimer solution in methylene chloride were uniformly deposited on the surface of a roughened Teflon plate followed by evaporation of the solvent for >12h under vacuum. Addition of aqueous hydration solution, (~290 milliosmolar ammonium sulfate solution and doxorubicin (DOX) (.2mg/ml), pH 7.3) followed by sonication led to spontaneous budding of drug encapsulated nanosized dendrosomes dendrosomes, off the teflon-deposited thin-film, into the aqueous solution. The sonication procedure involved placing the sample vial containing the aqueous based solution and dried thin-film formulation (of dendrimer uniformly deposited on Teflon) into a sonicator bath (Branson; Model 3510) @ 60-65°C for 30min followed by constant agitation for 60 minutes at 60-65°C. Subsequently, five

cycles of freeze-thaw extraction followed; freeze-thaw extraction was carried out by placing the sample vials in liquid N_2 and subsequently thawing in a water bath at 50-60°C.

After hydration and sonication, samples were placed into dialysis cassettes and dialyzed at 4°C in iso-osmotic citrate phosphate buffer (pH~7.4) to remove non-entrapped DOX. Dialysis solutions were changed 4 times over approximately 48 hours. After the dialysis, the samples were removed from the dialysis cassette, and diluted in the citrate phosphate buffer. Release studies of DOX from the loaded dendrosomes were initiated immediately following dilution in buffer.

3.3.2 Doxorubicin Release from Dendrisomes Studies

Doxorubicin release from the dendrisome core was was measured fluorometrically (using a SPEX Fluorolog-3 fluorimeter;λex = 480nm,λem = 590nm) at various intervals up to fourteen days. The fluorescence was obtained at time zero for all samples. Subsequently, a portion of the samples were acidified with 12.1N HCl to reduce the pH down to approximately 5.2 and the fluorescence was remeasured, with this new fluorescence being time zero for the acidified samples. Inside the aqueous core, the DOX is aggregated and its fluorescence is quenched. As the drug is released from the dendrosome core and diluted into the external solution its fluoreswcence is no longer quenched and thus increases. Thus, an increase in fluorescence over time can be correlated to doxorubicin release.

At the culmination of the study, the samples were solubilized using Triton X-100 and heat. The percent of Dox release over time was calculated as the ratio between the

fluorescence measured at each time point to the maximum final fluorescence obtained upon lysis of the vesicles with TritonX-100 at the culmination of the study according to the equation:

$$P\% = (I_t - I_{t0})/(I_{max(Tx)} - I_{t0}) \times 100 \qquad \textbf{Equation 3.1}$$

where $\mathbf{I_t}$ = fluorescence at each time point t

$\mathbf{I_{t0}}$ = fluorescence at time point 0

$\mathbf{I_{max(Tx)}}$ = maximum fluorescence upon lysis with Triton X

3.3.3 Cytotoxicity Studies of Various Dendrimers

Since endothelial cells are the first point of contact for intravenous drug formulations, the toxicity of the dendrosomes was evaluated *in vitro* on human umbilical vein endothelial cells (HUVECs). In order to estimate the toxicity of these dendrosomes, cell viability experiments were carried out on human umbilical vein endothelial cells (HUVECs). Dendrosomes from library 2 were incubated with HUVECs at varying concentrations for a period of four hours. Cell viability assays with Cell Titer-Blue^{TM}, a dye that becomes fluorescent in the presence of living cells, were carried out at 1, 2 and 4 h intervals Library 2 showed no discernable toxicity when compared to the control experiments (Figure 5) indicating an excellent biocompatibility for dendrosomes..

HUVECs were cultured in EGM Endothelial Growth Media (LONZA) supplemented with bovine brain extract (BBE) with heparin, h-EGF, hydrocortisone, gentamicin, amphotericin B (GA-1000), and fetal bovine serum (FBS). Cells were maintained in plastic culture flasks at 37□C in a humidified atmosphere containing 5% CO_2 and were further subcultured when the flasks were 70% to 90% confluent. The passage number of the cells for the HUVECs *in vitro* studies ranged from 5-8.

HUVECs were plated at a density of 3,200 cells per well (10,000cells/cm^2) in 96 well tissue culture plates and allowed to adhere overnight. Culture media was removed

from the wells and replaced with 250μL of either: 100% media, 94% media/6% PBS buffer, 87.5% media/12.5% PBS buffer, 75% media/25% PBS buffer, 100% PBS buffer, and various concentrations of sterile dendrosomes and PEO-b-PCL and PEO-b-PBD polymersomes ranging from 0.0625mg to 0.25mg in the three concentrations of media/PBS, and maintained at 37°C in a humidified atmosphere of 5% CO_2. The dendrosomes and polymersomes were prepared by film the hydration method as described in and manually extruded 25 times through 100 nm polycarbonate membrane. Dendrosomes and polymersomes were sterilized by exposing them for 30min to UV radiation.

The investigation of dendrosome toxicity and cell viability was assessed fluorometrically using the indicator dye resazurin (CellTiter-Blue Cell Viability Assay, Promega) which is reduced by viable cells from a non fluorescent form to a highly fluorescent form, resorufin, according to Equation 3.2. The viable cells retain the metabolic capacity to convert resazurin to resorufin while nonviable cells rapidly lose metabolic capacity and are not able to reduce the indicator dye hence no fluorescent signal is generated. As such, cell viability can be monitored by fluorescent changes.

Equation 3.2- Reduction of resazurin to resorufin in the presence of live cells.

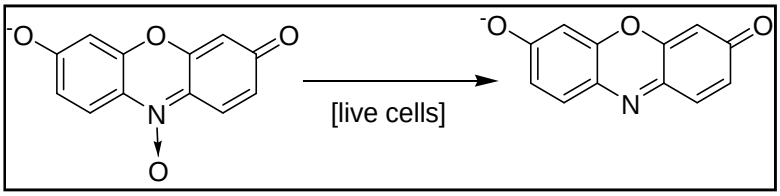

At various defined time points (1h, 2h, and 4h post vesicle administration), wells were washed three times with 250μL of PBS and 100μL of fresh media was added. To the fresh media, 20μL of Cell-Titer Blue (Promega) was added and cells were incubated at 37°C in a humidified atmosphere containing 5% CO_2 for 2 hours. Subsequently, 100μL of media containing Cell-Titer Blue was removed from the cells and placed in the wells of a 96 well black bottom plate. The fluorescence intensity at 590nm emanating from the wells when excited at 560nm was then determined using a TECAN Inifinite2000 plate reader.

3.4 RESULTS AND DISCUSSION

3.4.1 Doxorubicin Release from Dendrosomes

Selected dendrosomes from libraries 1 and 2 were loaded with the anthracyclin drug, Doxorubicin, and its release was monitored fluorometrically at 37□C at physiological pH (~7.2~7.4) and acidic pH (~5.2~5.4). Figure 3.1 shows selected experiments that illustrate a significantly higher release of drug at acidic pH than at physiological pH. As mentioned, Janus-amphiphiles contain cleavable bonds which breakdown under acidic conditions leading to destabilization of the vesicle structure; hence more drug is released at low pH. Since the vasculature surround the tumor has a lower than physiological pH (~5.2), hence, this increased release at low pH is quite beneficial for delivering drug to the tumor. For both conditions, the characteristic burst phase release is seen where approximately 20% of the drug is released within the first twelve hours. Subsequent release of the drug from dendrosomes at both pHs is slower.

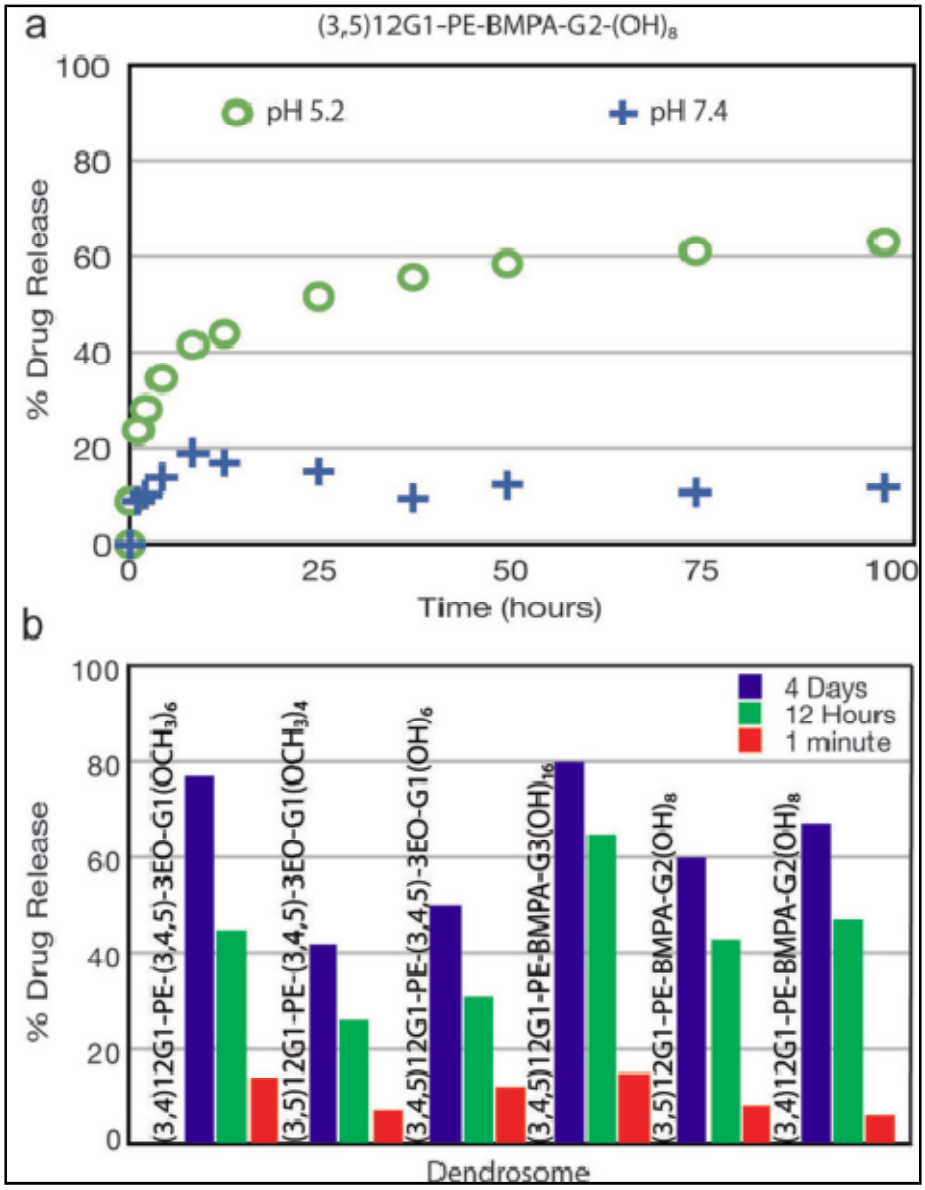

Figure 3.5- Characterization of the release of doxorubicin from dendrosomes (a) Release of Doxorubicin from dendrosomes assembled from (3,5)12G1-PE-BMPA-G2-(OH)8 showing excellent stability at physiological temperature and pH 7.4 and rapid release of the drug at physiological temperature and pH 5.2 (b) Comparative of release of doxorubicin dendrosomes from different libraries.

3.4.2 Dendrosome Cytotoxicity Studies

Since endothelial cells are the first point of contact for intravenous drug formulations, the toxicity of the unloaded dendrosomes was evaluated *in vitro* on human umbilical vein endothelial cells (HUVECs) over the course of four hours. Dendrosomes from library 2 were incubated

with HUVECs at varying concentrations for a period of four hours. Cell viability assays with Cell Titer-Blue^{TM}, a fluorometric agent that reports metabolic activity of cells, were carried out at 1h, 2h and 4h intervals. Live cells undergo metabolism causing a change in the fluorescence of the molecule, while dead cells do not undergo metabolism and hence do not change the fluorescence of the molecule; this can be quantified via the fluorescence of the CellTiter Blue substrate. Library 2 showed only slight toxicity when compared to the polymersome control experiments (Figure 3.6) after one and four hours. At 2 hours, the dendrosomes showed no discernable toxicity when compared to the control experiments (Figure 3.6); these results indicated an excellent biocompatibility for dendrosomes. Hence, the viability results demonstrate that the uptake of dendrosomes is well tolerated by the HUVECs.

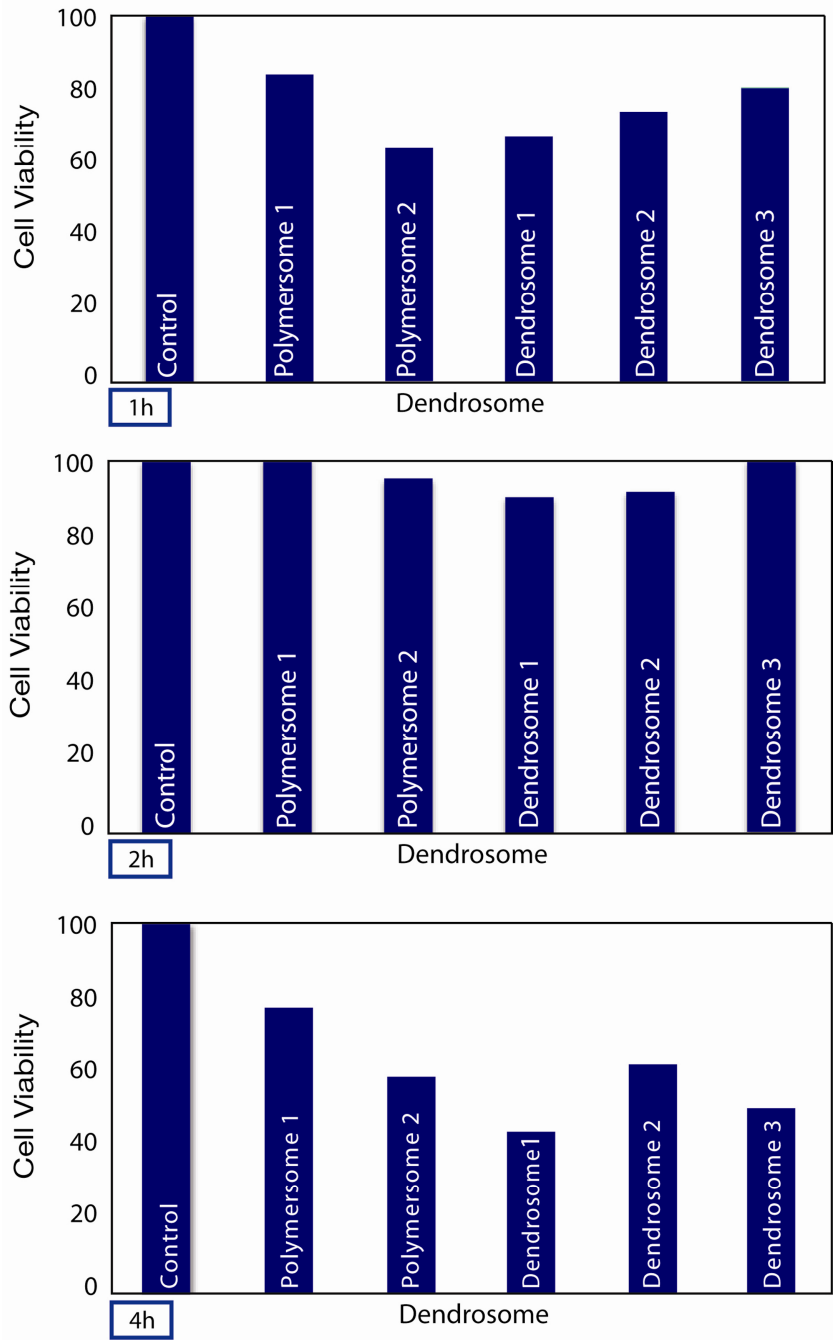

Figure 3.6- Cell viability studies conducted using various dendrosomes from library 2
with human umbilical vein endothelial cells (HUVEC) and CellTiter-BlueTM cell viability assay after 1h (top), 2h (middle) and 4h (bottom) from the moment the cell were fed with dendrosomes. Control: EGM Endothelial Growth Media (LONZA) Polymersome 1: hydrogenated polybutadiene-b-polyethyleneoxide; Polymersome 2: polycaprolactone-b-polyethyleneoxide; Dendrosome 1: (3,4)12G1-PE-(3,4,5)3EO-

G1-(OMe)6; Dendrosome 2: (3,5)12G1-PE-(3,4,5)3EO-G1-(OMe)6; Dendrosome 3: (3,4,5)12G1-PE-(3,4,5)3EO-G1-(OH)6

3.5 CONCLUSIONS

The results of studies described in this chapter demonstrate the potential use of self-assembled dendrimeric vesicles for drug delivery purposes. Here we show that libraries of amphiphilic Janus-dendrimers self-assemble into monodisperse and stable vesicles, termed dendrosomes. In addition to the classical spherical shape, these dendrimers self-assemble into a variety of less encountered shapes.

Doxorubicin, a chemotherapeutic, was successfully loaded into the aqueous core of vesicles self assembled from a variety of the amphiphilic Janus-dendrimers. In contrast to DOX loading in polymersomes (Chapter 2), DOX was not loaded actively across the membrane with a gradient, but rather passively in the hydration solution. The release of the drug from the vesicles was investigated at two physiologically relevant pH's and characterized. Furthermore, toxicity studies with these vesicles confirmed that these vesicles are non-toxic to Human Umbilical Vein Endothelial Cells (HUVECs) at short times. Based on the performance of the dendrimeric vesicles in laboratory experiments, it is expected that dendrosomes will extend the capabilities of synthetic amphiphiles, generating responsive membranes with permeability controllable for desirable drug delivery.

3.6 ACKNOWLEDGEMENTS

Financial support by the National Science Foundation and P. Roy Vagelos Chair at Penn is gratefully acknowledged.

3.7 REFERENCES

1. Singer, S.J. and G.L. Nicolson, *FLUID MOSAIC MODEL OF STRUCTURE OF CELL-MEMBRANES.* Science, 1972. **175**(4023): p. 720-&.
2. Bangham, A.D., M.M. Standish, and J.C. Watkins, *DIFFUSION OF UNIVALENT IONS ACROSS LAMELLAE OF SWOLLEN PHOSPHOLIPIDS.* Journal of Molecular Biology, 1965. **13**(1): p. 238-&.
3. Ghadiri, M.R., J.R. Granja, and L.K. Buehler, *ARTIFICIAL TRANSMEMBRANE ION CHANNELS FROM SELF-ASSEMBLING PEPTIDE NANOTUBES.* Nature, 1994. **369**(6478): p. 301-304.
4. Percec, V., et al., *Self-assembly of amphiphilic dendritic dipeptides into helical pores.* Nature, 2004. **430**(7001): p. 764-768.
5. Haluska, C.K., et al., *Time scales of membrane fusion revealed by direct imaging of vesicle fusion with high temporal resolution.* Proceedings of the National Academy of Sciences of the United States of America, 2006. **103**(43): p. 15841-15846.
6. Barenholz, Y., *Liposome application: problems and prospects.* Current Opinion in Colloid & Interface Science, 2001. **6**(1): p. 66-77.
7. Guo, X. and F.C. Szoka, *Chemical approaches to triggerable lipid vesicles for drug and gene delivery.* Accounts of Chemical Research, 2003. **36**(5): p. 335-341.
8. Ringsdorf, H., B. Schlarb, and J. Venzmer, *MOLECULAR ARCHITECTURE AND FUNCTION OF POLYMERIC ORIENTED SYSTEMS - MODELS FOR THE STUDY OF ORGANIZATION, SURFACE RECOGNITION, AND DYNAMICS OF BIOMEMBRANES.* Angewandte Chemie-International Edition in English, 1988. **27**(1): p. 113-158.
9. Thomas, J.L. and D.A. Tirrell, *POLYELECTROLYTE-SENSITIZED PHOSPHOLIPID-VESICLES.* Accounts of Chemical Research, 1992. **25**(8): p. 336-342.
10. Lasic, D.D. and D. Papahadjopoulos, *LIPOSOMES REVISITED.* Science, 1995. **267**(5202): p. 1275-1276.
11. Krafft, M.P., *Fluorocarbons and fluorinated amphiphiles in drug delivery and biomedical research.* Advanced Drug Delivery Reviews, 2001. **47**(2-3): p. 209-228.
12. Papahadjopoulos, D., et al., *STERICALLY STABILIZED LIPOSOMES - IMPROVEMENTS IN PHARMACOKINETICS AND ANTITUMOR THERAPEUTIC EFFICACY.* Proceedings of the National Academy of Sciences of the United States of America, 1991. **88**(24): p. 11460-11464.
13. Discher, B.M., et al., *Polymersomes: Tough vesicles made from diblock copolymers.* Science, 1999. **284**(5417): p. 1143-1146.
14. Discher, D.E. and A. Eisenberg, *Polymer vesicles.* Science, 2002. **297**(5583): p. 967-973.
15. Cornelissen, J., et al., *Helical superstructures from charged poly(styrene)-poly(isocyanodipeptide) block copolymers.* Science, 1998. **280**(5368): p. 1427-1430.
16. Kita-Tokarczyk, K. and W. Meier, *Biomimetic Block Copolymer Membranes.* Chimia, 2008. **62**(10): p. 820-825.

17. Chiruvolu, S., et al., *A PHASE OF LIPOSOMES WITH ENTANGLED TUBULAR VESICLES.* Science, 1994. **266**(5188): p. 1222-1225.
18. Walker, S.A., M.T. Kennedy, and J.A. Zasadzinski, *Encapsulation of bilayer vesicles by self-assembly.* Nature, 1997. **387**(6628): p. 61-64.
19. Dubois, M., et al., *Self-assembly of regular hollow icosahedra in salt-free catanionic solutions.* Nature, 2001. **411**(6838): p. 672-675.
20. Almgren, M., K. Edwards, and G. Karlsson, *Cryo transmission electron microscopy of liposomes and related structures.* Colloids and Surfaces a-Physicochemical and Engineering Aspects, 2000. **174**(1-2): p. 3-21.
21. Walter, A., et al., *INTERMEDIATE STRUCTURES IN THE CHOLATE-PHOSPHATIDYLCHOLINE VESICLE MICELLE TRANSITION.* Biophysical Journal, 1991. **60**(6): p. 1315-1325.
22. Percec, V., et al., *Controlling polymer shape through the self-assembly of dendritic side-groups.* Nature, 1998. **391**(6663): p. 161-164.
23. Percec, V., et al., *Self-organization of supramolecular helical dendrimers into complex electronic materials (vol 419, pg 384, 2002).* Nature, 2002. **419**(6909): p. 862-862.
24. Lee, C.C., et al., *Designing dendrimers for biological applications.* Nature Biotechnology, 2005. **23**(12): p. 1517-1526.
25. Esfand, R. and D.A. Tomalia, *Poly(amidoamine) (PAMAM) dendrimers: from biomimicry to drug delivery and biomedical applications.* Drug Discovery Today, 2001. **6**(8): p. 427-436.
26. Hillmyer, M.A., et al., *Complex phase behavior in solvent-free nonionic surfactants.* Science, 1996. **271**(5251): p. 976-978.
27. Walde, P. and S. Ichikawa, *Enzymes inside lipid vesicles: Preparation, reactivity and applications.* Biomolecular Engineering, 2001. **18**(4): p. 143-177.
28. Lasic, D.D., *Colloid chemistry - Liposomes within liposomes.* Nature, 1997. **387**(6628): p. 26-27.
29. Needham, D. and R.S. Nunn, *ELASTIC-DEFORMATION AND FAILURE OF LIPID BILAYER-MEMBRANES CONTAINING CHOLESTEROL.* Biophysical Journal, 1990. **58**(4): p. 997-1009.
30. Iyer, A.K., et al., *Exploiting the enhanced permeability and retention effect for tumor targeting.* Drug Discovery Today, 2006. **11**(17-18): p. 812-818.
31. Duncan, R., *Polymer-Drug Conjugates: Targeting Cancer*, in *Biomedical Aspects of Drug Targeting*, V.R. Muzykantov and V.P. Torchlin, Editors. 2002, Kluwer Academic Publishers: Boston. p. 197-199.
32. Vanhest, J.C.M., et al., *POLYSTYRENE-DENDRIMER AMPHIPHILIC BLOCK-COPOLYMERS WITH A GENERATION-DEPENDENT AGGREGATION.* Science, 1995. **268**(5217): p. 1592-1595.
33. Al-Jamal, K.T., T. Sakthivel, and A.T. Florence, *Dendrisomes: Vesicular structures derived from a cationic lipidic dendron.* Journal of Pharmaceutical Sciences, 2005. **94**(1): p. 102-113.
34. Ghoroghchian, P.P., et al., *Near-infrared-emissive polymersomes: Self-assembled soft matter for in vivo optical imaging.* Proceedings of the National Academy of Sciences of the United States of America, 2005. **102**(8): p. 2922-2927.

Chapter 4

POLYMERSOMES: SELF-ASSEMBLED VESICLES FOR IMAGING AND DRUG DELIVERY

ADAPTED FROM

Dalia Hope Levine, Nimil Sood, Julie Czupryna, Lanlan Zhou, Ramacharan Murali, Daniel A. Hammer, Manuscript in Preparation

4.1 SUMMARY

The bioresorbable poly(ethylene oxide)-b-poly(ε-caprolactone) polymersome, with its thick lamellar hydrophobic membrane, of approximately 22nm, and large aqueous core, holds great clinical promise for use in theranostic biomedical applications, where both drug and imaging agent are simultaneously loaded into the same vesicle for drug delivery and imaging purposes. This chapter discusses the generation of a near infrared (NIR) emissive polymersome, a self-assembled polymer vesicle, loaded with the NIR dye porphyrin in its hydrophobic compartment. Much of the seminal research regarding NIR-emissive polymersomes was carried out by Ghoroghchian et al. Yet, the ability to combine an imaging capability with drug delivery remained to be created and characterized. The following chapter illustrates the design of a polymersome with the capability to load both an imaging agent as well as a chemotherapeutic into one vesicle, creating an optimal platform for both drug delivery and imaging.

This chapter demonstrates the ability to encapsulate doxorubicin, a chemotherapeutic, into poly(ethylene oxide)-b-poly(ε-caprolactone) NIR-emissive polymersomes. In addition to loading studies, the release of doxorubicin from the vesicles was investigated. The increase in fluorescence from doxorubicin, as it is released from the vesicle, and the decrease in fluorescence from the porphyrin chromophore, as the polymersome membrane degrades, were examined and will be discussed in this chapter. Subsequent chapters will elaborate on the use of the NIR-emissive polymeric vesicles for *in vitro* cellular uptake studies (Chapter 5) and *in vivo*

imaging (Chapter 6). Furthermore, the use of the porphyrin-doxorubicin multi-modal polymersome for imaging drug delivery will be explored in Chapter 6.

4.2 INTRODUCTION

The attractive biomaterial properties of polymersomes such as prolonged circulation times [8], increased mechanical stability [7],and the ability to incorporate numerous large hydrophobic molecules within their thick lamellar membranes and hydrophilic molecules within their lumen [5, 6] render these vesicles useful in a variety of clinical applications. One such application is *in vivo* deep tissue fluorescence based optical imaging.

Currently, intravital microscopy (IVM), through the use of visible probes, has enabled anatomical, functional and molecular imaging of live animals [114]; however, due to light scattering and optical absorption by living tissue, the *in vivo* imaging potential of these visible probes decreases substantially at tissue depths great than 500 μM to 1 mm [115]. Since light scattering decreases with increasing wavelength and the absorbance spectra for hemoglobin and water reach their lowest values in the Near Infrared (NIR) region of the spectra (Figure 4.1) [115], research efforts have been focused on developing optical imaging probes in the NIR window for *in vivo* applications.

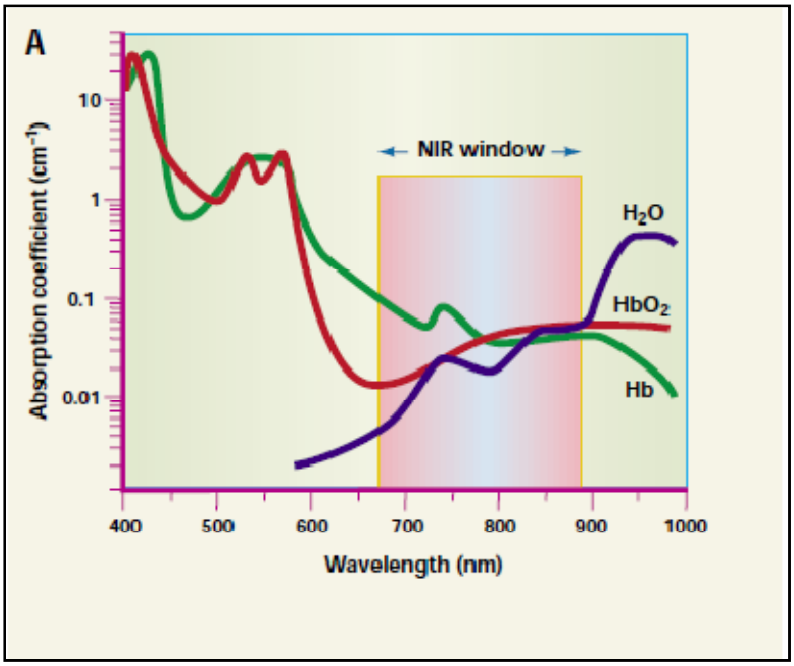

Figure 4.1- The absorbance spectra for water, hemoglobin, and water clearly showing a nadir in their optical absorption over the NIR window. Adapted from Weissleder [115].

A family of molecules which emit in the NIR has been developed by the Therien Laboratory. The chemical structure and absorption spectra of these porphyrin based fluorophores (PBF) is shown in Figure 4.2 and Figure 4.3A. These porphyrin molecules are derived from the linkage of (porphinato) zinc (II) (PZn) macrocycles by meso-to-meso, beta-to-meso, and beta-to-beta ethynyl- and butadiynyl-bridges [116-118]. The optical properties of these biologically inspired porphyrin molecules can be tuned over a large window of the visible and NIR spectra by varying the number of macrocycles per molecule, the bond type and location of the linkages between the macrocycles, and lastly by changing the side groups [117]. These subtle changes in porphyrin chemical structure can predictably change the optical properties of the fluorophores. The porphyrin trimer, (PZn_3), denoted as DDD in Figure 4.2, with its absorption maxima at 790nm and

emission maxima at 809nm, is optimal for biologically based imaging applications for reasons enumerated above. All NIR-emissive polymersome *in situ*, *in vitro*, and *in vivo* work to be discussed therein utilized this particular porphyrin molecule.

These porphyrin molecules, however, are very large, ranging from 2.1nm (monomer) to 5.3nm (pentamer) in length, and are highly hydrophobic, thus underscoring the need for an appropriate amphipathic delivery system with a large hydrophobic region [9]. Due to its large hydrophobic bilayer, the polymersome makes for a great delivery vehicle for the porphyrin molecules. Recall the polymersome hydrophobic membrane (~9nm-22nm), tuned by the length of the hydrophobic block of the copolymer, is at least double the thickness of the liposome membrane (~3nm-4nm) [9]. As such, only the monomeric or dimeric porphyrin molecules can be incorporated into liposomes, and only at loading levels of ~1 mol%. In contrast, the incorporation of larger porphyrin structures into the polymersome bilayer is easily obtained even at loading levels greater than 5 mol% (Figure 4.3B) with little effect on the spectral properties of the chromophore or the structural properties of the polymersome membrane [51]. In addition to the large hydrophobic membrane, which renders the polymersome ideal for the incorporation of porphyrin fluorophores, the optimal biological properties of polymersomes previously discussed, such as increased circulation due to the fully PEG-ylated brush [8] and increased mechanical and thermodynamic stability [3], make the porphyrin loaded polymersome quite useful for biological imaging applications.

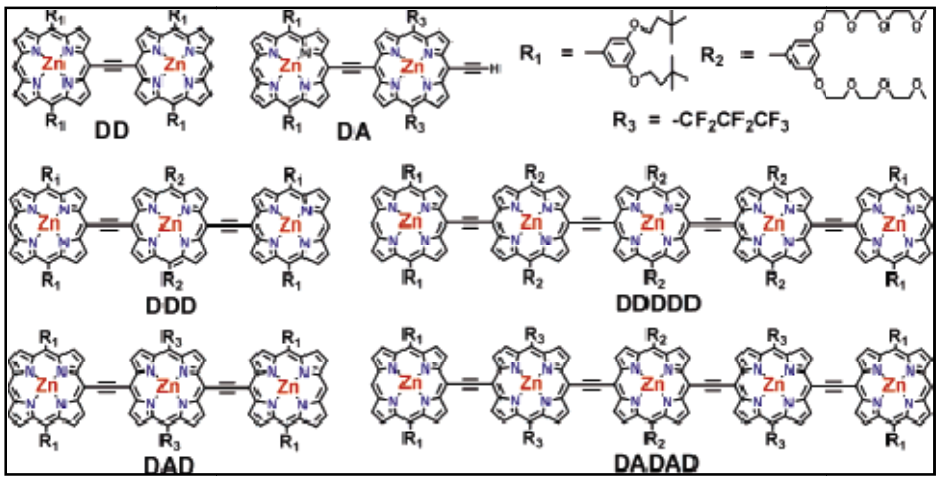

Figure 4.2-Some of the porphyrin molecules (PZn_2 to PZn_5) whose macrocycles are linked by meso-to-meso ethyne bridges. All *in situ*, *in vitro*, and *in vivo* studies use the porphyrin trimer, DDD. Image adapted from Duncan [118].

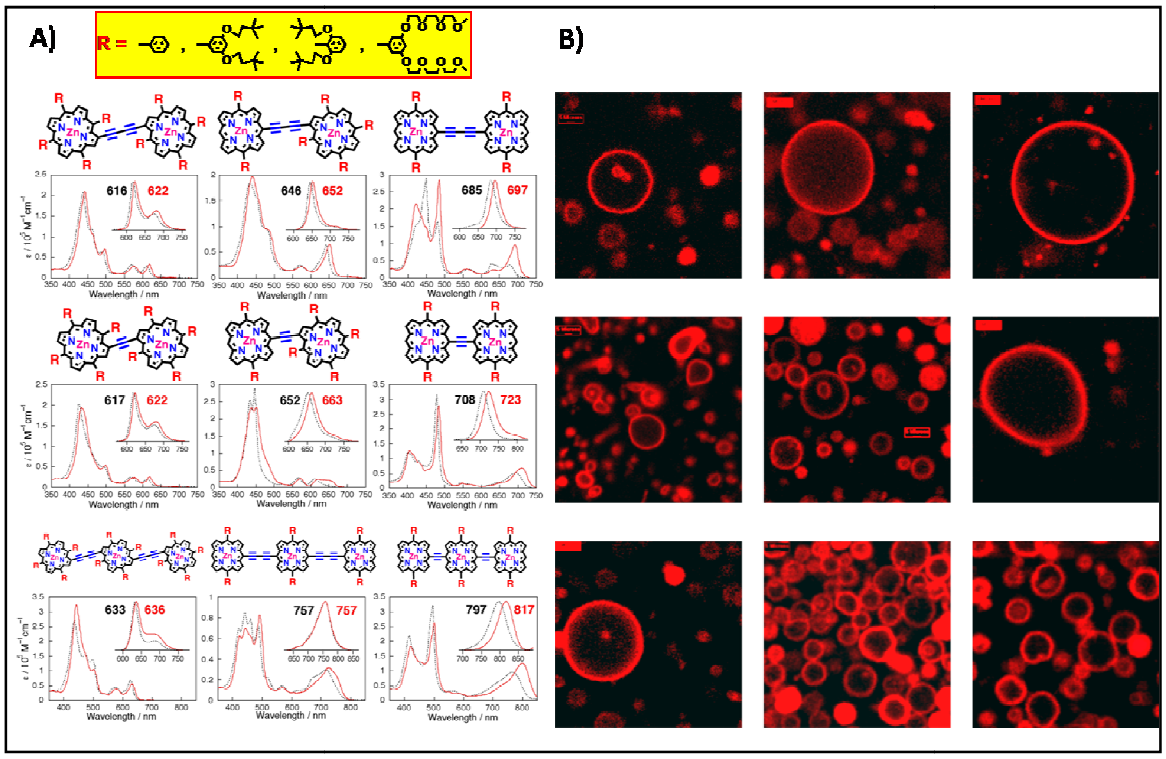

Figure 4.3- A) A subset of the family of porphyrin molecules, B) uniformly, stably, and non-covalently incorporated into the hydrophobic bilayer of poly(ethylene oxide)-b-polybutadiene polymersomes. Adapted from Ghoroghchian (2005) [10].

The NIR emissive polymersome soft matter complex, developed and extensively characterized by Ghoroghchian et al [9, 51, 52, 119], is formed through the cooperative self assembly of the diblock copolymer with the porphyrin molecules [9]. Following self assembly, the vesicles maintain an aqueous core free of dye and there is no need for further processing to remove unincorporated dye. Furthermore, no release of dye to the internal or external aqueous solution is observed [51]. Figure 4.3B depicts the stable, non-covalent, and uniform incorporation of multiple porphyrin molecules copies into the polymersome bilayer. Incorporating the family of porphyrin molecules into polymeric vesicles leads to a family of soft matter optical imaging agents with emission maxima that span the window from approximately 575nm to 1000nm [51].

The incorporation of therapeutics into the aqueous core of the porphyrin polymersome leads to the generation of multi-modal vesicles, with the capability to both track vesicle location *in vivo* and locally deliver therapeutics.

The ability to incorporate numerous porphyrin molecules into one polymersome creates an intensely bright fluorescent contrast agent with great promise for *in vivo* imaging applications. The additional encapsulation of therapeutics into these contrast agents lead to the creation of a *multi-functional* polymer vesicle with great theranostic utility.

4.3 EXPERIMENTAL METHODS

4.3.1 Preparation of Porphyrin Loaded PEO-b-PBD and PEO-b-PCL Vesicles

Self-assembly via thin-film hydration was used to assemble the PEO-b-PCL and PEO- b-PBD copolymers into their equilibrium morphologies. Film hydration has been

extensively utilized for preparing non-degradable polymersomes comprised of PEO-b-PBD and PEO-b-PEE diblock copolymers [4, 9]. Furthermore, Ghoroghchian, et al. demonstrated the ability to load porphyrin molecules of various sizes into polymer vesicles [9, 51, 52, 119].

Briefly, a PEO-b-PCL copolymer or PEO-b-PBD copolymer solution in methylene chloride was prepared (35mg/ml-100mg/ml polymer) and added to porphyrin at a 1:40 porphyrin:polymer molar ratio. Two hundred microliters of the polymer-porphyrin solution were uniformly deposited on the surface of a roughened Teflon plate followed by evaporation of the solvent for >12h. Addition of aqueous solution, (~290mOsM Phosphate Buffered Saline, PBS) and sonication at 65°C led to spontaneous budding of polymersomes, off the Teflon-deposited thin-film, into the aqueous solution. The sonication procedure involved placing the sample vial containing the aqueous based solution and dried thin-film formulation (of polymer-drug uniformly deposited on Teflon) into a sonicator bath (Branson; Model 3510) @ 60-65°C for 30min followed by constant agitation for 60 minutes at 60-65°C. Subsequently, five cycles of freeze-thaw extraction, which involved placing the sample vials in liquid N_2 followed by thawing in a water bath at 50-60°C. Extrusion using a pressure driven Lipex Thermobarrel Extruder (1.5 mL capacity) at 65°C was performed to yield small (<300-nm diameter) unilamellar polymersomes that possess appropriately narrow size distributions. The size distribution of the vesicle suspensions was determined by dynamic light scattering. The sample was centrifuged, filtrate removed, and additional PBS buffer was added to the concentrated sample for a total of nine times. The collected polymersome solution was centrifuged to concentrate the sample.

Absorbance spectra of the NIR-emissive polymersomes were obtained using an Ultrospec 2100pro Amersham Biosciences UV/Visible Spectrophotometer. Fluorescence spectra of NIR-emissive polymersomes were obtained with a Spex Fluorolog-3 spectrophotometer (Jobin Yvon, Edison, NJ) The concentration of porphyrin in the vesicles was determined by measuring the absorbance (molar extinction coefficient $1.29*10^5$ $cm^{-1}M^{-1}$ in polymersomes at 794nm [9]).

4.3.2 Preparation of Porphyrin and Doxorubicin Loaded PEO-b-PCL Vesicles and the Release of Doxorubicin and Porphyrin from PEO-b-PCL Vesicles

Similar to previous procedures, a PEO-b-PCL copolymer solution in methylene chloride was prepared (35mg/ml-100mg/ml polymer) and added to porphyrin at a 1:40 porphyrin:polymer molar ratio. The solution was deposited on the surface of a roughened Teflon plate followed by evaporation of the solvent for >12h. Hydration of the samples in Ammonium Sulfate Solution (~290mOsM, pH~5.4), equilibration at 60-65□C for 30 minutes, and finally sonication at 60-65°C using a sonicator bath (Branson; Model 3510) led to spontaneous budding of polymersomes, off the Teflon-deposited thin-film, into the aqueous solution. Five cycles of freeze-thaw extraction as described in Section 4.3.1 followed the sonication. Extrusion using a pressure driven Lipex Thermobarrel Extruder (1.5 mL capacity) at 65°C was performed to yield small (<300-nm diameter) unilamellar polymersomes that possess appropriately narrow size distributions. The size distribution of the vesicle suspensions was determined by dynamic light scattering.

Vesicles of the appropriate size were dialyzed against iso-osmotic acidified sodium chloride solution (pH~5.5—acidified with 12.N HCl, ~290mOsM) to establish a gradient across the vesicle membrane; three buffer exchanges were made in

approximately 30 hours. Similar to the loading in PEO-b-PmCL, dialysis into sodium acetate buffer at pH 5.5, as performed with PEO-b-PCL vesicles discussed in Chapter 2, did not yield stable loading as determined via fluorescence measurements. Hence, dialysis in various buffers was attempted, as will be elaborated upon in Section 4.4.2, and it was determined that stable fluorescence counts were obtained for loading when iso-osmotic acidified NaCl (pH~5.5) was used as the dialysis media.

Post dialysis, vesicles were incubated with doxorubicin at a ratio of .2:1 (drug:polymer) at 65□C for greater than 7 hours [77-79]. Non-entrapped DOX was removed from the *multi-functional* polymersome suspension using an HPLC (Acta Basic 10 HPLC with Frac 950) and the solution was passed through a HiTrap desalting column. The fractions containing only *multi-functional* polymersomes were collected, centrifuged and concentrated. Incorporation of porphyrin and encapsulation of DOX was confirmed spectrophotometrically using an Ultrospec 2100pro Amersham Biosciences UV/Visible Spectrophotometer.

The release of doxorubicin from the vesicles and the decrease in porphyrin fluorescence over time was determined fluorometrically. Aliquots of the samples were placed into either PBS buffer (290 mOsM at pH ~7.4) or sodium acetate buffer (50 mM sodium acetate and 100 mM sodium chloride, at pH ~ 5, 290mOsM) with N = 4 samples for each buffer. Release studies of DOX from the loaded polymersomes were initiated immediately following aliquoting; DOX and Porphyrin fluorescence were measured fluorometrically using a SPEX Fluorolog-3 fluorimeter (DOX: λ_{ex} = 480nm, λ_{em} = 590nm; Porphyrin: λ_{ex} = 480nm, λ_{em} = 800nm) at various intervals up to fourteen days.

As DOX is released from the polymersome core and diluted into the surrounding solution, its fluorescence emission increases over time. In contrast, as the vesicle membrane is hydrolyzed, the porphyrin fluorescence decreases upon membrane degradation. At the culmination of the study, the samples were solubilized using Triton X-100, which disrupts the vesicle membrane and releases the encapsulated DOX into the external solution. The percent release over time and release rate were calculated by comparing the measured DOX fluorescence at each time point to final DOX fluorescence, as determined upon solubilization of remaining intact polymersomes with TritonX-100, at the completion of the study.

4.4 RESULTS AND DISCUSSION

4.4.1 The Loading of Porphyrin into PEO-b-PCL and PEO-b-PBD Vesicles

Porphyrin trimer was successfully loaded into PEO-b-PCL and PEO-b-PBD vesicles at a molar ratio of 1:40 (Porphyrin to polymer) as previously described by P. Peter Ghoroghchian [9, 51]. In both cases, the incorporation of porphyrin was confirmed using absorbance spectroscopy, where the spectra clearly demonstrate both scatter due to the vesicles as well as the characteristic absorbance peaks of porphyrin (Figure 4.4). Porphyrin PEO-b-PBD vesicles were used in the initial vesicle biodistribution studies discussed in subsequent chapters. Once the biodistrbution was determined, biodegradable porphyrin PEO-b-PCL vesicles were used to further elucidate the biodistribution and degradation of the vesicles *in vivo*.

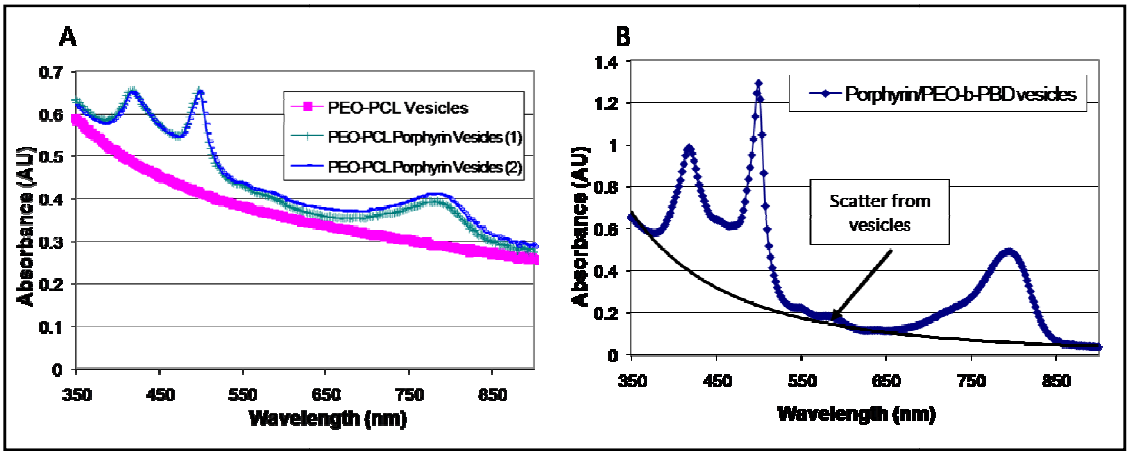

Figure 4.4- Absorbance spectra of porphyrin loaded vesicles showing the incorporation of porphyrin into A) PEO-b-PCL Vesicles and b) PEO-b-PBD Vesicles. The characteristic absorbance peaks as well as the scatter from the vesicles is clearly visible.

4.4.2 Loading and Release of Doxorubicin and Porphyrin in PEO-b-PCL Polymersomes

Doxorubicin and porphyrin were successfully loaded into polymersomes as per the method described in section 4.3.2. Successful loading of porphyrin and doxorubicin was determined by obtaining fluorescence spectra of the dual loaded vesicles and confirming the existence of the characteristic emission peaks (Figure 4.5). The encapsulation of doxorubicin was further confirmed by comparing fluorescence data pre and post incubation with the nonionic surfactant, Triton X-100 (Figure 4.5).

Doxorubicin was actively encapsulated into the aqueous compartment of porphyrin PEO-b-PCL vesicles (~200nm) though a gradient established by dialyzing samples in acidified NaCl solution [77, 79, 81] (See Section 4.3.2). Recall, PEO-b-PCL vesicles are dialyzed against sodium acetate buffer. When dialysis in this media was attempted, however, similar to the case for PEO-b-PmCL and PEO-b-PBD vesicles, the

fluorescence during loading did not stabilize. Hence, acidified sodium chloride solution was tested as dialysis exchange media and deemed acceptable.

In situ release studies were conducted at various physiological conditions (pH 5 and pH 7.4,@T=37□C) where changes in doxorubicin and porphyrin were monitored fluorometrically (λ_{ex}=480nm, $\lambda_{em\text{-}DOX}$=590nm, $\lambda_{em\text{-}porphyrin}$=794nm) over 14 days. At both pH's, the characteristic initial burst phase release (where approximately 20% of the initial payload within the first 12 hours) was observed followed by a more controlled pH dependent release over the 14 day release study (Figure 4.4 B,C). At a pH of 5, the initial release rate is significantly faster than the rate observed over the entire 14 days; furthermore, similar to the findings for PEO-b-PCL vesicles alone, it appears that the dominant mechanism of release at both short and long times at this pH is acid catalyzed hydrolysis of the PCL membrane. At a pH of 7.4, two distinct phases (α, β) were observed for DOX release from PEO-b-PCL vesicles. In contrast, when porphyrin is incorporated into the hydrophobic membrane, it appears that the large porphyrin molecules hinder extensive initial passive diffusion of the drug across the PCL membrane, and thus significant doxorubicin release from the polymersome core at pH 7.4 occurs at later times. This suggests that DOX release from the porphyrin vesicles is predominantly facilitated by hydrolytic matrix degradation of the caprolactone backbone (Figure 4.6 B, C), even in non-acidic environments. Since acid catalyzed hydrolysis of the membrane occurs at both short and long times at pH 5, DOX release at pH 5 is more rapid and more drug is released than that at pH 7.4

Figure 4.6A depicts the decrease in porphyrin fluorescence over the 14 day time period. Porphyrin fluorescence is highly environmentally dependent and changes in the environment are reflected as changes in the florescence. Thus, as the membrane breaks down and porphyrin is no longer in the hydrophobic environment of the PCL membrane, its fluorescence decreases. As expected, the porphyrin fluorescence decrease over the 14 days, as the membrane degrades, correlates nicely with the increase in DOX fluorescence (drug release).

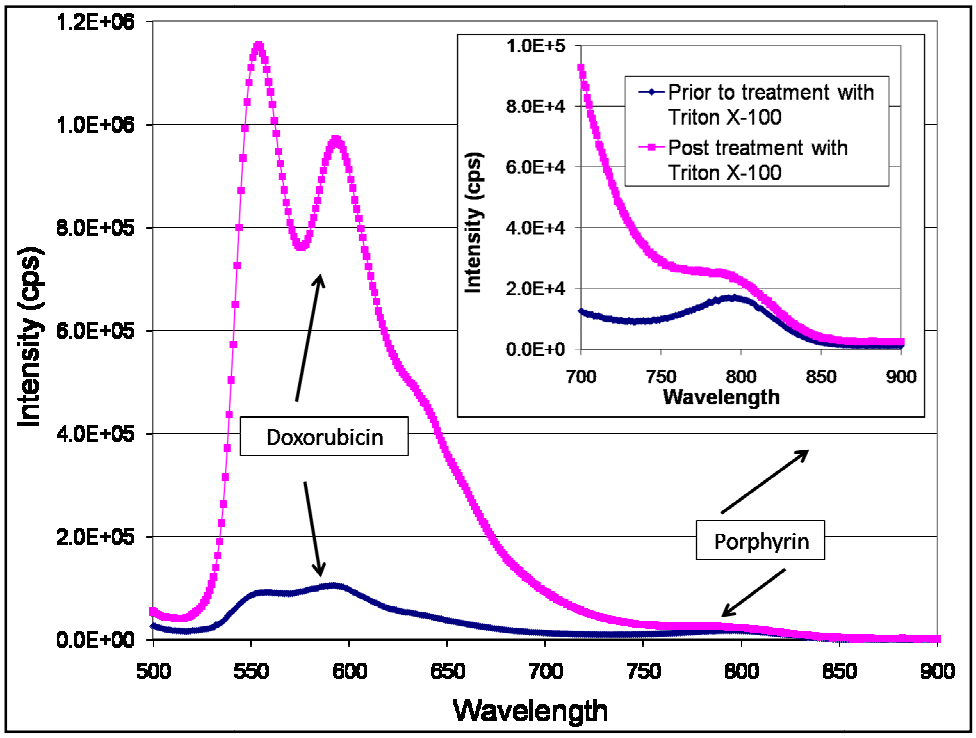

Figure 4.5- Fluorescence spectra of DOX/porphyrin PEO-b-PCL vesicles. The doxorubicin and porphyrin peaks are clearly visible. The inlay is a zoomed in version of the curve from 700nm to 900nm to show the porphyrin peak.

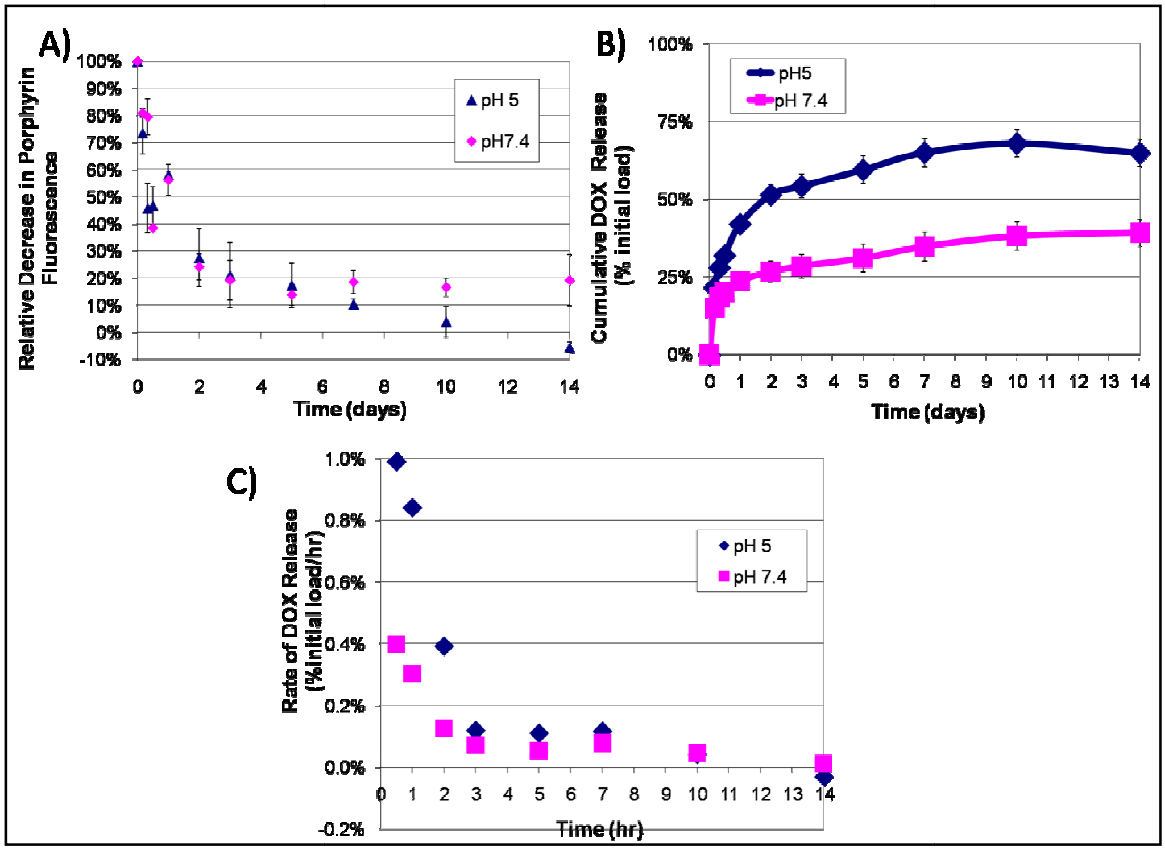

Figure 4.6- (A) Porphyrin decrease in fluorescence corresponds with (B) doxorubicin cumulative release as determined by doxorubicin increase in fluorescence and (C) rate of doxorubicin release from PEO-b-PCL polymeric vesicles.

4.5 CONCLUSIONS

The findings discussed in this chapter highlight the potential of polymersomes to be used simultaneously as contrast agents for imaging applications as well as drug delivery vehicles for therapeutic applications. The results demonstrated the method used to generate NIR-emissive polymersomes for imaging applications can be expanded upon to encapsulate a chemotherapeutic, doxorubicin, into the aqueous core, creating a *multi-functional* polymersome. Extensive doxorubicin loading studies established the use of both an ammonium sulfate and a pH gradient across the porphyrin incorporated

hydrophobic bilayer of the polymersome as the optimal loading environment. Once the loading parameters were determined, release studies were conducted and the release of DOX from the vesicle and vesicle breakdown was characterized.

The theranostic applications of these polymer vesicles loaded with therapeutics and imaging agents will be elaborated upon further in Chapter 7.

4.6 ACKNOWLEDGEMENTS

This work was supported by grants from the National Institutes of Health (EB003457-01 and CA115229), the National Cancer Institute (R33-NO1-CO-29008), Commonwealth Funds, Pennsylvania and Abramson Cancer Center, University of Pennsylvania, and infrastructural support was provided by a grant from the MRSEC Program of the National Science Foundation (DMR05-20020 and DMR-00-79909). A portion of the work discussed in this chapter was performed in the University of Minnesota I.T. Characterization Facility, which receives partial support from the NSF through the NNIN program.

4.7 REFERENCES

1. Photos, P.J., et al., *Polymer vesicles in vivo: correlations with PEG molecular weight.* Journal of Controlled Release, 2003. **90**(3): p. 323-334.
2. Bermudez, H., et al., *Molecular weight dependence of polymersome membrane structure, elasticity, and stability.* Macromolecules, 2002. **35**(21): p. 8203-8208.
3. Lee, J.C.M., et al., *Preparation, stability, and in vitro performance of vesicles made with diblock copolymers.* Biotechnology and Bioengineering, 2001. **73**(2): p. 135-145.
4. Meng, F., G.H.M. Engbers, and J. Feijen, *Biodegradable polymersomes as a basis for artificial cells: encapsulation, release and targeting.* Journal of Controlled Release, 2005. **101**(1-3): p. 187-198.
5. Jain, R.K., L.L. Munn, and D. Fukumura, *Dissecting tumour pathophysiology using intravital microscopy.* Nature Reviews Cancer, 2002. **2**(4): p. 266-276.
6. Weissleder, R., *A clearer vision for in vivo imaging.* Nature Biotechnology, 2001. **19**(4): p. 316-317.

7. Lin, V.S.Y. and M.J. Therien, *The role of porphyrin-to-porphyrin linkage topology in the extensive modulation of the absorptive and emissive properties of a series of ethynyl- and butadiynyl-bridged bis- and tris(porphinato)zinc chromophores.* Chemistry-a European Journal, 1995. **1**(9): p. 645-651.
8. Lin, V.S.Y., S.G. Dimagno, and M.J. Therien, *HIGHLY CONJUGATED, ACETYLENYL BRIDGED PORPHYRINS - NEW MODELS FOR LIGHT-HARVESTING ANTENNA SYSTEMS.* Science, 1994. **264**(5162): p. 1105-1111.
9. Duncan, T.V., et al., *Exceptional near-infrared fluorescence quantum yields and excited-state absorptivity of highly conjugated porphyrin arrays.* Journal of the American Chemical Society, 2006. **128**(28): p. 9000-9001.
10. Ghoroghchian, P.P., et al., *Near-infrared-emissive polymersomes: Self-assembled soft matter for in vivo optical imaging.* Proceedings of the National Academy of Sciences of the United States of America, 2005. **102**(8): p. 2922-2927.
11. Ghoroghchian, P.P., et al., *Broad spectral domain fluorescence wavelength modulation of visible and near-infrared emissive polymersomes.* Journal of the American Chemical Society, 2005. **127**(44): p. 15388-15390.
12. Discher, B.M., et al., *Polymersomes: Tough vesicles made from diblock copolymers.* Science, 1999. **284**(5417): p. 1143-1146.
13. Ghoroghchian, P.P., et al., *Controlling bulk optical properties of emissive polymersomes through intramembranous polymer-fluorophore interactions.* Chemistry of Materials, 2007. **19**(6): p. 1309-1318.
14. Ghoroghchian, P.P., et al., *Quantitative membrane loading of polymer vesicles.* Soft Matter, 2006. **2**(11): p. 973-980.
15. Discher, D.E. and A. Eisenberg, *Polymer vesicles.* Science, 2002. **297**(5583): p. 967-973.
16. Haran, G., et al., *Transmembrane Ammonium-Sulfate Gradients in Liposomes Produce Efficient and Stable Entrapment of Amphipathic Weak Bases.* Biochimica Et Biophysica Acta, 1993. **1151**(2): p. 201-215.
17. Lopes de Menezes, D.E., Pilarski, L.M., Allen, T.M., , Cancer Research, 1998. **58**: p. 3320-3330.
18. Bolotin, E.M., et al., *Ammonium Sulfate Gradients for Efficient and Stable Remote Loading of Amphiphathic Weak Bases into Liposomes and Ligandoliposomes.* Journal of Liposome Research, 1994. **4**(1): p. 455-479.
19. de Menezes, D.E.L., L.M. Pilarski, and T.M. Allen, *In vitro and in vivo targeting of immunoliposomal doxorubicin to human B-cell lymphoma.* Cancer Research, 1998. **58**(15): p. 3320-3330.

Chapter 5

POLYMERSOMES: DISCOVERING THEIR IMAGING AND DRUG DELIVERY POTENTIAL *IN VITRO*

ADAPTED FROM

D. H Levine, J. S. Katz, N. Dang, J. A. Burdick, J. Hadfield, and D. A. Hammer, Manuscript in Preparation

5.1 SUMMARY

Polymersomes (polymer vesicles) have been shown to possess a number of attractive biomaterial properties compared to liposomes (phospholipid vesicles), including prolonged circulation times, increased mechanical stability, as well as the unique ability to incorporate numerous large hydrophobic molecules within their thick lamellar membranes and hydrophilic molecules within their lumen. We have shown the ability to generate fully-bioresorbable self-assembled nanovesicles, from two FDA-approved building blocks, poly(ethylene oxide) (PEO) and polycaprolactone (PCL). We have successfully loaded imaging agents, such as porphyrin-based near infrared (NIR) fluorophores, and therapeutics such as doxorubicin and combretastatin A-4 into these polymersomes and tracked their release (See Chapters 2 and 4).

Tumors require a network of blood vessels to survive and grow; these blood vessels are required to provide oxygen and nutrients to the tumor cells and remove carbon dioxide and waste. However, these tumor blood vessels are immature and poorly developed. As a result, the combination of chemotherapeutics with anti-angiogenesis drugs/vascular disrupting agents (VDA) has emerged as a promising therapy for eradicating tumors. These agents target genetically stable endothelial cells that constitute the blood vessels around tumors rather than the transformed tumor cells themselves. Combretastatin A-4, a hydrophobic cytotoxic agent, inhibits the polymerization of tubulin and is highly toxic to tumor vasculature, but is believed not to affect healthy vasculature. Hence, in addition to delivering drug to tumorigenic cells, the ability to deliver

therapeutics to the endothelial cells lining the newly formed vasculature would be advantageous in cancer therapy.

Here, we determined the cytotoxic potential of combretastatin A-4 loaded polymeric vesicles and doxorubicin loaded polymeric vesicles on human umbilical vein endothelial cells (HUVECs) and SK-BR-3 tumorigenic cells both separately cultured, as well as in co-cultured. For both cell lines and both therapeutic agents, toxicity was both concentration and time dependent. Furthermore, we utilized NIR-emissive polymersomes formulated from PEO-b-PCL diblock copolymer and loaded with porphyrin (a NIR emissive fluorophore) to assess cellular uptake of polymersomes. Vesicle uptake by HUVECs was dependent on both concentration and incubation time. A viability assay using CellTiter-Blue™ (Promega) demonstrated biocompatibility of the unloaded polymersomes at short time for the SK-BR-3 cells and at extended time for the HUVECs. Thus, this study highlights the feasibility of using polymersomes to deliver vascular disrupting agents to endothelial cells simultaneously with treating tumors directly.

5.2 INTRODUCTION

Polymersomes (polymer vesicles) have been shown to possess a number of attractive biomaterial properties compared to liposomes (phospholipid vesicles), including prolonged circulation times [8], increased mechanical stability [7], as well as the unique ability to incorporate numerous large hydrophobic molecules within their thick lamellar membranes and hydrophilic molecules within their lumen [5, 6]. We have shown the ability to generate fully-bioresorbable self-assembled nanovesicles, from two

FDA-approved building blocks, poly(ethylene oxide) (PEO) and polycaprolactone (PCL) [10]. We have successfully loaded imaging agents, such as porphyrin-based near infrared (NIR) fluorophores, and therapeutics such as doxorubicin and combretastatin A-4 into these polymersomes and tracked their release (See Chapters 2 and 4).

Doxorubicin (DOX), an amphipathic antibiotic used to treat a wide array of malignancies, from solid tumors to leukemias [67-70], has been known to cause cardiotoxicity at cumulative doses [69, 120]. This has created a major therapeutic limitation. However, as discussed, encapsulating the drug into a vesicle has been shown to decrease cardiac toxicity thereby reducing the levels of DOX in heart muscle with minimal effects on the therapeutic efficacy of the drug [69, 120].

As discussed in Chapter 2, tumors require a network of blood vessels to survive and grow; these blood vessels are required to provide oxygen and nutrients to the tumor cells and remove carbon dioxide and waste. However, these tumor blood vessels are immature and poorly developed [73]. As a result, the combination of chemotherapeutics with anti-angiogenesis drugs/vascular disrupting agents (VDA) has emerged as a promising therapy for eradicating tumors [71, 73]. These agents target genetically stable endothelial cells that constitute the blood vessels around tumors, rather than the transformed tumor cells themselves [75]. Combretastatin A-4, a hydrophobic cytotoxic agent, inhibits the polymerization of tubulin and is highly toxic to tumor vasculature, but is believed not to affect healthy vasculature [76].

Hence, in addition to delivering drug to tumorigenic cells, the ability to deliver therapeutics to the endothelial cells lining the newly formed vasculature is highly

advantageous in cancer therapy. The therapeutic potential of the DOX/Combretastatin A-4 co-drug combination vesicles, as well as the single drug -vesicle, on Human Umbilical Vein Endothelial Cells (HUVECs) and the human breast cancer cells, SK-BR-3 cells, cultured separately and in co-culture was investigated.

It should be noted that the HUVECs are a good "surrogate" for the new endothelial cells making up the tumor vasculature since they are a well established cell line that mimics the endothelial cells partially because the HUVECs express some of the proteins upregulated on new endothelial near tumors [121].

The findings of the enumerated toxicity studies will be explored in this chapter. First, however, the biocompatibility of non-drug loaded vesicles, as well as cellular uptake of vesicles by HUVECs and SK-BR-3 cells, were examined and will be discussed.

5.3 EXPERIMENTAL METHODS

5.3.1 Preparation of Drug and Imaging Agent Loaded PEO-b-PCL Vesicles

Drug loaded vesicles were prepared as described in Chapter 2. Porphyrin loaded PEO-b-PCL and Porphyrin/DOX Vesicles were prepared as described in Chapter 3. Vesicles were concentrated post formation using Millipore Centricon Tubes.

To determine the concentration of combretastatin in the PEO-b-PCL vesicles, one hundred microliter sample aliquots were removed and the combretastatin was extracted from the vesicles by adding the aliquot to 400 microliters of PBS and 500 microliters of methylene chloride, and subsequently vortexing and centrifuging the sample. The resulting aqueous layer was carefully removed, and the remaining organic layer with drug

was placed in a vacuum. The dried powder resulting from evaporation of the methylene chloride was reconstituted in 1 milliliter of acetonitrile. The concentration of combretastatin was determined by measuring the absorbance (molar extinction coefficient 12, $579M^{-1}cm^{-1}$ in acetonitrile at 300nm). Polymer concentration was determined by a mathematical calculation, as the molar ratio of combretastatin to polymer is known to be 0.9:1.

To determine the concentration of Doxorubicin in the PEO-b-PCL polymersomes, sample aliquots were removed from the concentrated stock solution, and lyophilized to destroy the vesicle structure and release the encapsulated DOX from the core of the polymersome. The freeze-dried powder was reconstituted in tertiary butanol:water 9:1, v/v containing 0.075N HCl or 90% isopropyl alcohol containing 0.075 M HCl. The concentration of DOX was determined using Beer's Law by measuring the absorbance at 480nm using a molar extinction coefficient of $12{,}500cm^{-1}M^{-1}$ in either solvent [70, 122].

The concentration of the porphyrin vesicles in solution was determined by measuring the absorbance at 794nm using a molar extinction coefficient of $1.29*10^{5}M^{-1}cm^{-1}$ in THF[9]. Polymer concentration was determined by a mathematical calculation, since the ratio of porphyrin to polymer was set at 1:40 (molar ratio).

For cell studies, 10x concentrations of the drug-polymer vesicles and imaging agent-polymer vesicles were made by diluting the resulting concentrated sample in PBS. The 10x samples were further diluted in sterile culture media to yield final desired drug concentrations in a 90% media-10% PBS aqueous solution. The PBS-

Media-vesicle suspension was sterilized under UV light in a cell culture hood for 30 minutes, yielding sterile drug loaded vesicles in media-PBS.

5.3.2 Cell Culture

Human umbilical vein endothelial cells (HUVECs) were cultured in EGM Endothelia Growth Media (LONZA) supplemented with bovine brain extract (BBE) with heparin, h-EGF, hydrocortisone, GA-1000 (gentamicin, amphotericin B), and fetal bovine serum (FBS). Cells were maintained in plastic culture flasks at 37°C in a humidified atmosphere containing 5% CO_2 in air and subcultured when the flasks were 70% to 90% confluent. To subculture cells, growth media was removed from the HUVEC culture flask via aspiration and the flask was washed with Hepes Buffered Saline Solution (HBSS). The HBSS was removed and 0.025mg/ml trypsin-EDTA was added and the flask was returned to the incubator for 5min at 37□C and 5% CO_2 in air. Post trypsin incubation, trypsin neutralizing solution (TNS, LONZA) was added to the flask and the wall was washed in order to remove all cells. The cell suspension was then transferred to a conical tube and centrifuged at 1000rpm for 5 minutes to pellet the cells. The supernatant was aspirated and the cells were resuspended in fresh growth media and a cell count was performed with a hemocytometer for future culturing and well-plating. HUVECs *in vitro* studies were conducted with cells between passages 4-8.

The human breast cancer cells, SK-BR-3 cells, were cultured in McCoy's 5a Medium Modified (base media), 10% fetal bovine serum (FBS), and 1% Pen/Strep 100X (10000u/ml P - 10mg/ml S). Cells were maintained in plastic culture flasks at 37°C in a humidified atmosphere containing 5% CO_2 in air and subcultured at subcultivation ratio of 1:3 when the flasks were 70% to 90% confluent. When cells were deemed 70%-90%

confluent, growth media was removed from the culture flask via aspiration and the flask was washed with Phosphate Buffered Saline (PBS). The PBS was removed and trypsin-EDTA (0.25%)was added and the flask was returned to the incubator for 5min at 37□C and 5% CO_2 in air. Post trypsin incubation, media was added to the flask and the wall was washed in order to remove all cells. The cell suspension was then transferred to a conical tube and centrifuged at 1000rpm for 5 minutes to pellet the cells. The supernatant was aspirated and the cells were resuspended in fresh growth media and a cell count was performed with a hemocytometer for future culturing and well-plating. For *in vitro* experiments, SK-BR-3 cells between passages 15 to 30 were used.

5.3.3 Determining Cellular Uptake of PEO-b-PCL Vesicles by HUVECs and SK-BR-3 Cells

In order to investigate the cellular uptake of PEO-b-PCL vesicles as a function of cell number, vesicle concentration, and incubation time, HUVECs and SK-BR-3 cells were plated at varying densities ranging from $3.0*10^4$ cells/well to $0.7*10^4$ cells/well in 96 well (black frame, clear well) cell culture plates (Isoplate-96 TC, Perkin Elmer) in complete growth media and allowed to adhere overnight (~20-24hours). Culture media was removed from the wells, wells were washed once with 250uL of PBS and replaced with 250uL of either: 90% media/10% PBS without polymersomes, or 90% media/10% PBS with various concentrations of porphyrin polymersomes and maintained at 37°C in a humidified atmosphere containing 5% CO_2 in air. The suspensions were sterilized with 30 min exposure to a UV lamp in the culture hood prior to addition to cells. At various defined time points (.75H, 1.5H, 3H, and 5H post vesicle administration), plates were removed from the incubator, wells were washed three times with 250uL of PBS to

remove free vesicles and 100uL of fresh media was added. The fluorescence intensity emanating from the wells as a result of vesicles that had been taken up was then determined using a LICOR Odyssey, an Infrared (IR) Imaging System.

5.3.4 Investigating the Biocompatibility and Viability of Unloaded PEO-b-PCL on HUVECs and SK-BR-3 Cells

In addition to determining vesicle uptake, viability studies were carried out to determine the biocompatibility of unloaded PEO-b-PCL polymersomes on HUVECs and SK-BR-3 cells *in vitro*. HUVECs and SK-BR-3 cells were plated in 96 well plates in complete growth media and allowed to adhere overnight (~20~24hours). Cells were removed from the flasks as per the procedure described in Section 5.3.2. When examining the effects on HUVECs, HUVECs were plated at a density of 3,200 cells per well; in separate plates, SK-BR-3 cells were plated at a density of 5,000 cells per well to examine the effect on SK-BR-3 cells. In each case, cells were allowed to adhere for 20 to 24 hours. Culture media was removed from the wells, wells were washed once with 250uL of PBS and replaced with 250uL of either: 90% media/10% PBS without polymersomes, or 90% media/10% PBS with various concentrations of unloaded polymersomes and maintained at 37°C in a humidified atmosphere containing 5% CO_2 in air. The suspensions were sterilized with 30 min exposure to a UV lamp in the culture hood prior to addition to cells. At various defined time points (.12H, 24H, 48H, and 72H post vesicle administration), plates were removed from the incubator, wells were washed three times with 250uL of PBS to remove free vesicles, and 100uL of fresh media was added. 20ul of CellTiter-Blue® (Promega) was added to each well and the plate was returned to the incubator. After two hours of incubation, 20ul of the CellTiter-Blue™

/Media from the wells was added to 80ul of PBS in a 96-well black bottom assay plate, and the fluorescence emanating from the wells, which is a measure of cell viability, was determined using a TECAN Infinite® 2000 Multimode microplate reader.

5.3.5 Investigating the Anti-vasculature Potential of Combretastatin PEO-b-PCL Polymersomes on HUVECs and SK-BR-3 Cells Cultured Separately

In order to investigate the anti-vasculature potential of combretastatin loaded PEO-b-PCL vesicles, HUVECs were plated at a density of 3,200 cells per well (10,000cells/cm^2) in 96 well cell culture plates and SK-BR-3 cells were plated in separate 96 well cell cultures plates at a density of 5,000 cells per well; in each instance, cells were allowed to adhere overnight (~20-24hours). Culture media was removed from the wells, wells were washed with 250uL of PBS, and replaced with 250uL of either: 100% media, 90% media/10% PBS, 100% PBS, and various concentrations of drug in 90% media/10% PBS, and maintained at 37°C in a humidified atmosphere containing 5% CO_2 in air. The suspensions were sterilized with 30 min exposure to a UV lamp in the culture hood prior to addition to cells. At various defined time points (12H, 24H, 48H, and 72H post drug administration), wells were washed with 250uL of PBS and 100uL of fresh media was added. To the fresh media, 20uL of CellTiter-Blue® (Promega) was added to each well and the cells and Titer Blue were incubated at 37°C in a humidified atmosphere containing 5% CO_2 in air for 2 hours. Subsequently, 20uL of media containing CellTiter-Blue™ was removed from the wells and diluted into 80uL of PBS in the wells of a 96-well black bottom assay plate. The fluorescence intensity emanating from the wells, which is a measure of cell viability, was then determined using a TECAN Infinite® 2000 Multimode microplate reader.

5.3.6 Investigating the Cytotoxic Effects of Doxorubicin Loaded PEO-b-PCL Vesicles on HUVECs and SK-BR-3 Cells Cultured Separately

Doxorubicin single culture cytotoxicity studies were carried out in a manner similar to the previously discussed studies. HUVECs were plated at a density of 3,200 cells per well (10,000cells/cm^2) in 96 well cell culture plates and SK-BR-3 cells were plated in separate 96 well cell cultures plates at a density of 5,000 cells per well; in each instance, cells were allowed to adhere overnight (~20-24hours). Culture media was removed from the wells, wells were washed with 250uL of PBS, and replaced with 250uL of either: 100% media, 90% media/10% PBS, 100% PBS, and various concentrations of drug in 90% media/10% PBS, and maintained at 37°C in a humidified atmosphere containing 5% CO_2 in air. The suspensions were sterilized with 30 min exposure to a UV lamp in the culture hood prior to addition to cells. At various defined time points (12H, 24H, 48H, and 72H post drug administration), wells were washed with 250uL of PBS and 100uL of fresh media was added. To the fresh media, 20uL of CellTiter-Blue® (Promega) was added to each well and the cells and Titer Blue were incubated at 37°C in a humidified atmosphere containing 5% CO_2 in air for 2 hours. Subsequently, 20uL of media containing CellTiter-Blue™ was removed from the wells and diluted into 80uL of PBS in the wells of a 96-well black bottom assay plate. The fluorescence intensity emanating from the wells, which is a measure of cell viability, was then determined using a TECAN Infinite® 2000 Multimode microplate reader.

5.3.7 Investigating the Anti-vasculature and Anti-tumor Potential of Combretastatin and Doxorubicin Loaded PEO-b-PCL Polymersomes on HUVECs and SK-BR-3 Cells in Co-Culture

In order to determine the cytotoxic effects of drug loaded vesicles in co-culture, HUVECs and SK-BR-3 cells were stained using Cellvue ® NIR815($\lambda_{Ex\ max}$ =786nm, $\lambda_{Em\ max}$ =814nm) and Cellvue ® Burgundy ($\lambda_{Ex\ max}$ =683nm and $\lambda_{Em\ max}$ =707nm) from Molecular Targeting Technologies Inc.(MTTI), respectively. These dyes provide stable labeling of the lipid regions of the cell membrane. Labeling was carried out as per protocol obtained from MTTI, but scaled down for 2 million cells. Stained cells were plated at a density of 3,200 cells per well (10,000cells/cm^2) in 96 well (black frame, clear well) cell culture plates (Isoplate-96 TC, Perkin Elmer) and were allowed to adhere overnight (~20~24hours). Culture media was removed from the wells, wells were washed with 250uL of PBS, and replaced with 250uL of either: 100% media, 90% media/10% PBS, 100% PBS, and various concentrations of drug loaded vesicles in 90% media/10% PBS, and maintained at 37°C in a humidified atmosphere containing 5% CO_2 in air. The suspensions were sterilized with 30 minute exposure to a UV lamp in the culture hood prior to incubation with cells. Immediately following addition of drug loaded polymersomes, the fluorescence intensity was measured using a LICOR Odyssey, an Infrared (IR) Imaging System and this fluorescence was deemed to be the initial fluorescence per well. At various defined time points (12H, 24H, 48H, and 72H) post drug administration, wells were washed with 250uL of PBS to removed dead cells and 250uL of fresh media was added to the wells. The fluorescence intensity emanating from the washed wells, as a result of live stained cells in the wells, was then determined using a LICOR Odyssey.

5.4 RESULTS AND DISCUSSION

5.4.1 Cellular Uptake of Porphyrin Loaded PEO-b-PCL Vesicles by HUVECs and SK-BR-3 Cells

To determine the cellular uptake of polymer vesicles by HUVECs and SK-BR-3 cells, we utilized ~200nm NIR-emissive polymersomes formulated from PEO-b-PCL diblock copolymer and loaded with porphyrin (a NIR emissive fluorophore) and the LICOR Odyssey, an Infrared (IR) Imaging System. Figure 5.1 shows the raw data obtained for the uptake of ~200nm porphyrin polymersomes by HUVECs after 5 hours of incubation; similar images were obtained for the other time points as well as for SK-BR-3 cells.

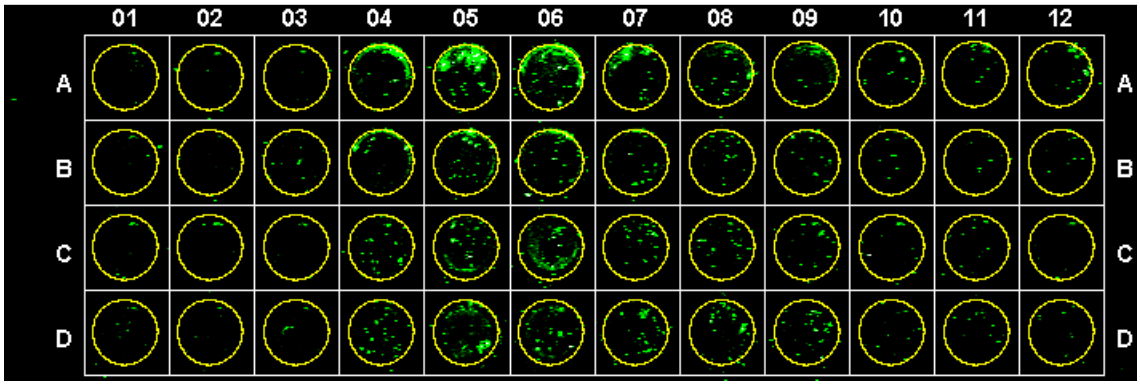

Figure 5.1- Raw HUVEC uptake data from the Odyssey.
Row A: $3*10^4$ Cells/Well; Row B: $2.25*10^4$ Cells/Well; Row C: $1.5*10^4$ Cells/Well; Row D: $0.75*10^4$ Cells/Well Column 1-3: Media Only; Column 4-6: 9uM PEO-b-PCL; Column 7-9: 4.5uM PEO-b-PCL; Column 10-12: 1.125uM PEO-b-PCL; Porphyrin Vesicles=Green (800 channel)

The vesicle uptake by HUVECs was both concentration and incubation time dependent. In general, as vesicle concentration in the media increased, cellular uptake also increased, until the saturation capacity of the cell was reached, especially at low cell numbers (Figure 5.2). Furthermore, increased incubation time or higher concentration of

vesicles generally resulted in increased uptake by both cell types (Figure 5.3). At higher cell densities, uptake was seen as early as 45 minutes and increased with extended incubation times. At lower vesicle concentrations, extended time was necessary for significant vesicle uptake.

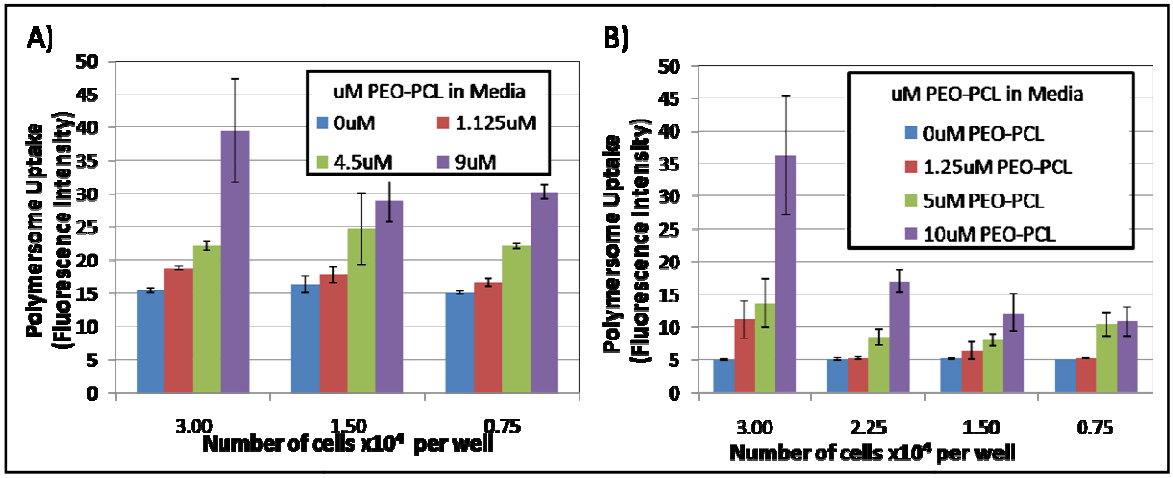

Figure 5.2- The effect of concentration and cell number on polymersome uptake by HUVECs
(A) and SK-BR-3 cells (B) after 5 hours of incubation with porphyrin polymersomes. (n=3; error bars ± S.E.)

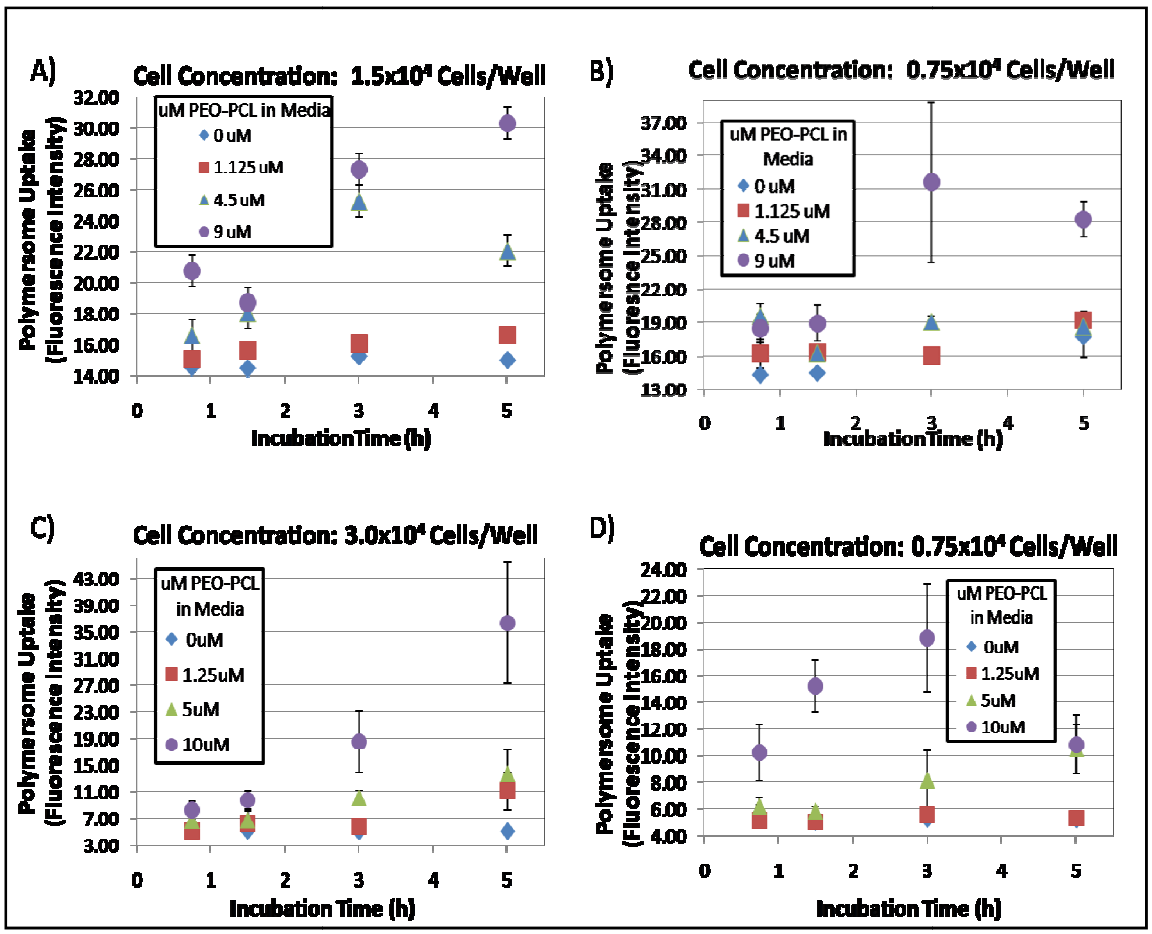

Figure 5.3- The effect of concentration and incubation time on polymersome uptake by HUVECs (A-B) and SK-BR-3 cells (C-D). (n=3; error bars ± S.E.)

5.4.2 Determination of the Viability and Biocompatibility of Unloaded PEO-b-PCL Vesicles on HUVECs and SK-BR-3 Cells in vitro

A viability assay using CellTiter-Blue™ was used to demonstrate the biocompatibility of the PEO-b-PCL nanoparticles without drug or imaging agent on cells in culture. HUVECs and SK-BR-3 cells were cultured with ~200nm unloaded PEO-b-PCL polymer vesicles at varying concentrations for up to 72 hours. A moderate drop in viability (~55-75%) was observed with the HUVECs, which did not appear to be concentration or time dependent (Figure 5.4A). For the case of SK-BR-3 cells, toxicity

appeared to be both concentration and time dependent. After 12 hours of incubation with vesicles, the viability dropped to approximately 50%, and after 24 hours, the viability decreased to ~35-40% Figure 5.4B. At the 48 hour time point and beyond, there appears to be a great loss in viability at the high concentrations of PEO-b-PCL vesicles, however the cells cultured with .28uM of vesicles appear to be 50% viable (Figure 5.4B).

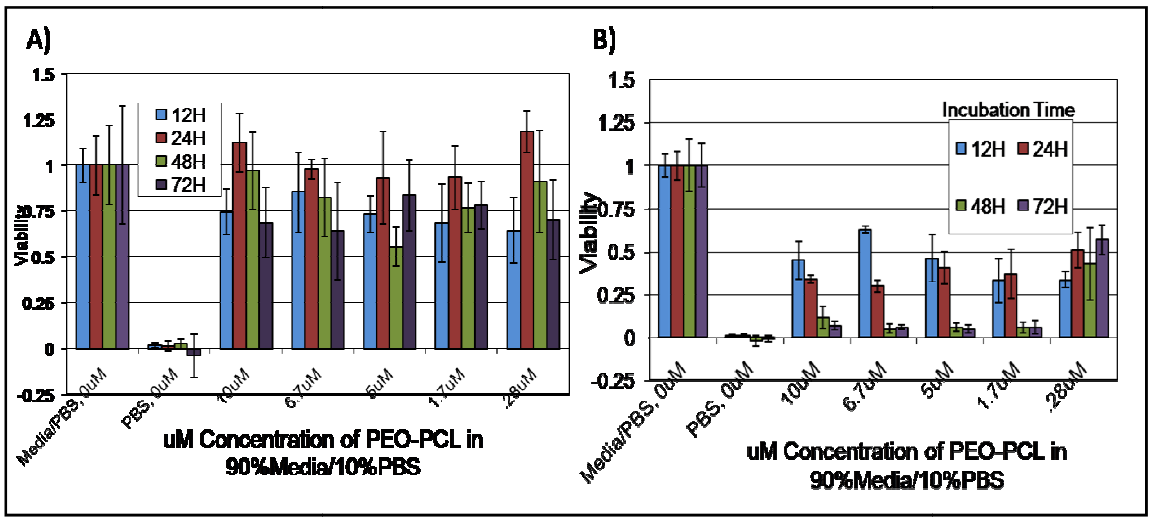

Figure 5.4- The viability of HUVECs (A) SK-BR-3 cells (B) when cultured with PEO-b-PCL vesicles at varying concentrations for 12hours to 72 hours.
Each bar represents the mean of four samples and error bars are standard deviation. All conditions are normalized to cultures grown in Media(90%)/PBS(10%) without vesicles present.

5.4.3 Determination of the Anti-vasculature Potential of Combretastatin PEO-b-PCL Polymersomes on HUVECs and Cytotoxic Effect on SK-BR-3 Cells Cultured Separately

Anti-vasculature potential of combretastatin A-4 loaded polymeric vesicles on HUVECs and SK-BR-3 tumorigenic cells was determined over 72 hours. Both cell lines were separately cultured in the presence of ~200nm combretastatin loaded PEO-b-PCL vesicles at varying concentrations and for up to 72 hours. For both cell lines incubated

with combretastatin vesicles, viability decreased over the 72 hours in both a time and dose dependent manner (Figure 5.5).

For HUVECs cultured with combretastatin vesicles for 12 hours, viability appears to be highly concentration dependent and ranged from ~40% viable at 9uM concentration of combretastatin to ~100% viable for the 0.25uM combretastatin condition. At later times however, while viability still appears to be concentration dependent, the viability has significantly decreased and by 72 h, viability dropped to less than ~35% for all doses of combretastatin (Figure 5.5A).

For SK-BR-3 cells, cell growth for drug treated cells was arrested, and at extended times cells appeared to be dying. After the first 24 hours, the cellular viability decreased to 50% or less for all concentrations, and by 72 hours, viability was less than ~25% for all concentrations of combretastatin in polymersomes (Figure 5.5B). Recall however, that a portion of the toxic effects are due to the vesicles themselves as evidenced in Figure 5.4B and thus some of the toxic effects seen may be due to the vesicles and not only the drug.

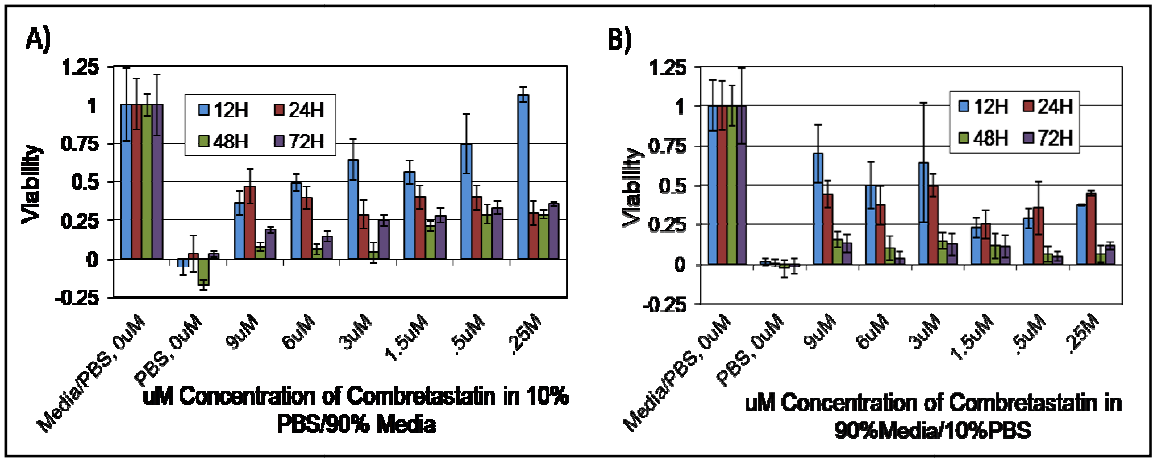

Figure 5.5- The effect of varying concentrations of combretastatin loaded polymersomes on HUVECs (A) and SK-BR-3 cells (B) viability over 72 hours. Each bar represents the mean of four samples and error bars are standard deviation. All conditions are normalized to cultures grown in Media(90%)/PBS(10%) without vesicles.

5.4.4 Determination of the Cytotoxic Potential of Doxorubicin Loaded PEO-b-PCL Polymersomes on HUVECs and SK-BR-3 Cells Cultured Separately

The cytotoxic potential of doxorubicin loaded PEO-b-PCL polymeric vesicles on HUVECs and SK-BR-3 tumorigenic cells was examined for both concentration and incubation time dependence. Both cell lines were separately cultured in the presence of ~200nm doxorubicin loaded PEO-b-PCL polymersomes at varying concentrations and for up to 72 hours. For both cell lines incubated with doxorubicin vesicles, viability decreased over the 72 hours in both a time and concentration dependent manner (Figure 5.6).

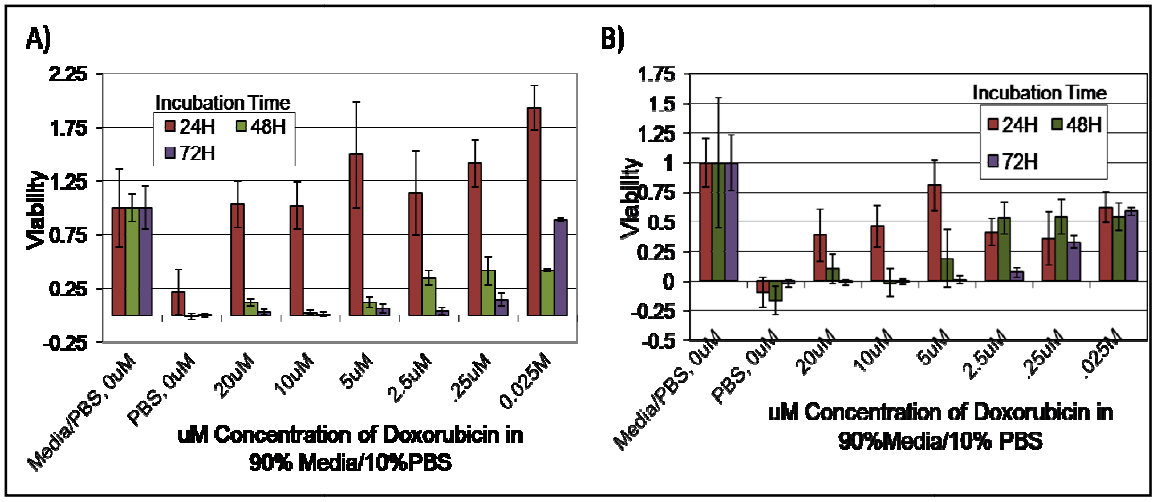

Figure 5.6- The effect of varying concentrations of doxorubicin loaded polymersomes on HUVECs (A) and SK-BR-3 cells (B) viability over 72 hours. Each bar represents the mean of four samples and error bars are standard deviation. All conditions are normalized to cultures grown in Media(90%)/PBS(10%) without vesicles.

After 24 hours of incubation, HUVEC viability does not appear to be effected by doxorubicin vesicles, even at high concentration. However, the cellular viability decreased sharply after the first 48 hours, where the viability is less than ~10% for cells incubated with doxorubicin at concentrations greater than 2.5uM. After 72 hours, cellular viability is less than ~25% for all concentrations of DOX greater than .025uM (Figure 5.6A). While one might expect to observe a less dramatic effect on HUVEC viability after incubation with the chemotherapeutic, one must consider that nearly all chemotherapeutics have anti-angiogenesis or antivascular effects; this has been show both *in vitro* and *in vivo* [71].

For SK-BR-3 tumorigenic cells, the cytotoxic effect of doxorubicin was more prevalent after 24hours. In fact, viability is less than ~75% in for all concentration, and less than ~50% for most concentrations of DOX. Similar to the HUVEC response, by 48

hours, the cellular viability dropped to less than ~25% for DOX concentrations greater than 2.5uM and after 72 hours, only cells incubated with concentrations less than 0.25uM were greater than ~25% viable (Figure 5.6B).

5.4.5 Investigating the Anti-vasculature and Anti-tumor Potential of Combretastatin and Doxorubicin Loaded PEO-b-PCL Polymersomes on HUVECs and SK-BR-3 Cells in Co-culture

HUVECs and SK-BR-3 cells were each stained using MTTI's Cellvue ® Burgundy and Cellvue ® NIR815, respectively. Post staining, cells were plated in 96 well (black frame, clear well) cell culture plates (Isoplate-96 TC, Perkin Elmer) for further examination of the effects of drug loaded vesicles on HUVECs and SK-BR-3 cells in co-culture. Figure 5.7 shows the initial fluorescence emanating from the wells of the 96 well plates, post plating with stained HUVECs and SK-BR-3 cells. In order to determine cell viability, cells incubated with drug loaded vesicles were washed to remove non-adherent cells and then assayed for fluorescence. Specifically, the fluorescence emanating from each well post incubation with drug vesicles was normalized against its original fluorescence intensity, post initial wash and prior to incubation with drug. Subsequent to that normalization step, intensity per well was normalized against the normalized value for wells without drug. This double normalization accounted for the fact that the washing step can remove some viable loosely adherent cells.

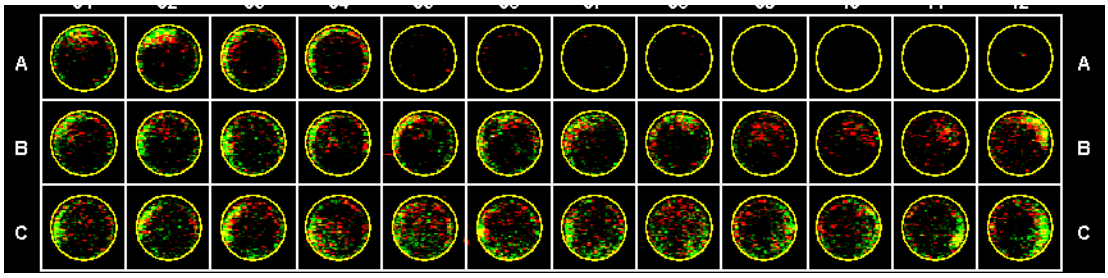

Figure 5.7- Image of stained co-cultured HUVECs and SK-BR-3 cells using the LICOR Odyssey prior to incubation with drug loaded vesicles. Green=HUVECs (700 Channel); Red= SK-BR-3 (800 Channel)

When combretastatin loaded PEO-b-PCL polymersomes are administered to HUVECs and SK-BR-3 cells in co-culture, the anti-vasculature effect of the drug on HUVECs appears to be less pronounced than when the drug is administered to cells in single culture; however, viability of cells cultured with drug loaded polymersomes is compared to the viability of cells cultured in PBS only (negative control as all cells will be dead), there is a noticeable effect after 12 hours (Figure 5.8A). Noting that the viability of the PBS only cells is quite high, a CellTiter-Blue™ Cell Viability Assay (Promega) was carried out to determine if the PBS only wells still contained viable cells. Though this assay, it was confirmed that these wells were devoid of living cells. From this, it is believed that the non-viable stained HUVECs stick to the wells even post washing and this sticking increases with increased incubation time in the wells. Hence, the fluorescence from the PBS only wells increases over time, even though it was confirmed that the cells were dead after culturing in PBS for 72 hours. Data not shown.

Post 12 hour incubation with combretastatin polymersomes, SK-BR-3 cell viability appeared to be adversely effected by the administration of combretastatin loaded polymersomes as well (Figure 5.8B). After 24 hours, the viability drops to ~75% or less,

and 48 hours post administration of drug loaded vesicles the cellular viability is less than ~50%. For the SK-BR-3 cells, the toxicity in co-culture appears to be less than when the cells are cultured separately; this may be the result of having the same concentration of polymer and drug, but 1.25 times more cells.

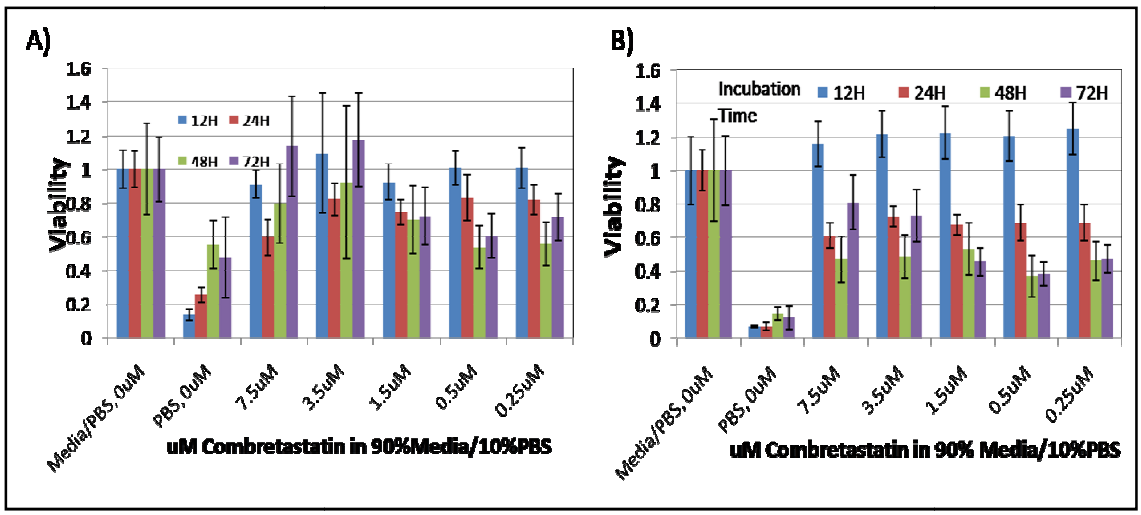

Figure 5.8- The effect of combretastatin loaded polymersomes on HUVECs (A) SK-BR-3 cells (B) in co-culture. Each bar represents the mean of four samples and error bars are standard deviation. All conditions are normalized to the initial fluorescence and then to cultures grown in Media(90%)/PBS(10%) without vesicles.

Twenty four hours post incubation with doxorubicin vesicles, the cellular viability of HUVECs appears to decrease to about 60% (when the viability is compared against that of the cells cultured in PBS only). When comparing against the fluorescence emanating from PBS cultured cells against the fluorescence from cells cultured with drug loaded vesicles, it appears that the viability drops greatly after a 72 hour incubation with drug loaded vesicles. Again however, it must be noted, that sticking of the non-viable cells cultured in PBS only was observed and from this we can surmise that cells cultured

with drug at high concentrations over extended periods of time are also sticking to the wells yielding a false positive reading for the fluorescence.

The effect of doxorubicin loaded polymersomes on SK-BR-3 cells in co-culture with HUVECs is apparent after 24 hours, when cellular viability decreased to less than ~80% after administration of drug loaded polymersomes. For concentrations of drug 2.5uM and greater, the decrease in SK-BR-3 viability over time at a single drug concentration is demonstrated by cellular viability decreasing from ~100% at 12 hours to less than 20% after 72 hours at the higher concentrations. At 48 and 72 hours post incubation with drug loaded polymersomes, the time and concentration dependence becomes apparent as decreasing concentration of drug at a particular time point leads to an increase in viability. In contrast to the combretastatin co-culture studies, here we see that although there are more cells in culture with the same amount of polymer and drug, the SK-BR-3 cells are still adversely affected by incubation with doxorubicin.

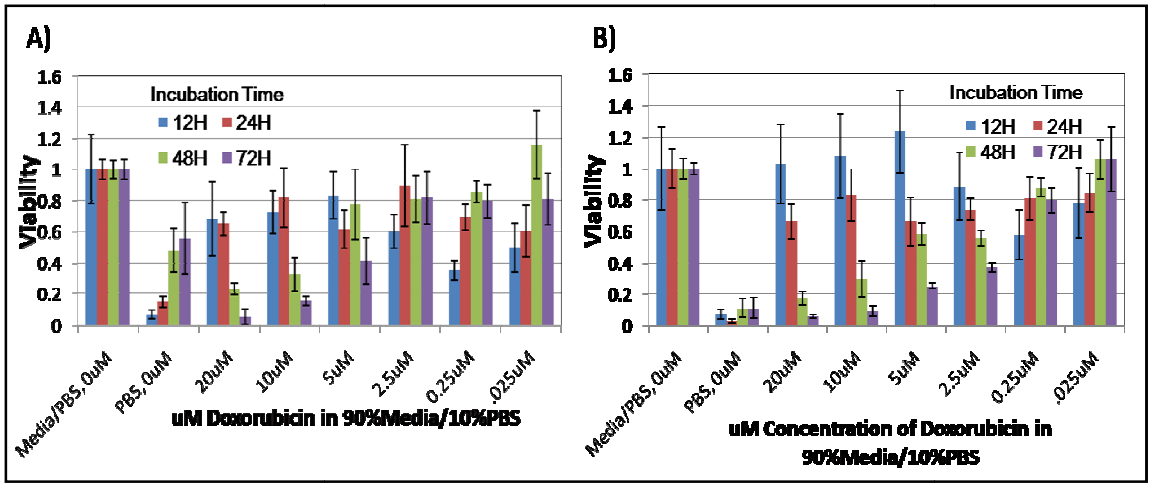

Figure 5.9- The effect of doxorubicin loaded PEO-b-PCL polymersomes on HUVECs (A) SK-BR-3 cells (B) in co-culture.

Each bar represents the mean of four samples and error bars are standard deviation. All conditions are normalized to the initial fluorescence and then to cultures grown in Media(90%)/PBS(10%) without vesicles.

As a final proof of concept, the following preliminary studies were carried out to investigate the effect of dual drug (DOX and combretastatin) loaded polymersomes on co-cultures of SK-BR-3 cells and HUVECs. Similar to the single drug loaded vesicles, we see a strong dependence on both concentration and time for the SK-BR-3 cells, especially at the higher drug concentrations where viability decreases with each time point after the first 24 hours. In addition, at the 72 hour time point, a clear drug concentration dependence is exhibited where the viability ranges from ~100% at the lowest concentration to ~20% at the highest concentration of drug (Figure 5.10B). The HUVEC response to the dual drug loaded vesicles is not nearly as strong as what is observed for the SK-BR-3 cells. A loose dependence on concentration and time is observed (Figure 5.10A), however, additional studies are required to precisely determine the effect of the dual drug vesicles on HUVECs in co-culture. Follow up studies will be described in Chapter 7.

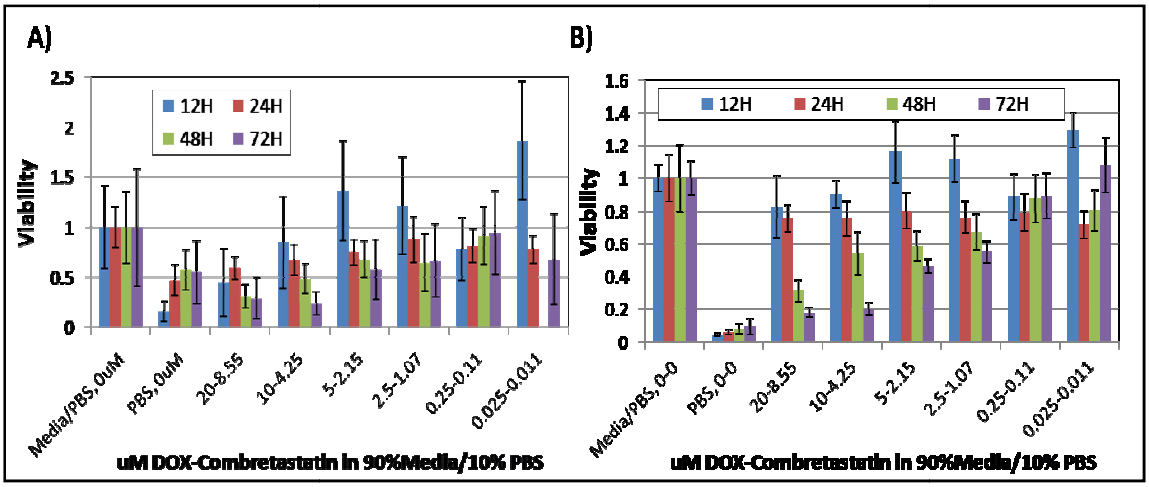

Figure 5.10- The effect of doxorubicin-combretastatin dual loaded PEO-b-PCL polymersomes on HUVECs (A) and SK-BR-3 cells (B) in co culture.
Each bar represents the mean of four samples and error bars are standard deviation. All conditions are normalized to the initial fluorescence and then to cultures grown in Media(90%)/PBS(10%) without vesicles.

5.5 CONCLUSIONS

We successfully utilized nano-polymersomes formulated from PEO-b-PCL diblock copolymer for *in vitro* delivery of both imaging agents as well as therapeutics. NIR-emissive polymersomes were used to determine uptake of polymersomes in human umbilical vein endothelial cells (HUVECs) and SK-BR3 tumorigenic cells. Vesicle uptake for both cell lines was dependent on concentration and incubation time. As vesicle concentration in the media increased, cellular uptake also increased. Furthermore, increased incubation time generally resulted in increased uptake. At higher HUVEC densities and/or high vesicle concentration, uptake was seen as early as 45 minutes and increased with extended incubation times. At lower concentrations, extended time was necessary for significant vesicle uptake.

Toxicity studies on drug loaded as well as empty vesicles were carried out using CellTiter-Blue™ Cell Viability Assay (Promega). A viability assay demonstrated

biocompatibility of the nanoparticles without drug or imaging agent at all concentrations with HUVECs. The SK-BR-3 cells demonstrate a 50% loss in viability after 12 hour incubation with empty vesicles at high and intermediate concentrations of polymer. At low concentration of polymer, SK-BR-3 viability does not appear to be effected. The cytotoxic potential of combretastatin A-4 loaded polymeric vesicles and doxorubicin loaded polymeric vesicles on HUVECs and SK-BR3 tumorigenic cells were determined. For both cell lines, toxicity was generally both concentration and time dependent. For HUVECs, a 50% reduction in viability is seen within 12 hours at high concentrations of combretastatin A-4; at longer times, cellular viability is decreased to approximately 25% viable even at low concentrations of combretastatin A-4. For SK-BR3 cells, cell growth for drug treated cells was arrested, and at extended times cells appeared to be dying. Similar results were observed for HUVECs and SK-BR-3 cells treated with doxorubicin loaded vesicles. When co-cultured, the effect of the drug is less pronounced then when the cells are treated separately, but at high concentrations of drug and/or extended incubation times, the cytotoxic effect of the drug loaded vesicles is observed.

Thus, this study highlights the feasibility of using polymersomes to deliver vascular disrupting agents to endothelial cells simultaneously with treating tumors.

5.6 ACKNOWLEDGEMENTS

This work was supported by grants from the National Institutes of Health (CA115229), and the University of Pennsylvania's Institute for the Translational Medicine and Therapeutics (ITMAT).

5.7 REFERENCES

1. Photos, P.J., et al., *Polymer vesicles in vivo: correlations with PEG molecular weight.* Journal of Controlled Release, 2003. **90**(3): p. 323-334.
2. Bermudez, H., et al., *Molecular weight dependence of polymersome membrane structure, elasticity, and stability.* Macromolecules, 2002. **35**(21): p. 8203-8208.
3. Lee, J.C.M., et al., *Preparation, stability, and in vitro performance of vesicles made with diblock copolymers.* Biotechnology and Bioengineering, 2001. **73**(2): p. 135-145.
4. Meng, F., G.H.M. Engbers, and J. Feijen, *Biodegradable polymersomes as a basis for artificial cells: encapsulation, release and targeting.* Journal of Controlled Release, 2005. **101**(1-3): p. 187-198.
5. Ghoroghchian, P.P., et al., *Bioresorbable vesicles formed through spontaneous self-assembly of amphiphilic poly(ethylene oxide)-block-polycaprolactone.* Macromolecules, 2006. **39**(5): p. 1673-1675.
6. Carter, S.K., *ADRIAMYCIN (NSC-123127) - THOUGHTS FOR FUTURE.* Cancer Chemotherapy Reports Part 3 Program Information-Supplement, 1975. **6**(2): p. 389-397.
7. Young, R.C., R.F. Ozols, and C.E. Myers, *THE ANTHRACYCLINE ANTI-NEOPLASTIC DRUGS.* New England Journal of Medicine, 1981. **305**(3): p. 139-153.
8. Barenholz, Y., et al., *STABILITY OF LIPOSOMAL DOXORUBICIN FORMULATIONS - PROBLEMS AND PROSPECTS.* Medicinal Research Reviews, 1993. **13**(4): p. 449-491.
9. Gabizon, A.A., *SELECTIVE TUMOR-LOCALIZATION AND IMPROVED THERAPEUTIC INDEX OF ANTHRACYCLINES ENCAPSULATED IN LONG-CIRCULATING LIPOSOMES.* Cancer Research, 1992. **52**(4): p. 891-896.
10. Gabizon, A., et al., *LIPOSOMES AS INVIVO CARRIERS OF ADRIAMYCIN - REDUCED CARDIAC UPTAKE AND PRESERVED ANTI-TUMOR ACTIVITY IN MICE.* Cancer Research, 1982. **42**(11): p. 4734-4739.
11. Tozer, G., C. Kanthou, and B. Baguley, *Disrupting Tumor Blood Vessels.* Nature Rev. Cancer, 2005. **5**: p. 423-435.
12. Kerbel, R.S. and B.A. Kamen, *The anti-angiogenic basis of metronomic chemotherapy.* Nature Rev. Cancer, 2004. **4**: p. 423-436.
13. Hanahan, D., G. Bergers, and E. Bergsland, *Less is more, regularly: metronomic dosing of cytotoxic drugs can target tumor angiogenesis in mice.* The Journal of Clinical Investigation, 2000. **105**: p. 1045-1047.
14. Gaukroger, K., et al., *Novel syntheses of cis and trans isomers of combretastatin A-4.* Journal of Organic Chemistry, 2001. **66**(24): p. 8135-8138.
15. Discussions with Dr. B. Barnhart, U.o.P., Abramson Family Cancer Research Institute.
16. Eliaz, R.E. and F.C. Szoka, *Liposome-encapsulated doxorubicin targeted to CD44: A strategy to kill CD44-overexpressing tumor cells.* Cancer Research, 2001. **61**(6): p. 2592-2601.

17. Ghoroghchian, P.P., et al., *Near-infrared-emissive polymersomes: Self-assembled soft matter for in vivo optical imaging.* Proceedings of the National Academy of Sciences of the United States of America, 2005. **102**(8): p. 2922-2927.

Chapter 6

POLYMERSOMES: DISCOVERING THEIR DRUG DELIVERY AND IMAGING POTENTIAL *IN VIVO*

ADAPTED FROM

Dalia Hope Levine, P. Peter Ghoroghchian, Jaclyn Freudenberg, Geng Zhang, Michael J. Therien, Mark I. Greene, Daniel A. Hammer, and Ramachandran Murali, *Methods*, 2008, vol. 46, p. 25-32.

6.1 SUMMARY

Polymersomes (polymer vesicles) have been shown to possess a number of attractive biomaterial properties compared to liposomes (phospholipid vesicles), including prolonged circulation times, increased mechanical stability, as well as the unique ability to incorporate numerous large hydrophobic molecules within their thick lamellar membranes and hydrophilic molecules within their core. We have previously shown the ability to generate two types of self-assembled nano-sized vesicles ranging in size from 100's of nanometers to 10's of microns; one type comprised of a biocompatible diblock copolymer consisting of polyethyleneoxide (PEO) and polybutadine (PBD) and a second fully-bioresorbable vesicle consisting of two FDA-approved building blocks: polyethyleneoxide (PEO) and polycaprolactone (PCL). In addition, we have successfully loaded imaging agents, such as porphyrin-based near infrared (NIR) fluorophores, and therapeutics such as doxorubicin, an anti-neoplastic agent, into these polymersomes and tracked their release *in situ* and *in vivo*.

NIR-emissive polymersomes, loaded with porphyrin, can be used for biodistribution studies, to track the location of the polymersomes, and potentially for diagnostic studies. Here, we utilize NIR-emissive polymersomes to determine polymersome biodistribution in tumor bearing mice using a noninvasive small animal optical imaging instrument which detects the NIR fluorescence signal. Passive accumulation of NIR-emissive polymersomes in tumor tissues of mice, as well as other organs, is evidenced. Using porphyrin polymersomes for biodistribution studies will greatly decrease the number of animals required for such studies since the location of the

polymersomes can be determined without sacrificing animals at multiple time points to perform histology on the excised organs.

Doxorubicin, an anti-neoplastic agent, was encapsulated to serve as a model system for the release of a physiologically relevant compound from the PEO-b-PCL polymersomes. The therapeutic potential of doxorubicin loaded polymersomes is shown; drug loaded bioresorbable polymersomes were administered *in vivo* and their capability to retard tumor growth was assessed using such metrics as tumor size and body weight. Doxorubicin loaded polymersomes were able to retard tumor growth in a live animal on a par with the commercially available DOXIL, liposomal doxorubicin. Furthermore, mouse weights remained within +/-1.5g, for all treatment groups throughout the study.

Lastly, the marriage of the porphyrin polymersome with the doxorubicin polymersome was attempted *in vivo*. Results are promising suggesting with further work that the *multi-functional* polymersome for theranostic applications could be a reality.

6.2 INTRODUCTION

The fully PEG-ylated polymersome, with its thick hydrophobic membrane and large aqueous core, posses a number of superior biomaterial properties [4-6, 8] which make it ideally suited to facilitate biomedical applications such as deep tissue optical imaging and drug delivery.

Chapter 4 discusses the basis and rationale for using near infrared imaging (NIR) agents in contrast to visible probes for *in vivo* imaging applications and the tunable spectral properties of the porphyrin fluorophores used in the *in vivo* imaging studies

discussed in this chapter. This chapter will build upon those concepts highlight in the previous chapters and discuss some of the principles of *in vivo* fluorescence based imaging.

In vivo deep tissue fluorescence based imaging characterizes the interaction of photons with tissue through three basic parameters, namely absorption, light scattering, and emission. As discussed in Chapter 4, light absorption by the oxy and deoxyhemoglobin, water, and other molecules found in tissues [123, 124] is greatest below 700nm, causing significant auto-fluorescence in the visible spectra [125] and limiting the penetration depth to less than a few millimeters [126]. However, owing to the small tissue absorption coefficient in the NIR window (700nm-900nm) of the spectrum, light can penetrate much deeper into the tissues, enabling imaging deeper imaging into the tissues in contrast to imaging with probes in the visible region of the spectra [115].

In addition to the tissue properties which complicate *in vivo* imaging, the contrast agent itself must be nontoxic and overcome certain challenges *in vivo* such as absorption, distribution, metabolism, and excretion [127]. Furthermore, the contrast agent must be able localize and remain at the site with enough fluorescent intensity to be imaged [127, 128].

Hence, the development of NIR contrast agents with appropriate biological parameters is crucial for in depth optical imaging of living tissues. We have investigated the performance of NIR-emissive porphyrin polymersomes, polymeric vesicles loaded with porphyrin contrast agents, in both a biocompatible and bioresorbable formulation

and demonstrated their ability to assist in diagnostic applications as well as drug biodistribution studies.

Chapter 2 and Chapter 4 discuss the fabrication of the drug loaded polymersomes and the drug loaded polymersome for imaging purposes, while Chapter 5 demonstrates the potential of these vesicles *in vitro*. In addition to the use of polymersomes for *in vivo* optical imaging in the NIR, this chapter will investigate use of drug loaded vesicles for *in vivo* applications.

Currently many pharmaceutical agents exist whose systemic toxicity is too great to be administered clinically. Other compounds, would be clinically beneficial, however their hydrophobicity precludes them from being administered by conventional methods. Hence, a delivery vehicle with the ability to deliver such toxic and hydrophobic molecules at a high payload to the site of interest is imperative for advancing therapies.

Previously, researchers have demonstrated the therapeutic benefits of encapsulating pharmaceutical agents with low bioavailabilty or high systemic toxicity in PEG-ylated lipid vesicles, termed liposomes [120, 129, 130]. As described throughout this thesis, polymersomes, polymeric vesicles, have unique biological properties [4-6, 8] to render them superior to liposomes for drug delivery applications. Hence considerable effort has been made in developing polymeric vesicles for drug delivery tools [27, 43, 131, 132]. The *in vivo* performance of the fully bioresorbable PEO-b-PCL polymersome for the delivery of doxorubicin, a chemotherapeutic agent known to causes cardiotoxicty will be examined in this chapter. Lastly, the chapter will close by demonstrating the potential for using polymersomes as both drug and imaging delivery agents.

6.3EXPERIMENTAL METHODS

Nude athymic mice used in the studies discussed below were housed under USDA- and AAALAC-approved conditions with free access to food and water. The University of Pennsylvania Institutional Animal Care and Use Committee and Small Animal Imaging Facility (SAIF) Animal Oversight Committee approved all experimental procedures. All *in vivo* imaging was conducted at the SAIF in the Department of Radiology at the University of Pennsylvania.

6.3.1 Preparation of Drug and Imaging Agent Loaded Polymersomes

Drug loaded vesicles, porphyrin loaded vesicles, as well as drug-porphyrin vesicles were prepared as described in Chapter 2 and Chapter 4. Briefly, thin-film hydration was used to assemble the ~200nm PEO-b-PCL copolymers into equilibrium morphologies [10]. Polymersomes were incubated with doxorubicin in a ratio of 1:.4 polymer:drug (w/w) for ~9h at a temperature above their main gel to liquid-crystalline phase transition temperature, trapping the drug in the aqueous core. Nonentraped DOX was removed using HPLC; the solution was passed through two HiTrap desalting columns and further removed using a Centricon tube to ensure the absorbance of drug in the subnatant was undetectable at 480nm. The collected DOX polymersome suspension was concentrated and passed through a 1um membrane prior to injection.

To determine the concentration of doxorubicin in the PEO-b-PCL polymersomes, sample aliquots were removed from the concentrated stock solution, and lyophilized to destroy the vesicle structure and release the encapsulated DOX from the core of the polymersome. The freeze-dried powder was reconstituted in tertiary butanol:water 9:1,

v/v containing 0.075N HCl or 90% isopropyl alcohol containing 0.075 M HCl. The concentration of DOX was determined using Beer's Law by measuring the absorbance at 480nm using a molar extinction coefficient of 12,5000$cm^{-1}M^{-1}$ in either solvent [70, 122].

6.3.2Preparation of Porphyrin Imaging Agent Loaded PEO-b-PBD and PEO-b-PCL Polymersomes

Porphyrin loaded PEO-b-PCL and PEO-b-PBD polymersomes were prepared as described in Chapter 4. Briefly, self-assembly via thin-film hydration followed by freeze thawing and extrusion were used to yield small porphyrin PEO-b-PBD polymer vesicles or porphyrin PEO-b-PCL polymersomes (~200nm diameter)[9]. The porphyrin dye is localized to the vesicle membrane. The suspension was centrifuged using Millipore Centricon Tubes to obtain a porphyrin concentration of 15uM as determined by absorbance spectroscopy. Prior to injection, vesicles were passed through a sterile 200nm membrane.

The concentration of the porphyrin vesicles in solution was determined by measuring the absorbance at 794nm using a molar extinction coefficient of $1.29*10^{5}M^{-1}cm^{-1}$ [9]. Polymer concentration was determined by a mathematical calculation, since the ratio of porphyrin to polymer was set at 1:40 (molar ratio).

6.3.3 Cell Culture and Establishment of Tumors in Nude Mice

The T6-17 cell line which is derived from NIH-3T3 cells by over-expressing the human erbB2 receptor was used for all *in vivo* studies; these cells are HER2-expressing transformed tumor cells with the ability to develop tumors in nude mice [133].

The T6-17 cells, were cultured in DMEM - high glucose 4.5 gm/L (base media), 10% fetal bovine serum (FBS), 1% Pen/Strep 100X (10000u/ml P - 10mg/ml S), and 1% glutamine. Cells were maintained in plastic culture flasks at 37°C in a humidified atmosphere containing 5% CO_2 in air and subcultured at subcultivation ratio of 1:10 when the flasks were 70% to 90% confluent. When cells were deemed 70%-90% confluent, growth media was removed from the culture flask via aspiration and the flask was washed with Phosphate Buffered Saline (PBS). The PBS was removed and 0.25%trypsin-EDTA was added and the flask was returned to the incubator for 5min at 37□C and 5% CO_2 in air. Post trypsin incubation, media was added to the flask and the wall was washed in order to remove all cells. The cell suspension was then transferred to a conical tube and centrifuged at 1000rpm for 5 minutes to pellet the cells. The supernatant was aspirated and the cells were resuspended in fresh growth media. When cells were to be used for tumor studies, a cell count was performed.

6.3.4 In vivo Biodistribution and Diagnostic Studies Using Porphyrin loaded PEO-b-PBD Polymersomes

To establish the tumor *in vivo*, T6-17 tumor cells ($1x10^6$) were injected s.c. into the flank of athymic nude female mice. At least ten days after inoculation of tumor cells, when tumors were visible and palpable, treatment with polymersomes commenced as described.

In order to reduce background fluorescence for extended imaging studies, lasting more than 12 hours, mice were switched from a fenbendazole-impregnated diet for prophylaxis purposes to AIN-76A, a low-autofluorescence rodent diet (Research Diets,

Inc.; New Brunswick, NJ). 5 to 7 days prior to imaging and remained on the low-fluorescence feed until the culmination of the study.

Once the tumors were visible and palpable, 100ul of the porphryin polymersome solution (15uM porphyrin) was injected intravenously into the tail vein of a tumor bearing (T6-17 cells) nude mouse. Fluorescent signal was measured prior to injection, as well as at specific time points ranging from hours to days, post injection, using one of the following small animal imagers: a) the GEART eXplore Optics, 2) the LICOR Pearl Imager. At the culmination of the study, the mice were sacrificed according to protocol. At the culmination of the extended study, sacrificed mice were carefully dissected and their organs were excised for further analysis.

6.3.5 In vivo Intratumor Studies Using Porphyrin loaded PEO-b-PBD Polymersomes

To establish the tumor *in vivo*, T6-17 tumor cells ($1x10^6$) were injected s.c. into the flank of athymic nude female mice. At least ten days after inoculation of tumor cells, when tumors were at least visible and palpable, 100uL of a 15uM solution of porphyrin PEO-b-PBD polymersomes was injected intravenously into the tail vein of the tumor bearing nude mouse. Approximately eight hours post injection of vesicles, 100ul of AngioSense-IVM 680 (VisEn Medical), a large fluorescence agent (250k MW) that remains localized in the vasculature for extended periods of time (λ_{ex}=680±10nm, λ_{ex}=700±10nm), was intravenously injected into the retro-orbital vein of the mouse.

Immediately following the injection of AngioSense-IVM 680, a full body scan of the mouse in the prone position was taken using the GEArt. Subsequently, a small portion the skin was removed from the tumor and the tumor was imagined using the

Olympus IV-100. At the culmination of the study, the mice were euthanized as per protocol. .

6.3.6 In vivo Therapeutic Study Using Doxorubicin Loaded PEO-b-PCL Polymersomes

To establish the tumor *in vivo*, T6-17 tumor cells ($1x10^6$) were injected s.c. into the flank of athymic nude female mice. One week after inoculation of tumor cells, when tumors were visible and palpable, treatment with polymersomes commenced as described.

Once the tumors were visible and palpable, the mice were injected through the tail vein with 200uL of (1) polymersomes loaded with DOX at a concentration of 1mg/ml, (2) DOXIL (liposomal formulation of DOX) at a DOX concentration of 1mg/ml, (3) free DOX (unencapsulated drug) at a DOX concentration of 1mg/ml, and (4) PBS. Each group consisted of five mice. The concentration of DOX in all administrations was 1mg/ml and 200ul of solution was administered to each mouse, to yield a dose of 10mg of drug/kg.

After the administration of treatment (i.e. post i.v. injection), tumors were measured daily and mice were weighed every other day. Tumor volume was determined by the equation, l*w*h. Nine days after the start of treatment, the mice were sacrificed, bled from the retrooribital sinuses, and organs were harvested. Using a HEMAVET, blood work was performed to be used as a metric for systemic toxicity resulting from each of the treatment groups. Physical appearance and behavior were recorded as well.

6.3.7 In vivo Theranostic Study Using Doxorubicin and Porphyrin Loaded PEO-b-PCL Polymersome

To establish the tumor *in vivo*, T6-17 tumor cells ($1x10^6$) were injected s.c. into the right flank of athymic nude female mice. Nine days after inoculation of tumor cells, when tumors were visible and palpable, treatment with polymersomes commenced as described in the following sections.

In order to reduce background fluorescence for extended imaging studies, lasting more than 12 hours, mice were switched from a fenbendazole-impregnated diet for prophylaxis purposes to AIN-76A, a low-autofluorescence rodent diet (Research Diets, Inc.; New Brunswick, NJ). 5 to 7 days prior to imaging and remained on the low-fluorescence feed until the culmination of the study.

Once the tumors were visible and palpable, the mice were injected through the tail vein with 250uL of:

(1) Doxorubicin-Porphyrin PEO-b-PCL polymersomes at a concentration of 0.122mgDOX/ml (4.65uM porphyrin and 2.6 mgPEO-b-PCL/ml as determined by the porphyrin absorbance),

(2) Porphyrin PEO-b-PCL polymersome at a concentration of 2.6mgPEO-b-PCL/ml (4.65uM porphyrin)

(3) PEO-b-PCL polymersomes without DOX or porphyrin at a concentration of 2.6mgPEO-b-PCL/ml

(4) free DOX drug at a DOX concentration of 0.122mg/ml.

Each group consisted of four mice. The concentration of DOX delivered to the mice in this study was approximately 10% of the concentration delivered in the Therapeutic Study described above. Furthermore the porphyrin concentration was approximately 1/3 the concentration delivered in the Diagnostic Studies described above, however, twice the volume of porphyrin vesicle suspension was delivered, making the total porphyrin injected approximately 2/3 of the amount injected in previous studies. Recall from Chapter 4, the loading of DOX into porphyrin vesicles is difficult and inefficient; this is most likely the result of the large hydrophobic porphyrin molecules hampering the diffusion of the DOX molecules across the hydrophobic bilayer.

Post treatment, tumors were measured daily and mice were weighed every day. Tumor volume was determined by the equation, l*w*h.

Prior to treatment, mice that were to be administered porphyrin vesicles and porphyrin-DOX vesicles were pre-scanned using the Licor Odyssey Infrared Imaging System equipped with the Odyssey MousePOD *In vivo* Imaging Accessory. Mice were then scanned at regular intervals using the Odyssey and MousePOD Accessory. Five days after the start of treatment, the mice were sacrificed and carefully dissected. Organs were imaged post excision using the LICOR Odyssey.

6.4 RESULTS AND DISCUSSION

6.4.1 In vivo Biodistribution Studies Using Porphyrin Polymersomes

When Porphyrin loaded NIR-emissive nanopolymersomes are injected into the tail-vein of mice, the biodistribution of the nanoparticles can be tracked *in vivo* via non-invasive NIR fluorescence-based optical imaging. Figure 6.1 demonstrates the ability to

track PEO-b-PBD polymer vesicles in tumor bearing mice over 12 h. Additional extended studies using porphyrin loaded PEO-b-PBD (Figure 6.2) and PEO-b-PCL polymersomes demonstrated the ability to track vesicles *in vivo* for up to 9 days and will be discussed in this section and in Section6.4.4. It is important to note that initial studies were carried out using the biocompatible vesicle since it was known not to degrade *in vivo*. Nonetheless, it is envisioned that the bioresorbable vesicles generated from PEO-b-PCL diblock, might be able to link changes in fluorescence not only to the clearance of the vesicle but also to degradation of the vesicle.

Porphyrin NIR- emissive polymersomes injected into the tail vein of a tumor bearing mouse accumulated at the tumor site of non-necrotic tumors within four hours and remain at the tumor site for at least 72hours. Furthermore, these vesicles are observed *in vivo* for at least 9 days and are cleared by organs of the reticuloendothelial system (RES) as determined by imaging of fluorescence signals. Upon culmination of the extended studies and excision of the organs, it was determined, though fluorescence imaging of the organs, that there was significant vesicles accumulation in the spleen, and liver. Furthermore, even 7 days post treatment, a significant fluorescent signal is observed from the tail.

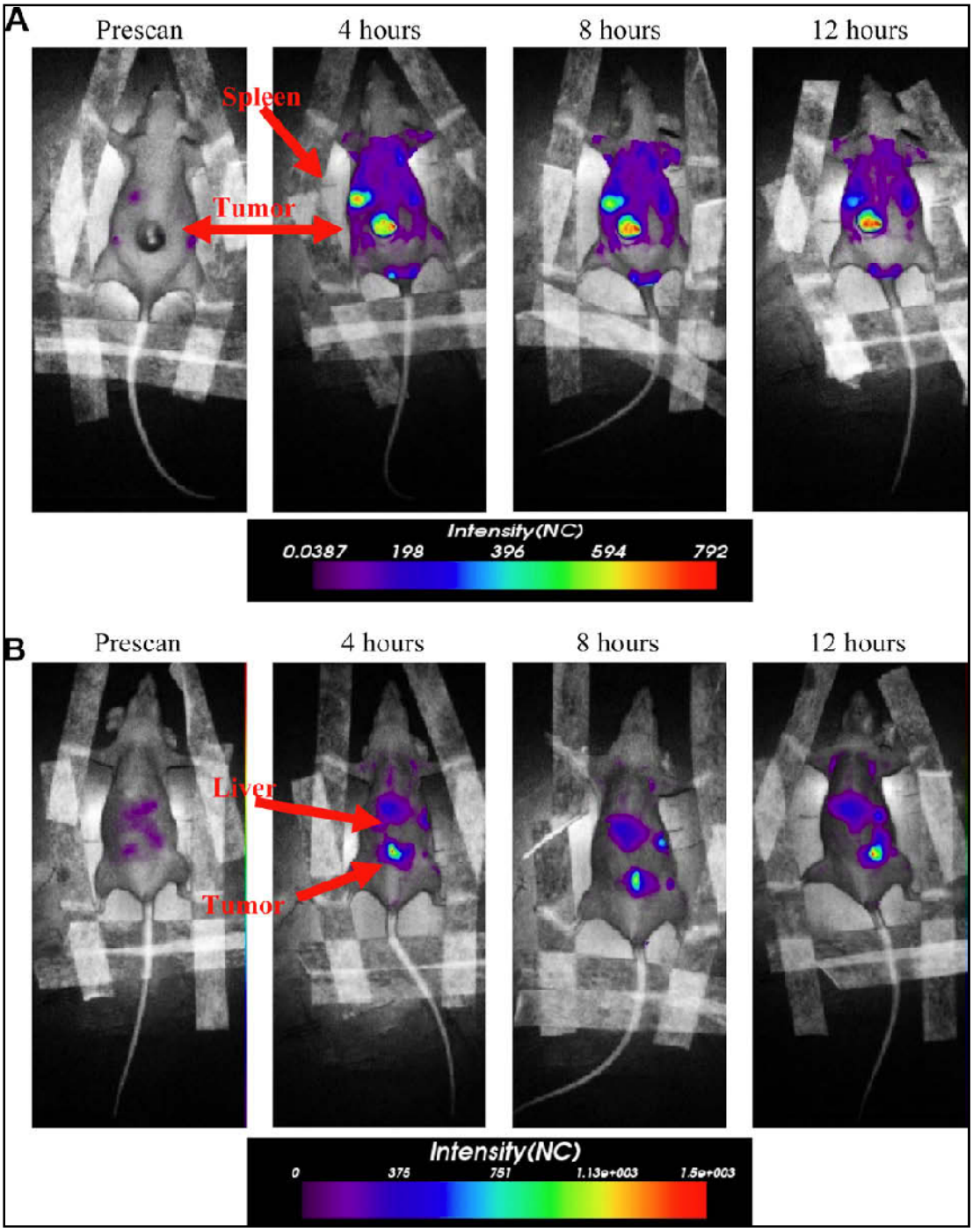

Figure 6.1- Tumor imaging by NIR-emmisive PEO-b-PBD polymersome.
Fluorescence images obtained using eXplore Optix instrument of the same mouse taken prior to administration of NIR-emissive polymersomes, and at 4, 8, and 12 h post tail-vein injection. (A) Prone position, (B) supine position (k_{ex} = 785 nm, k_{em} = 830–900 nm). The arrows in the prone and supine positions suggest location of organs. In the supine position, the arrow suggests the fluorescence emanating from

the lower portion of the mouse body is from the tumor; it may also be emanating from the gut of the mouse due to break down of food.

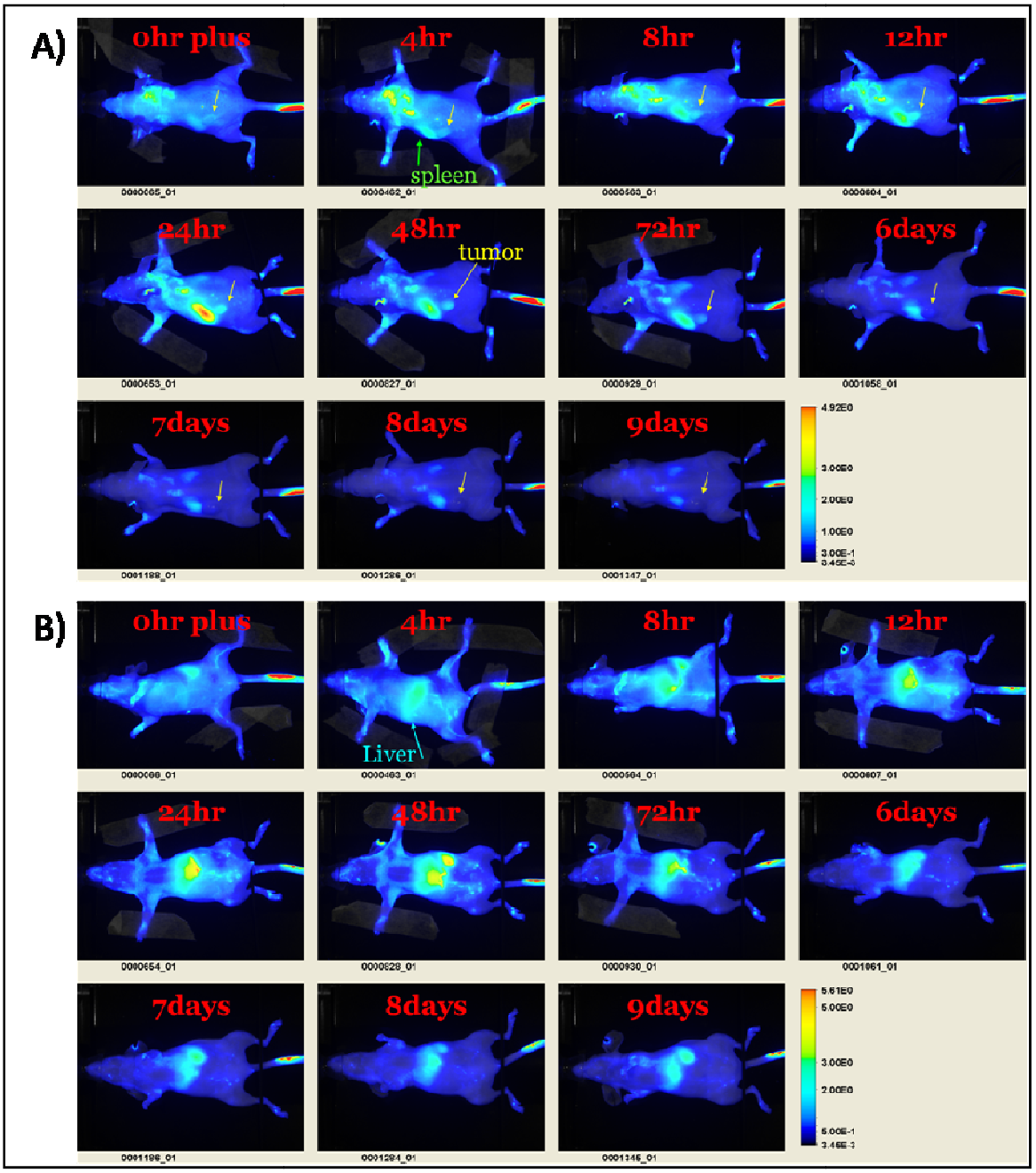

Figure 6.2- Fluorescence images of the same mouse taken right after administration of NIR-emissive PEO-b-PBD polymersomes, and at 4, 8,12, 48, 72, 144, 168, 192, and 216 hours post tail-vein injection.
Images were acquired using the Licor Pearl Imager. (A) Prone Position (B) Supine Position (λex =785nm, λem=830-900nm)

6.4.2 In vivo Intratumor Studies Using Porphyrin loaded PEO-b-PBD Polymersomes

The Olympus IV-100, intravital laser scanning microscope for small animal imaging, was used to examine the location of polymersome in relation to the tumor vasculature. Prior imaging with the Olympus IV-100, the mouse was imaged using the GEArt to confirm the distribution of porphyrin vesicles and AngioSense-IVM 680 in the mouse's body; furthermore the localization of porphyrin vesicles at the tumor site was verified using the GEArt.

Once the distribution of dye and vesicles was confirmed using the GEArt, the tissue on the tumor just below skin was imaged using the Olympus IV-100. Figure 6.3 clearly shows the co-localization of AngioSense IVM-680 in the vasculature and the porphyrin PEO-b-PBD vesicles, confirming their location in the tumor vasculature. The left hand panel of Figure 6.3 used the signal from AngioSense IVM-680 to show the tumor vasculature (700 channel), while the middle panel shows the fluorescent signal from the polymersomes in the same area (800channel); the right hand panel is an overlay of the left and middle panels and clearly shows the localization of porphyrin vesicles within the tumor vasculature.

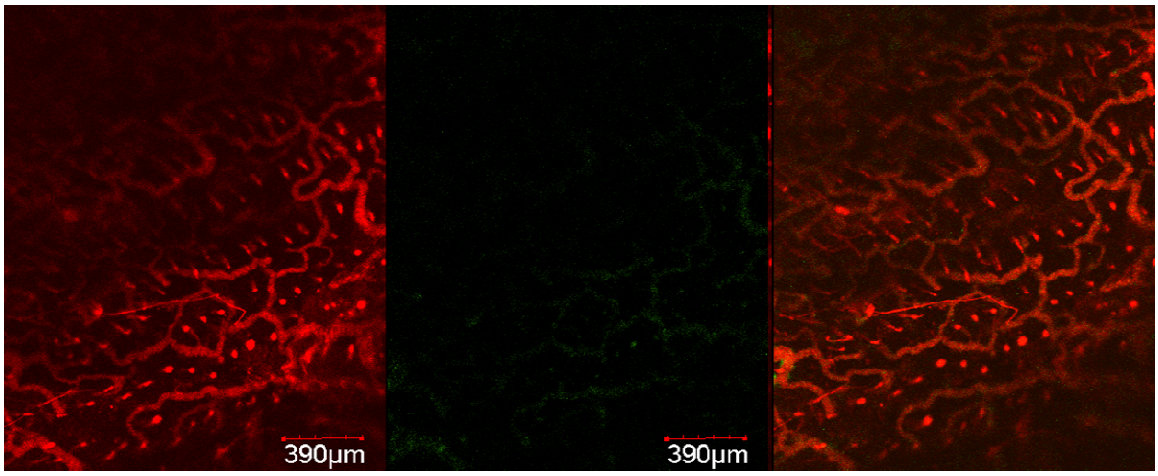

Figure 6.3- Intravital microscopy of the tumor tissue using the Olympus IV-100. Left hand pannel shows the tumor vasculature (using AngioSense IVM 680, 700 channel); Middle pannel shows the localization of porphyrin polymersomes (800 channel); Right pannel is the overly of the images from each channel clearly showing the co-localization of porphyrin vesicles in the blood vessels.

6.4.3 In vivo Therapeutic Study Using Doxorubicin loaded PEO-b-PCL Polymersomes

Doxorubicin loaded bioresorbable PEO-b-PCL polymersomes were administered *in vivo* to xenotransplanted (T6-17 cells) tumor-bearing mice and their therapeutic capability to retard tumor growth was assessed using such metrics as tumor size and body weight.

As demonstrated in Figure 6.4**Error! Reference source not found.**, doxorubicin loaded PEO-b- PCL polymersomes were able to retard tumor growth in mice on a par with the commercially available agent DOXIL ® (a clinically administered liposomal formulation of doxorubicin), and better than free drug and PBS alone. Further, mouse weights remained within ±1.5 g of the initial weight, for all treatment groups throughout the study.

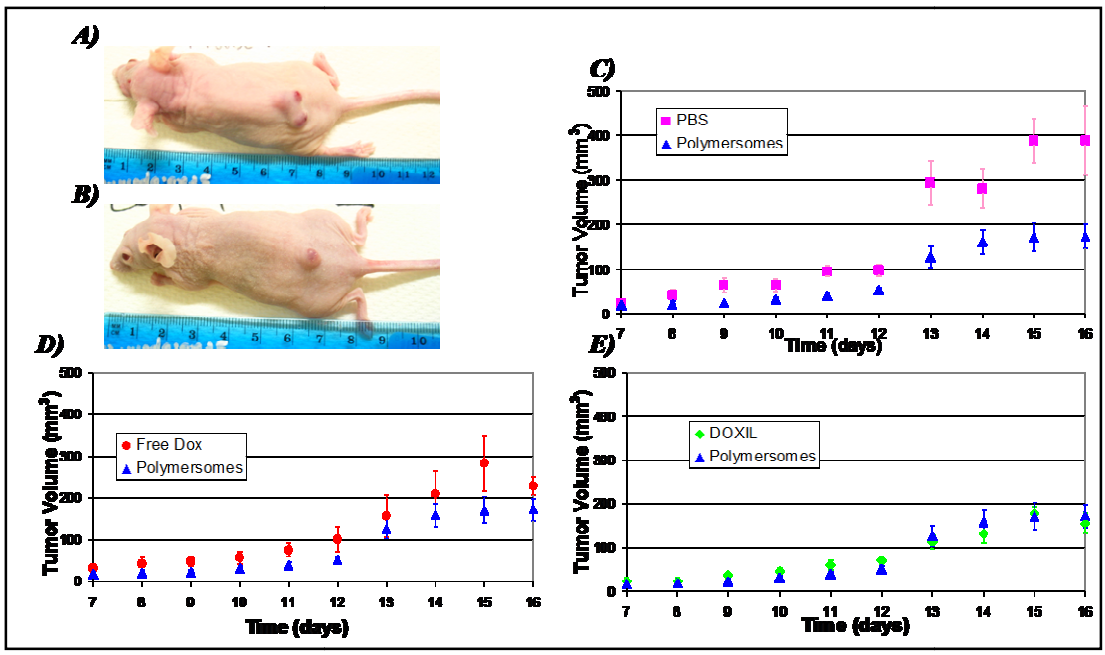

Figure 6.4- Anti-tumor effects of doxorubicin loaded PEO-b-PCL polymersome in mice.
Mice were inoculated with tumor cells on day 0, were administered drug (free dox, dox loaded polymersome, or DOXIL) or PBS on day 7, and sacrificed on day 16. Images of tumor bearing mice administered PBS (A) and DOX polymersomes at the culmination of the study, day 16. (B); (C–E) Average tumor Volume vs. Time, Tumor volumes of the 5 mice per group averaged. Error bars are reported as standard error.

A blood sampled was drawn from each mouse and analyzed using a HEMAVET (Figure 6.5). White blood cell (WBC) count and neutrophil (NE) count are slightly elevated in control mice receiving PBS only, but similar for the mice administered DOX in any form. Since WBC is a measure of the body's response to cytotoxic agents, the results demonstrate that all DOX treatments have the same level of systemic toxicity. RBC counts, HB, HCT and PLT values are similar for the various treatment groups.

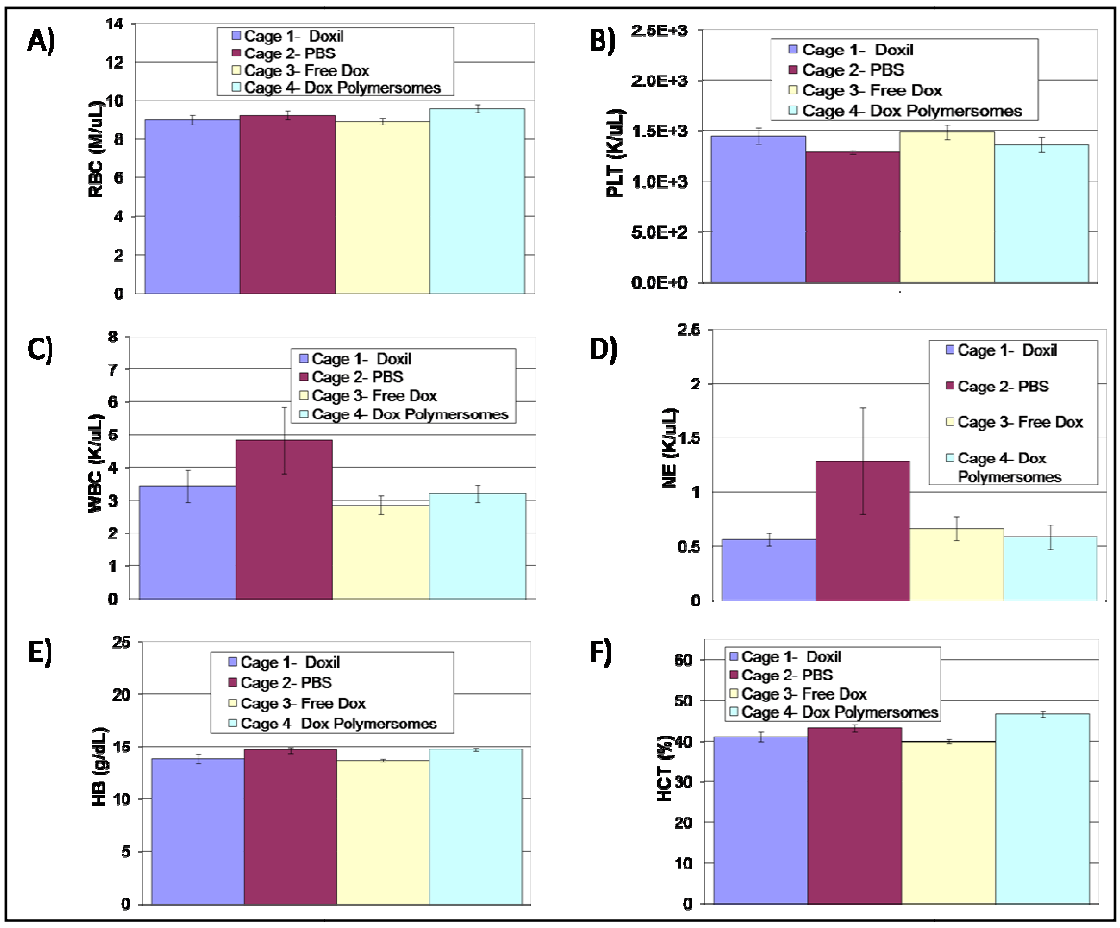

Figure 6.5- The effect of different treatments on the red blood cell (RBC) count (A), platelet (PLT) count (B), white blood cell (WBC) count (C), neutrophil (NE) count (D), hemoglobin (HB) count (E), and hematocrit (HCT) (F).
n=5. Error bars= ±S.E.

The tails and bodies of mice administered Doxil (cage 1) turned pink one day after drug was administered (Figure 6.6A,B) while those administered polymersomes (cage 4) (Figure 6.6C) and PBS or free DOX were not nearly as pink. Pictures of the mouse bodies and tails were taken two days after drug administration. Infected, oozing and/or scabbing tails were observed on 3/5 of the mice receiving free DOX (cage 3) (Figure 6.6A,B) while the tails of mice receiving DOX polymersomes as a treatment (cage 4) showed only slight signs of irritation (Figure 6.7C,D). Images were obtained at the culmination of the study. It should be noted that mice some of the mice that received

Doxil treated mice exhibited aggressive behavior and were difficult to handle in comparison to the mice receiving other treatments suggesting that DOX polymersome is better tolerated than DOXIL.

Figure 6.6- Images of mouse bodies and tails two days after administration of (A, B) Doxil and (C) DOX polymersomes.
Images were taken two days after treatment.

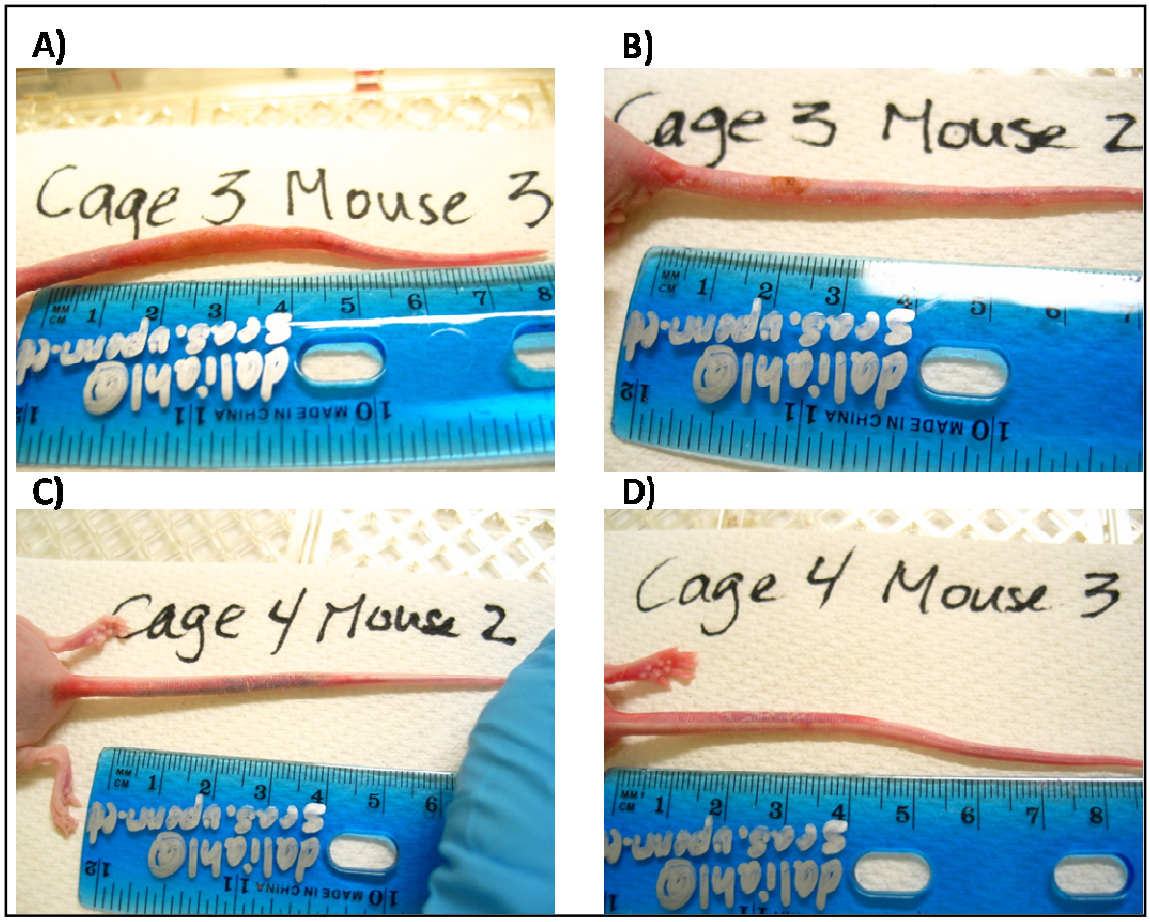

Figure 6.7- Images of mouse tails post free DOX treatment (A,B) and DOXpolymersomes (C,D).
Images were taken at the culmination of the study.

6.4.4 In vivo Theranostic Study Using Doxorubicin and Porphyrin Loaded PEO-b-PCL Polymersome

This study married the two main goals of this thesis linking drug delivery with imaging. As described, mice were administered one of the following treatments: doxorubicin-porphyrin polymersomes, porphyrin polymersomes, unloaded polymersomes or free doxorubicin in PBS, all at the same concentration of drug (doxorubicin), imaging agent (porphyrin), and polymer where applicable.

Figure 6.8 demonstrates the ability to track bioresorbable PEO-b-PCL vesicles loaded with porphyrin *in vivo* using an Odyssey Imager with MousePOD Accessory. It should be noted that there was considerable background on many of the images due to residual dye on the skin or skin distress; when the skin is distressed, the laser light gets trapped in the nicks of the roughened skin, and is detected erroneously as fluorescent signal.

Similar to the imaging study described in Section 6.4.1 using biocompatible PEO-b-PBD vesicles, fully bioresorbable PEO-b-PBD vesicles localize to the tumor within 12 hours, and clear over the course of 120 hours, with the greatest accumulation occurring 24-48 hours post administration. At 24 hours post vesicle administration, signal was observed *in vivo* from 100% of the mice administered porphyrin vesicles and 75% of the mice administered doxorubicin-porphyrin vesicles. At 120 hours post vesicle administration, signal is observed ex vivo from 100% of the tumors of mice administered porphyrin vesicles and porphyrin-doxorubicin vesicles (Figure 6.10). As expected, excised tumors of mice administered PEO-b-PCL polymersomes without porphyrin only

showed fluorescent signal in the 700 channel (red) due to auto fluorescence, but did not show any fluorescent signal in the 800 channel (green) (Figure 6.10).

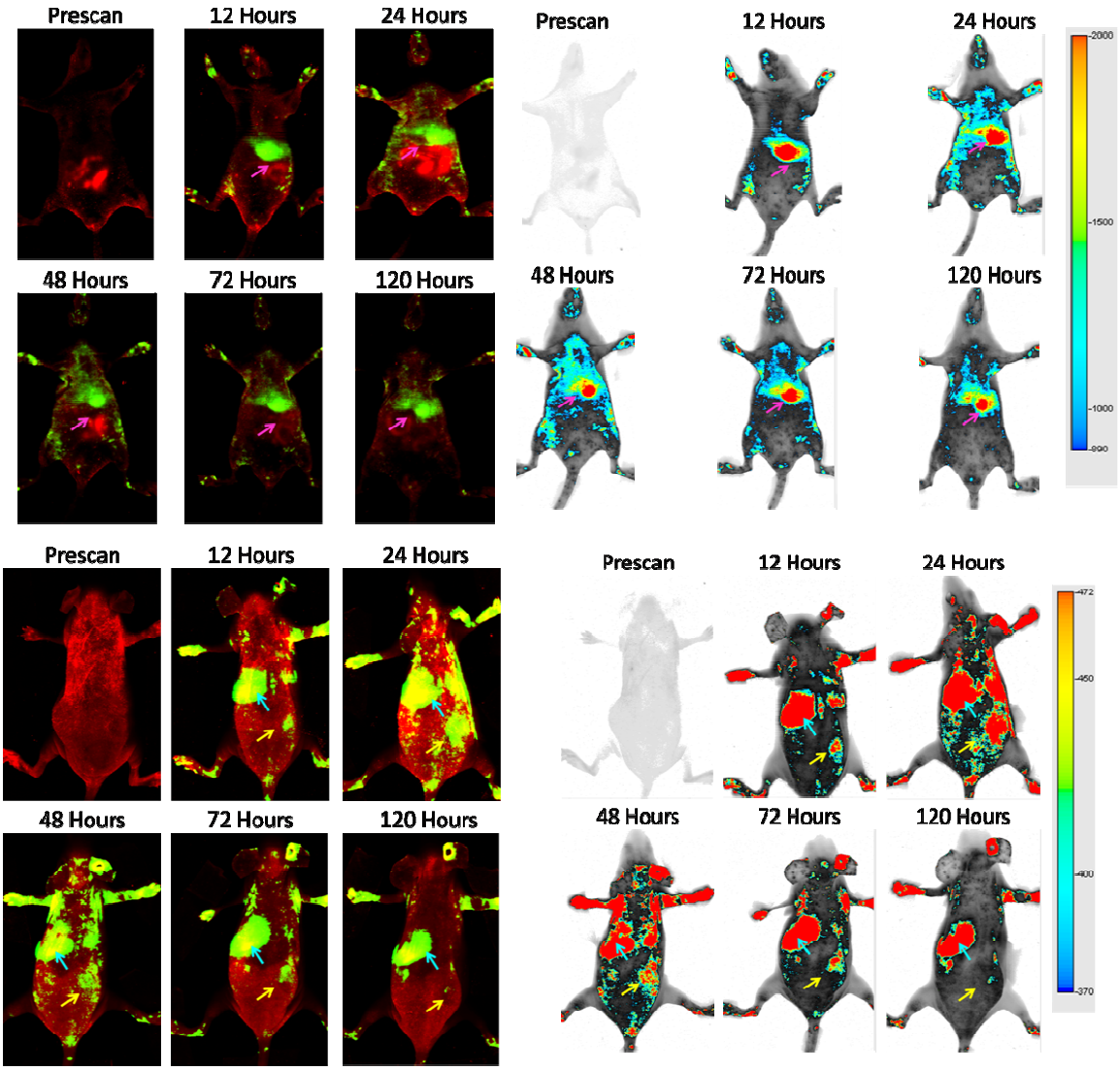

Figure 6.8- Representative fluorescent images of a mouse administered porphyrin PEO-b-PCL vesicles.
Left hand panel: two color images showing 700 channel (red, auto fluorescence) and 800 channel (green, porphyrin polymersomes). Right hand panel: Pseudo-colored rendering of the 800 channel showing the intensity of the signal from various organs. Top (890 to 5000), Bottom (370-472). Top- supine position; Bottom- prone position. Pink arrow- liver; Cyan arrow: spleen; Yellow arrow: tumor.

Figure 6.9- White light image of mouse shown in Figure 6.8.

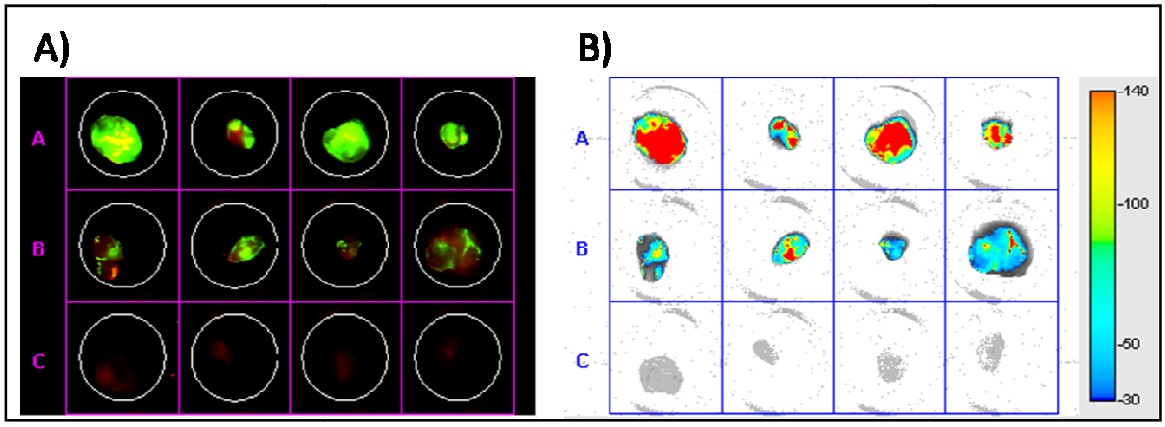

Figure 6.10- Ex vivo imaging of tumors excised 120 hours post administration of vesicles.
A) Two color images showing 700 channel (red, auto fluorescence) and 800 channel (green, porphyrin polymersomes); B) Pseudo-colored rendering of the 800 channel showing the intensity of the signal from various tumors (Range 300-140). Row A- Tumors excised from mice administered porphyrin PEO-b-PCL vesicles; Row B- Tumors excised from mice administered porphyrin-doxorubicin PEO-b-PCL vesicles; Row C- Tumors excised from mice administered PEO-b-PCL vesicles without porphyrin.

Vesicle accumulation in the spleen and liver is apparent in the images in Figure 6.8 and Figure 6.11A. Vesicles are cleared by the kidneys as evidenced Figure 6.11A as well as the fluorescence emanating from the mouse paws and underbelly (observed in Figure 6.8); this results from residual fluorophore on the skin from the urine. Figure 6.11

B and C demonstrate that the accumulation of vesicles in the tumor is heterogeneous and most likely dictated by the blood vesicles or lack thereof in portions of the tumor. Note that after 120 hours, a majority of the vesicles have been cleared from the tumor and have localized to the organs of the RES. Note that there is minimal accumulation of the vesicles in the heart (Figure 6.11). Figure 6.12B shows vesicles sequestered in the tail at the site of injection, while Figure 6.12A shows the tail almost entirely cleared of vesicles; this difference is probably caused by variability in the tail vein injections. It appears that sequestering of vesicles in the tail is predominantly observed when multiple injections (as evidenced by multiple fluorescent sites) are required to deliver the volume of vesicles.

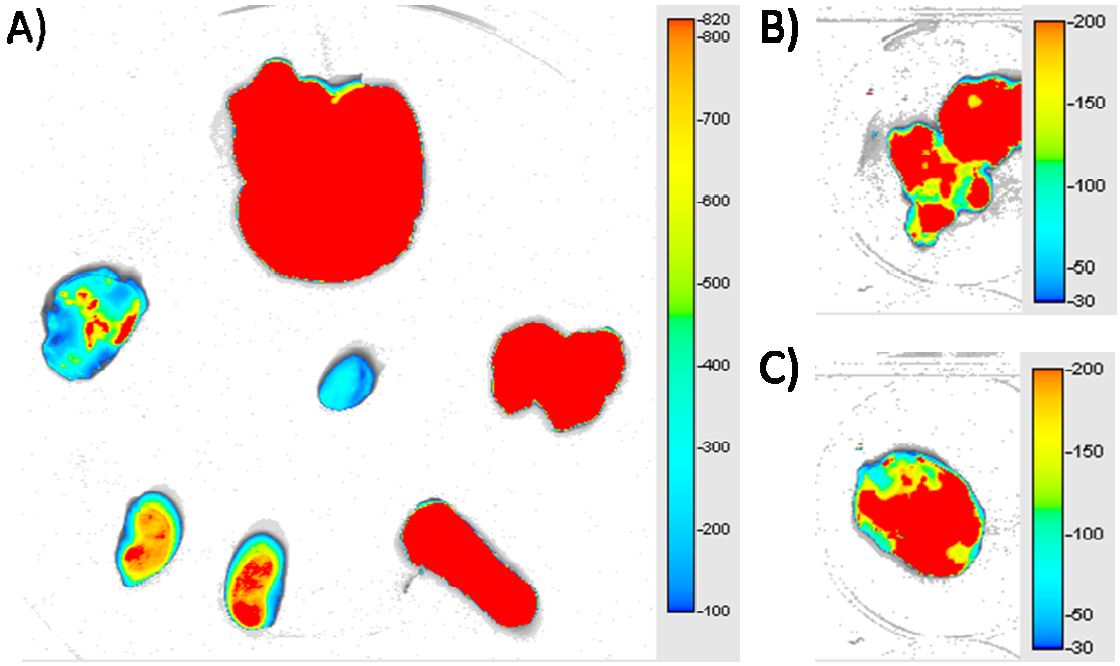

Figure 6.11- Pseudo colored images from fluorescence in the 800 channel emanating from A) excised organs (clockwise: liver, lungs, spleen, kidneys, and tumor. Center position: heart) B) sliced tumor and C) whole tumor.

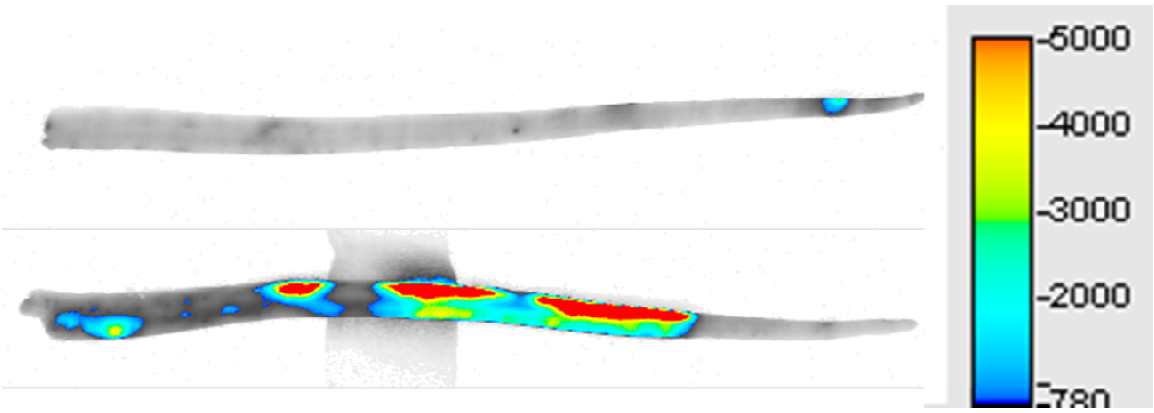

Figure 6.12- Excised tails from two different mice imaged ex vivo. Top tail shows clearance of the vesicles, while the bottom tail shows considerable accumulation of the vesicles in the tumor at the sites of injection.

Figure 6.13 shows the tumor volumes in millimeters cubed for the mice administered the different treatments. It is clear that mice administered porphyrin only vesicles had larger tumors than mice administered doxorubicin-porphyrin vesicles up to four days after treatment. The tumors of the mice administered porphyrin-doxorubicin vesicles were on par with mice administered vesicles only and larger than the tumors of mice administered free DOX after four days of treatment. This most likely results from the fact that at the start of the administration of treatment two populations of tumor sizes were present—large and small. We used mice with tumors in the "large population" for the imaging-drug studies and mice with tumors in the "small population" for the control studies (free DOX and vesicles only). As such, the growth potential for tumors in the "small population" was much less than that of the tumors in the "large population. Hence, although mice administered doxorubicin-porphyrin vesicles had tumors that were on par or greater than mice administered vesicles only or free DOX, respectively, this is probably the result of different tumor sizes at the beginning of the study. Additionally, the amount of drug administered was approximately 10% of that administered in the

therapeutic study. At such a low concentration of drug, variability in the success of the t.v. injection can also lead to a significant variation in the amount of drug delivered.

After five days, there is a great increase in the size of the tumors of the mice administered free DOX, while the size of those administered DOX in vesicles does not increase nearly as much even though they were larger. This is possibly due to the fact that the free drug is cleared much more rapidly from the tumor site than the vesicles.

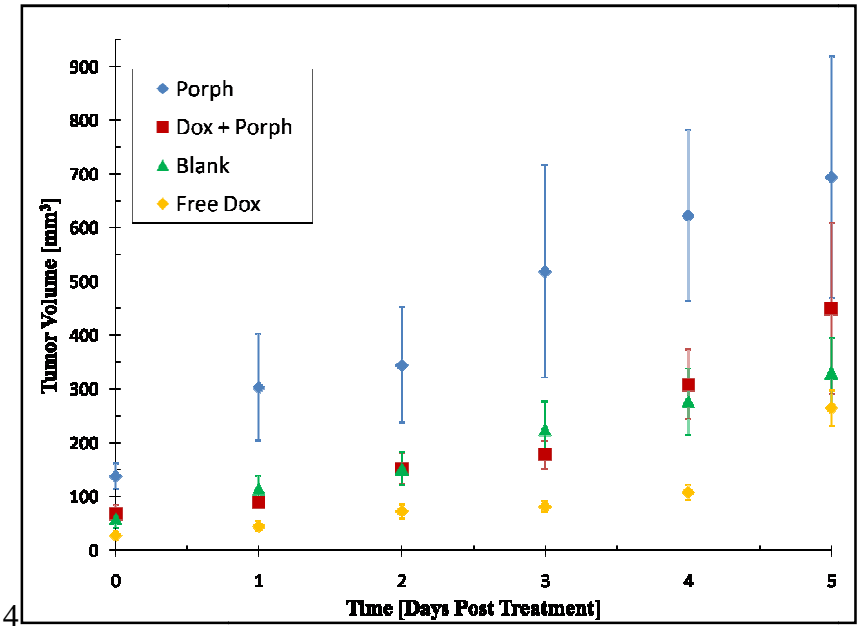

4

Figure 6.13- Tumor Volume (mm3) for mice administered porphyrin PEO-b-PCL Vesicles (blue diamonds), Doxorubicin-Porphyrin PEO-b-PCL Vesicles (red squares), PEO-b-PCL Vesicles (green triangles), and Free Doxorubicin (yellow circles).
Four mice per group, error bars are reported as ±SEM

Results from this study demonstrate the possibility that with an increased dosage and tumors of the same size at the start of the study, a dramatic difference in tumor size between mice administered porphyin-DOX vesicles and all other treatments could be observed.

6.5 CONCLUSIONS

We have shown that porphyrin PEO-b-PBD and PEO-b-PCL polymersomes can be used to non-invasively track the location of polymersomes, and may potentially be applied for diagnostic studies. Porphyrin polymersomes will greatly decrease the number of animals required for biodistribution since the location of the polymersomes can be determined without sacrificing animals at multiple time points to perform histology on the excised organs. Furthermore, the localization of the vesicles in the tumor vasculature was confirmed using intravital microscopy.

The ability of doxorubicin loaded PEO-b-PCL polymersomes to retard tumor growth on par with DOXIL® (the clinically administered liposomal formulation of doxorubicin) and better than free DOX was confirmed. *Multi-functional* polymersomes loaded with doxorubicin and porphyrin were tracked *in vivo* for 120 hours and were able to retard tumor growth in comparison to porphyrin polymersomes. Due to tumor size variation at the start of the study, the porphyrin-doxorubicin PEO-b-PCL polymersomes did not did not perform as expected. However, based on overall polymersome performance, it is believed that with minor modifications which will be discussed in Chapter 7, multimodal polymersomes hold promised for theranostic applications.

The ability to load components into the polymersome membrane and core shows enormous promise for dual modality polymersomes which will allow for the continuous noninvasive monitoring of drug-loaded nanopolymersomes *in vivo*, obviating the need to sacrifice animals at each time point to determine basic pharmacokinetic and biodistribution profiles, thereby greatly reducing animal load. Hence, polymersomes

hold enormous potential to be nanostructured biomaterials for future drug delivery and imaging applications.

6.6 ACKNOWLEDGEMENTS

This work was supported by grants from the National Institutes of Health (EB003457-01 and CA115229), the National Cancer Institute (R33-NO1-CO-29008), Commonwealth Funds, Pennsylvania and Abramson Cancer Center, University of Pennsylvania, and University of Pennsylvania's Institute for the Translational Medicine and Therapeutics (ITMAT). Infrastructural support was provided by a grant from the MRSEC Program of the National Science Foundation (DMR05-20020 and DMR-00-79909). Additional, assistance with image analysis by Dr. Wasserman, LICOR, is noted and greatly appreciated.

6.7 REFERENCES

1. Cegnar, M., J. Kristl, and J. Kos, *Nanoscale polymer carriers to deliver chemotherapeutic agents to tumours.* Expert Opinion on Biological Therapy, 2005. **5**(12): p. 1557-1569.
2. Antonietti, M. and S. Forster, *Vesicles and liposomes: A self-assembly principle beyond lipids.* Advanced Materials, 2003. **15**(16): p. 1323-1333.
3. Discher, B.M., et al., *Polymersomes: Tough vesicles made from diblock copolymers.* Science, 1999. **284**(5417): p. 1143-1146.
4. Discher, D.E. and A. Eisenberg, *Polymer vesicles.* Science, 2002. **297**(5583): p. 967-973.
5. Lee, J.C.M., et al., *Preparation, stability, and in vitro performance of vesicles made with diblock copolymers.* Biotechnology and Bioengineering, 2001. **73**(2): p. 135-145.
6. Meng, F., G.H.M. Engbers, and J. Feijen, *Biodegradable polymersomes as a basis for artificial cells: encapsulation, release and targeting.* Journal of Controlled Release, 2005. **101**(1-3): p. 187-198.
7. Bermudez, H., et al., *Molecular weight dependence of polymersome membrane structure, elasticity, and stability.* Macromolecules, 2002. **35**(21): p. 8203-8208.
8. Photos, P.J., et al., *Polymer vesicles in vivo: correlations with PEG molecular weight.* Journal of Controlled Release, 2003. **90**(3): p. 323-334.

9. Ghoroghchian, P.P., et al., *Near-infrared-emissive polymersomes: Self-assembled soft matter for in vivo optical imaging.* Proceedings of the National Academy of Sciences of the United States of America, 2005. **102**(8): p. 2922-2927.
10. Ghoroghchian, P.P., et al., *Bioresorbable vesicles formed through spontaneous self-assembly of amphiphilic poly(ethylene oxide)-block-polycaprolactone.* Macromolecules, 2006. **39**(5): p. 1673-1675.
11. Zupancich, J.A., F.S. Bates, and M.A. Hillmyer, *Aqueous dispersions of poly(ethylene oxide)-b-poly(gamma-methyl-epsilon-caprolactone) block copolymers.* Macromolecules, 2006. **39**(13): p. 4286-4288.
12. Hillmyer, M.A., et al., *Complex phase behavior in solvent-free nonionic surfactants.* Science, 1996. **271**(5251): p. 976-978.
13. Hillmyer, M.A. and F.S. Bates, *Synthesis and characterization of model polyalkane-poly(ethylene oxide) block copolymers.* Macromolecules, 1996. **29**(22): p. 6994-7002.
14. Discher, D.E. and F. Ahmed, *Polymersomes.* Annual Review of Biomedical Engineering, 2006. **8**: p. 323-341.
15. Savic, R., et al., *Micellar nanocontainers distribute to defined cytoplasmic organelles.* Science, 2003. **300**(5619): p. 615-618.
16. O'Reilly, R.K., C.J. Hawker, and K.L. Wooley, *Cross-linked block copolymer micelles: functional nanostructures of great potential and versatility.* Chemical Society Reviews, 2006. **35**(11): p. 1068-1083.
17. O'Reilly, R.K., et al., *Facile syntheses of surface-functionalized micelles and shell cross-linked nanoparticles.* Journal of Polymer Science Part a-Polymer Chemistry, 2006. **44**(17): p. 5203-5217.
18. Sun, X.K., et al., *An assessment of the effects of shell cross-linked nanoparticle size, core composition, and surface PEGylation on in vivo biodistribution.* Biomacromolecules, 2005. **6**(5): p. 2541-2554.
19. Christian, N.A., et al., *Tat-functionalized near-infrared emissive polymersomes for dendritic cell labeling.* Bioconjugate Chemistry, 2007. **18**(1): p. 31-40.
20. Lin, J.J., et al., *Adhesion of polymer vesicles.* Physical Review Letters, 2005. **95**(2).
21. Lin, J.J., et al., *Adhesion of antibody-functionalized polymersomes.* Langmuir, 2006. **22**(9): p. 3975-3979.
22. Lin, J.J., et al., *The effect of polymer chain length and surface density on the adhesiveness of functionalized polymersomes.* Langmuir, 2004. **20**(13): p. 5493-5500.
23. Matsumura, Y. and H. Maeda, *A New Concept for Macromolecular Therapeutics in Cancer-Chemotherapy - Mechanism of Tumoritropic Accumulation of Proteins and the Antitumor Agent Smancs.* Cancer Research, 1986. **46**(12): p. 6387-6392.
24. Iyer, A.K., et al., *Exploiting the enhanced permeability and retention effect for tumor targeting.* Drug Discovery Today, 2006. **11**(17-18): p. 812-818.
25. Duncan, R., *Polymer-Drug Conjugates: Targeting Cancer*, in *Biomedical Aspects of Drug Targeting*, V.R. Muzykantov and V.P. Torchlin, Editors. 2002, Kluwer Academic Publishers: Boston. p. 197-199.

26. Ahmed, F. and D.E. Discher, *Self-porating polymersomes of PEG-PLA and PEG-PCL: hydrolysis-triggered controlled release vesicles.* Journal of Controlled Release, 2004. **96**(1): p. 37-53.
27. Ahmed, F., et al., *Biodegradable polymersomes loaded with both paclitaxel and doxorubicin permeate and shrink tumors, inducing apoptosis in proportion to accumulated drug.* Journal of Controlled Release, 2006. **116**(2): p. 150-158.
28. Ahmed, F., et al., *Shrinkage of a rapidly growing tumor by drug-loaded polymersome: pH-triggered release through copolymer degradation.* Molecular Pharmaceutics 2006. **3**(3): p. 340-250.
29. Bei, J.Z., et al., *Polycaprolactone-poly(ethylene-glycol) block copolymer .4. Biodegradation behavior in vitro and in vivo.* Polymers for Advanced Technologies, 1997. **8**(11): p. 693-696.
30. Borchert, U., et al., *pH-induced release from P2VP-PEO block copolymer vesicles.* Langmuir, 2006. **22**(13): p. 5843-5847.
31. Cerritelli, S., D. Velluto, and J.A. Hubbell, *PEG-SS-PPS: Reduction-sensitive disulfide block copolymer vesicles for intracellular drug delivery.* Biomacromolecules, 2007. **8**(6): p. 1966-1972.
32. Napoli, A., et al., *New synthetic methodologies for amphiphilic multiblock copolymers of ethylene glycol and propylene sulfide.* Macromolecules, 2001. **34**(26): p. 8913-8917.
33. Valentini, M., et al., *Precise determination of the hydrophobic/hydrophilic junction in polymeric vesicles.* Langmuir, 2003. **19**(11): p. 4852-4855.
34. Napoli, A., et al., *Lyotropic behavior in water of amphiphilic ABA triblock copolymers based on poly(propylene sulfide) and poly(ethylene glycol).* Langmuir, 2002. **18**(22): p. 8324-8329.
35. Napoli, A., et al., *Oxidation-responsive polymeric vesicles.* Nature Materials, 2004. **3**(3): p. 183-189.
36. Sun, J., et al., *Direct formation of giant vesicles from synthetic polypeptides.* Langmuir, 2007. **23**(16): p. 8308-8315.
37. Berezov, A., et al., *Disabling ErbB receptors with rationally designed exocyclic mimetics of antibodies: Structure-function analysis.* Journal of Medicinal Chemistry, 2001. **44**(16): p. 2565-2574.
38. Sengupta, S., et al., *Temporal targeting of tumour cells and neovasculature with a nanoscale delivery system.* Nature, 2005. **436**(7050): p. 568-572.
39. Waterhouse, D.N., et al., Drug Safety, 2001. **24**: p. 903-920.
40. Choucair, A., P.L. Soo, and A. Eisenberg, *Active loading and tunable release of doxorubicin from block copolymer vesicles.* Langmuir, 2005. **21**(20): p. 9308-9313.
41. Sharma, U.S., S.V. Balasubramanian, and R.M. Straubinger, *Pharmaceutical and Physical-Properties of Paclitaxel (Taxol) Complexes with Cyclodextrins.* Journal of Pharmaceutical Sciences, 1995. **84**(10): p. 1223-1230.
42. Weiss, R.B., et al., *Hypersensitivity Reactions from Taxol.* Journal of Clinical Oncology, 1990. **8**(7): p. 1263-1268.

43. Li, S.L., et al., *Self-assembled poly(butadiene)-b-poly(ethylene oxide) polymersomes as paclitaxel carriers.* Biotechnology Progress, 2007. **23**(1): p. 278-285.
44. Gustafson, D.L., A.L. Merz, and M.E. Long, *Pharmacokinetics of combined doxorubicin and paclitaxel in mice.* Cancer Letters, 2005. **220**(2): p. 161-169.
45. Arifin, D.R. and A.F. Palmer, *Polymersome encapsulated hemoglobin: A novel type of oxygen carrier.* Biomacromolecules, 2005. **6**(4): p. 2172-2181.
46. Pressly, E.D., et al., *Structural effects on the biodistribution and positron emission tomography (PET) imaging of well-defined Cu-64-labeled nanoparticles comprised of amphiphilic block graft copolymers.* Biomacromolecules, 2007. **8**(10): p. 3126-3134.
47. Sun, G., et al., *Strategies for optimized radiolabeling of nanoparticles for in vivo PET Imaging.* Advanced Materials, 2007. **19**(20): p. 3157-+.
48. Kelly, K.A., et al., *Detection of vascular adhesion molecule-1 expression using a novel multimodal nanoparticle.* Circulation Research, 2005. **96**(3): p. 327-336.
49. Perez, J.M., et al., *Peroxidase substrate nanosensors for MR imaging.* Nano Letters, 2004. **4**(1): p. 119-122.
50. Tsourkas, A., et al., *In vivo imaging of activated endothelium using an anti-VCAM-1 magnetooptical probe.* Bioconjugate Chemistry, 2005. **16**(3): p. 576-581.
51. Ghoroghchian, P.P., et al., *Broad spectral domain fluorescence wavelength modulation of visible and near-infrared emissive polymersomes.* Journal of the American Chemical Society, 2005. **127**(44): p. 15388-15390.
52. Ghoroghchian, P.P., et al., *Controlling bulk optical properties of emissive polymersomes through intramembranous polymer-fluorophore interactions.* Chemistry of Materials, 2007. **19**(6): p. 1309-1318.
53. Ghoroghchian, P.P., *Emissive Polymer Vesicles: Soft Nanoscale Probes for In Vivo Optical Imaging*, in *Bioengineering*. 2006, University of Pennsylvania: Philadelphia. p. 364.
54. Figdor, C.G., et al., *Dendritic cell immunotherapy: mapping the way.* Nature Medicine, 2004. **10**(5): p. 475-480.
55. Christian, N.A., *Development and Application of Tat-Near-Infrared-Emissive Polymersomes for In Vivo Optical Imaging of Dendritic Cells*, in *Bioengineering*. 2007, University of Pennsylvania: Philadelphia.
56. Zhou, W., et al., *Biodegradable polymersomes for targeted ultrasound imaging.* Journal of Controlled Release, 2006. **116**(2): p. e62-e64.
57. Park, B.W., et al., *Rationally designed anti-HER2/neu peptide mimetic disables p185(HER2/neu) tyrosine kinases in vitro and in vivo.* Nature Biotechnology, 2000. **18**(2): p. 194-198.
58. Brooks, H., B. Lebleu, and E. Vives, *Tat peptide-mediated cellular delivery: back to basics.* Advanced Drug Delivery Reviews, 2005. **57**(4): p. 559-577.
59. Lee, K.Y. and S.H. Yuk, *Polymeric protein delivery systems.* Progress in Polymer Science, 2007. **32**(7): p. 669-697.
60. Nobs, L., et al., *Current methods for attaching targeting ligands to liposomes and nanoparticles.* Journal of Pharmaceutical Sciences, 2004. **93**(8): p. 1980-1992.

61. Ahmed, F., et al., *Block copolymer assemblies with cross-link stabilization: From single-component monolayers to bilayer blends with PEO-PLA.* Langmuir, 2003. **19**(16): p. 6505-6511.
62. Discher, B.M., et al., *Cross-linked polymersome membranes: Vesicles with broadly adjustable properties.* Journal of Physical Chemistry B, 2002. **106**(11): p. 2848-2854.
63. Dudia, A., et al., *Biofunctionalized lipid-polymer hybrid nanocontainers with controlled permeability.* Nano Letters, 2008. **8**(4): p. 1105-1110.
64. Jofre, A., et al., *Amphiphilic block copolymer nanotubes and vesicles stabilized by photopolymerization.* Journal of Physical Chemistry B, 2007. **111**(19): p. 5162-5166.
65. Lee, S.M., et al., *Polymer-caged lipsomes: A pH-Responsive delivery system with high stability.* Journal of the American Chemical Society, 2007. **129**(49): p. 15096-+.
66. Li, F., et al., *Stabilization of polymersome vesicles by an interpenetrating polymer network.* Macromolecules, 2007. **40**(2): p. 329-333.
67. Carter, S.K., *ADRIAMYCIN (NSC-123127) - THOUGHTS FOR FUTURE.* Cancer Chemotherapy Reports Part 3 Program Information-Supplement, 1975. **6**(2): p. 389-397.
68. Young, R.C., R.F. Ozols, and C.E. Myers, *THE ANTHRACYCLINE ANTI-NEOPLASTIC DRUGS.* New England Journal of Medicine, 1981. **305**(3): p. 139-153.
69. Barenholz, Y., et al., *STABILITY OF LIPOSOMAL DOXORUBICIN FORMULATIONS - PROBLEMS AND PROSPECTS.* Medicinal Research Reviews, 1993. **13**(4): p. 449-491.
70. Gabizon, A.A., *SELECTIVE TUMOR-LOCALIZATION AND IMPROVED THERAPEUTIC INDEX OF ANTHRACYCLINES ENCAPSULATED IN LONG-CIRCULATING LIPOSOMES.* Cancer Research, 1992. **52**(4): p. 891-896.
71. Kerbel, R.S. and B.A. Kamen, *The anti-angiogenic basis of metronomic chemotherapy.* Nature Rev. Cancer, 2004. **4**: p. 423-436.
72. Weinberg, r.A., *The Biology of Cancer*. 2007: Garland Science, Taylor & Francis Group.
73. Tozer, G., C. Kanthou, and B. Baguley, *Disrupting Tumor Blood Vessels.* Nature Rev. Cancer, 2005. **5**: p. 423-435.
74. Okaji, Y., et al., *Vaccines targeting tumour angiogenesis - a novel strategy for cancer immunotherapy.* Ejso, 2006. **32**(4): p. 363-370.
75. Hanahan, D., G. Bergers, and E. Bergsland, *Less is more, regularly: metronomic dosing of cytotoxic drugs can target tumor angiogenesis in mice.* The Journal of Clinical Investigation, 2000. **105**: p. 1045-1047.
76. Gaukroger, K., et al., *Novel syntheses of cis and trans isomers of combretastatin A-4.* Journal of Organic Chemistry, 2001. **66**(24): p. 8135-8138.
77. Haran, G., et al., *Transmembrane Ammonium-Sulfate Gradients in Liposomes Produce Efficient and Stable Entrapment of Amphipathic Weak Bases.* Biochimica Et Biophysica Acta, 1993. **1151**(2): p. 201-215.

78. Lopes de Menezes, D.E., Pilarski, L.M., Allen, T.M., , Cancer Research, 1998. **58**: p. 3320-3330.
79. Bolotin, E.M., et al., *Ammonium Sulfate Gradients for Efficient and Stable Remote Loading of Amphiphathic Weak Bases into Liposomes and Ligandoliposomes.* Journal of Liposome Research, 1994. **4**(1): p. 455-479.
80. Abraham, S.A., et al., *The liposomal formulation of doxorubicin*, in *Liposomes, Pt E*. 2005. p. 71-97.
81. de Menezes, D.E.L., L.M. Pilarski, and T.M. Allen, *In vitro and in vivo targeting of immunoliposomal doxorubicin to human B-cell lymphoma.* Cancer Research, 1998. **58**(15): p. 3320-3330.
82. Beijnen, J.H., O. Vanderhouwen, and W.J.M. Underberg, *ASPECTS OF THE DEGRADATION KINETICS OF DOXORUBICIN IN AQUEOUS-SOLUTION*. International Journal of Pharmaceutics, 1986. **32**(2-3): p. 123-131.
83. Janssen, M.J.H., et al., *DOXORUBICIN DECOMPOSITION ON STORAGE - EFFECT OF PH, TYPE OF BUFFER AND LIPOSOME ENCAPSULATION.* International Journal of Pharmaceutics, 1985. **23**(1): p. 1-11.
84. Ifkovits, J.L. and J.A. Burdick, *Review: Photopolymerizable and degradable biomaterials for tissue engineering applications.* Tissue Engineering, 2007. **13**(10): p. 2369-2385.
85. Kwon, G.S., et al., *PHYSICAL ENTRAPMENT OF ADRIAMYCIN IN AB BLOCK-COPOLYMER MICELLES.* Pharmaceutical Research, 1995. **12**(2): p. 192-195.
86. Singer, S.J. and G.L. Nicolson, *FLUID MOSAIC MODEL OF STRUCTURE OF CELL-MEMBRANES.* Science, 1972. **175**(4023): p. 720-&.
87. Bangham, A.D., M.M. Standish, and J.C. Watkins, *DIFFUSION OF UNIVALENT IONS ACROSS LAMELLAE OF SWOLLEN PHOSPHOLIPIDS.* Journal of Molecular Biology, 1965. **13**(1): p. 238-&.
88. Ghadiri, M.R., J.R. Granja, and L.K. Buehler, *ARTIFICIAL TRANSMEMBRANE ION CHANNELS FROM SELF-ASSEMBLING PEPTIDE NANOTUBES.* Nature, 1994. **369**(6478): p. 301-304.
89. Percec, V., et al., *Self-assembly of amphiphilic dendritic dipeptides into helical pores.* Nature, 2004. **430**(7001): p. 764-768.
90. Haluska, C.K., et al., *Time scales of membrane fusion revealed by direct imaging of vesicle fusion with high temporal resolution.* Proceedings of the National Academy of Sciences of the United States of America, 2006. **103**(43): p. 15841-15846.
91. Barenholz, Y., *Liposome application: problems and prospects.* Current Opinion in Colloid & Interface Science, 2001. **6**(1): p. 66-77.
92. Guo, X. and F.C. Szoka, *Chemical approaches to triggerable lipid vesicles for drug and gene delivery.* Accounts of Chemical Research, 2003. **36**(5): p. 335-341.
93. Ringsdorf, H., B. Schlarb, and J. Venzmer, *MOLECULAR ARCHITECTURE AND FUNCTION OF POLYMERIC ORIENTED SYSTEMS - MODELS FOR THE STUDY OF ORGANIZATION, SURFACE RECOGNITION, AND DYNAMICS OF BIOMEMBRANES.* Angewandte Chemie-International Edition in English, 1988. **27**(1): p. 113-158.

94. Thomas, J.L. and D.A. Tirrell, *POLYELECTROLYTE-SENSITIZED PHOSPHOLIPID-VESICLES.* Accounts of Chemical Research, 1992. **25**(8): p. 336-342.
95. Lasic, D.D. and D. Papahadjopoulos, *LIPOSOMES REVISITED.* Science, 1995. **267**(5202): p. 1275-1276.
96. Krafft, M.P., *Fluorocarbons and fluorinated amphiphiles in drug delivery and biomedical research.* Advanced Drug Delivery Reviews, 2001. **47**(2-3): p. 209-228.
97. Papahadjopoulos, D., et al., *STERICALLY STABILIZED LIPOSOMES - IMPROVEMENTS IN PHARMACOKINETICS AND ANTITUMOR THERAPEUTIC EFFICACY.* Proceedings of the National Academy of Sciences of the United States of America, 1991. **88**(24): p. 11460-11464.
98. Cornelissen, J., et al., *Helical superstructures from charged poly(styrene)-poly(isocyanodipeptide) block copolymers.* Science, 1998. **280**(5368): p. 1427-1430.
99. Kita-Tokarczyk, K. and W. Meier, *Biomimetic Block Copolymer Membranes.* Chimia, 2008. **62**(10): p. 820-825.
100. Chiruvolu, S., et al., *A PHASE OF LIPOSOMES WITH ENTANGLED TUBULAR VESICLES.* Science, 1994. **266**(5188): p. 1222-1225.
101. Walker, S.A., M.T. Kennedy, and J.A. Zasadzinski, *Encapsulation of bilayer vesicles by self-assembly.* Nature, 1997. **387**(6628): p. 61-64.
102. Dubois, M., et al., *Self-assembly of regular hollow icosahedra in salt-free catanionic solutions.* Nature, 2001. **411**(6838): p. 672-675.
103. Almgren, M., K. Edwards, and G. Karlsson, *Cryo transmission electron microscopy of liposomes and related structures.* Colloids and Surfaces a-Physicochemical and Engineering Aspects, 2000. **174**(1-2): p. 3-21.
104. Walter, A., et al., *INTERMEDIATE STRUCTURES IN THE CHOLATE-PHOSPHATIDYLCHOLINE VESICLE MICELLE TRANSITION.* Biophysical Journal, 1991. **60**(6): p. 1315-1325.
105. Percec, V., et al., *Controlling polymer shape through the self-assembly of dendritic side-groups.* Nature, 1998. **391**(6663): p. 161-164.
106. Percec, V., et al., *Self-organization of supramolecular helical dendrimers into complex electronic materials (vol 419, pg 384, 2002).* Nature, 2002. **419**(6909): p. 862-862.
107. Lee, C.C., et al., *Designing dendrimers for biological applications.* Nature Biotechnology, 2005. **23**(12): p. 1517-1526.
108. Esfand, R. and D.A. Tomalia, *Poly(amidoamine) (PAMAM) dendrimers: from biomimicry to drug delivery and biomedical applications.* Drug Discovery Today, 2001. **6**(8): p. 427-436.
109. Walde, P. and S. Ichikawa, *Enzymes inside lipid vesicles: Preparation, reactivity and applications.* Biomolecular Engineering, 2001. **18**(4): p. 143-177.
110. Lasic, D.D., *Colloid chemistry - Liposomes within liposomes.* Nature, 1997. **387**(6628): p. 26-27.

111. Needham, D. and R.S. Nunn, *ELASTIC-DEFORMATION AND FAILURE OF LIPID BILAYER-MEMBRANES CONTAINING CHOLESTEROL*. Biophysical Journal, 1990. **58**(4): p. 997-1009.
112. Vanhest, J.C.M., et al., *POLYSTYRENE-DENDRIMER AMPHIPHILIC BLOCK-COPOLYMERS WITH A GENERATION-DEPENDENT AGGREGATION*. Science, 1995. **268**(5217): p. 1592-1595.
113. Al-Jamal, K.T., T. Sakthivel, and A.T. Florence, *Dendrisomes: Vesicular structures derived from a cationic lipidic dendron.* Journal of Pharmaceutical Sciences, 2005. **94**(1): p. 102-113.
114. Jain, R.K., L.L. Munn, and D. Fukumura, *Dissecting tumour pathophysiology using intravital microscopy*. Nature Reviews Cancer, 2002. **2**(4): p. 266-276.
115. Weissleder, R., *A clearer vision for in vivo imaging.* Nature Biotechnology, 2001. **19**(4): p. 316-317.
116. Lin, V.S.Y. and M.J. Therien, *The role of porphyrin-to-porphyrin linkage topology in the extensive modulation of the absorptive and emissive properties of a series of ethynyl- and butadiynyl-bridged bis- and tris(porphinato)zinc chromophores.* Chemistry-a European Journal, 1995. **1**(9): p. 645-651.
117. Lin, V.S.Y., S.G. Dimagno, and M.J. Therien, *HIGHLY CONJUGATED, ACETYLENYL BRIDGED PORPHYRINS - NEW MODELS FOR LIGHT-HARVESTING ANTENNA SYSTEMS.* Science, 1994. **264**(5162): p. 1105-1111.
118. Duncan, T.V., et al., *Exceptional near-infrared fluorescence quantum yields and excited-state absorptivity of highly conjugated porphyrin arrays.* Journal of the American Chemical Society, 2006. **128**(28): p. 9000-9001.
119. Ghoroghchian, P.P., et al., *Quantitative membrane loading of polymer vesicles.* Soft Matter, 2006. **2**(11): p. 973-980.
120. Gabizon, A., et al., *LIPOSOMES AS INVIVO CARRIERS OF ADRIAMYCIN - REDUCED CARDIAC UPTAKE AND PRESERVED ANTI-TUMOR ACTIVITY IN MICE*. Cancer Research, 1982. **42**(11): p. 4734-4739.
121. Discussions with Dr. B. Barnhart, U.o.P., Abramson Family Cancer Research Institute.
122. Eliaz, R.E. and F.C. Szoka, *Liposome-encapsulated doxorubicin targeted to CD44: A strategy to kill CD44-overexpressing tumor cells.* Cancer Research, 2001. **61**(6): p. 2592-2601.
123. Tromberg, B.J., et al., *Non-invasive in vivo characterization of breast tumors using photon migration spectroscopy*. Neoplasia, 2000. **2**(1-2): p. 26-40.
124. Frangioni, J.V., *In vivo near-infrared fluorescence imaging.* Current Opinion in Chemical Biology, 2003. **7**(5): p. 626-634.
125. Wagnieres, G.A., W.M. Star, and B.C. Wilson, *In vivo fluorescence spectroscopy and imaging for oncological applications.* Photochemistry and Photobiology, 1998. **68**(5): p. 603-632.
126. Licha, K., *Contrast agents for optical imaging*, in *Contrast Agents Ii*. 2002, Springer-Verlag Berlin: Berlin. p. 1-29.
127. Olive, D.M., *Near Infrared Technology And Optical Agents for Molecular Imaging*. July 2009, LI-COR Bioscience: LI-COR Proucts and Applications Guide. p. 25-27.

128. Lopes, L.B., et al., *Studies on the encapsulation of diclofenac in small unilamellar liposomes of soya phosphatidylcholine.* Colloids and Surfaces B-Biointerfaces, 2004. **39**(4): p. 151-158.
129. Sharma, A., E. Mayhew, and R.M. Straubinger, *ANTITUMOR EFFECT OF TAXOL-CONTAINING LIPOSOMES IN A TAXOL-RESISTANT MURINE TUMOR-MODEL.* Cancer Research, 1993. **53**(24): p. 5877-5881.
130. Sharma, A. and R.M. Straubinger, *NOVEL TAXOL FORMULATIONS - PREPARATION AND CHARACTERIZATION OF TAXOL-CONTAINING LIPOSOMES.* Pharmaceutical Research, 1994. **11**(6): p. 889-896.
131. Xu, J.P., et al., *Novel biomimetic polymersomes as polymer therapeutics for drug delivery.* Journal of Controlled Release, 2005. **107**(3): p. 502-512.
132. Levine, D.H., et al., *Polymersomes: A new multi-functional tool for cancer diagnosis and therapy.* Methods, 2008. **46**(1): p. 25-32.
133. Berezov, A., et al., *Disabling receptor ensembles with rationally designed interface peptidomimetics.* Journal of Biological Chemistry, 2002. **277**(31): p. 28330-28339.
134. Sengupta, S., T. Kiziltepe, and R. Sasisekharan, *A dual-color fluorescence imaging-based system for the dissection of antiangiogenic and chemotherapeutic activity of molecules.* FASEB Journal, 2004. **18**(11): p. 1565-+.
135. Arap, W., R. Pasqualini, and E. Ruoslahti, *Cancer Treatment by Targeted Drug Delivery to Tumor Vasculature in a Mouse Model.* Science, 1998. **279**: p. 377-380.
136. Pasqualini, R., E. Koivunen, and E. Ruoslahti, *alpha v Integrins as receptors for tumor targeting by circulating ligands.* Nature Biotechnology, 1997. **15**(6): p. 542-546.
137. Ruoslahti, E., *Vascular zip codes in angiogenesis and metastasis.* Biochemical Society Transactions, 2004. **32**: p. 397-402.

Chapter 7

SUMMARY, MAJOR FINDINGS, AND SUGGESTED FUTURE RESEARCH FOR THE DEVELOPMENT OF FULLY BIORESORBABLE MULTI-FUNCTIONAL POLYMERSOMES

7.1 SUMMARY

The ability to deliver systemically toxic pharmaceutical agents or hydrophobic therapuetics with low bioavailability is a major challenge in treating malignancies. Combination therapies, consisting of either two different small molecules or a combination of small molecules and biologically active ligands, are currently used for the treatment of various cancers; thus, the capability co-administer and simultaneously deliver them is of great importance. In addition to treatment challenges, noninvasive diagnostic tools for the screening, diagnosis, and post treatment monitoring, are of particular clinical interest. The ability to coencapsulate drug and imaging agent, enabling the "imaging of drug delivery", can greatly enhance exploration into various treatment options and elucidate the efficacy of these treatments. Liposomes are presently used in various biotechnological and pharmaceutical applications to improve therapeutic indices and enhance cellular uptake [4], but it appears that polymersomes can offer superior advantages for future clinical therapeutic and diagnostic applications.

In this thesis, I develop, characterize, and evaluate *in situ*, *in vitro*, and *in vivo*, polymersomes (polymeric vesicles):

a) with the ability to co-encapsulate doxorubicin, a chemotherapeutic, and combretastatin, a vascaular disrupting agent, for the co-administration of two different therapeutics, creating a tool for the eradication of both tumorigenic cells and vascular cells.

b) and with the ability to co-incorporate doxorubicin and porphyrin, a highly hydrophobic near infrared fluorophore, for the capability to simultaneously

image and deliver pharamacetuical agents, essentially creating a tool for therapy and diagnosis.

7.2 Major Results with Respect to the Aims Delineated in Chapter 1

7.2.1 Aim 1: To load physiologically relevant molecules and imaging agents into the polymersome and characterize release kinetics

Doxorubicin was successfully loaded into the PEO-b-PCL polymersome, as well as polymeric vesicles compromised of other diblock copolymers. The different loading parameters were explored and it was determined that loading DOX into PEO-b-PCL vesicles could be accomplished using only an ammonium sulfate gradient, but the loading of DOX into PEO-b-PBD and PEO-b-PmCL required the generation of a pH gradient as well as an ammonium sulfate gradient. This difference in loading environment was attributed to the differences in hydrophobicity between the different hydrophobic backbones. Combretastatin incorporation into PEO-b-PCL vesicles was also established.

The insight gained from loading doxorubicin into these polymeric vesicles, enabled the successful encapsulation of doxorubicin into combretatstatin incorporated vesicles and into porophyrin encapusulated vesicles. Similar to the encapsulation of DOX into PEO-b-PBD and PEO-b-PmCL vesicles, these encapsulations required the use of both a pH and ammonium sulfate gradient.

Doxorubicin release kinetics from the various vesicles and co-encapsulations was characterized. The cumulative release of drug from the vesicles interior occur though the diffusion of the amphiphilic molecule across the vesicle membrane and by degradation of

the hydrophobic backbone of the vesicle. These release mechanisms depend upon both the pH of the external solution and the polymer and hydrophobic encapsulant composition of the vesicles. The successful co-encapsulation of DOX and combretastatin lead to the generation of a polymersome with the potential to treat tumors by affecting both the vasculature and tumor cells. The encapsulation of DOX into porphyrin incorporated vesicles lead to the creation of vesicles with therapeutic and diagnostic capabilities.

7.2.2 Aim2 Load Doxorubicin into the Aqueous Core of Dendrosomes

Doxorubicin was successfully encapsulated into the aqueous core of dendrosomes, vesicles self-assembled from various amphiphilic Janus-dendrimers. Due to stability issues of the dendrosomes at low pH, doxorubicin was not actively loaded across a gradient as it was for the case of polymersomes, but rather it was loaded passively by incorporation in the hydration solution. Release studies were performed and show a significantly higher release of drug at acidic pH than at physiological pH. Drug release was observed to vary depending on both pH of the external solution and dendrosome library.

The toxicity of the dendrosomes was evaluated *in vitro* on human umbilical vein endothelial cells (HUVECs) using Cell Titer-Blue^{TM}. The results indicate only minimal toxicity as compared to polymersomes after four hours of incubation with vesicles.

The results of dendrosome studies establish their the potential use as of self-assembled dendrimeric vesicles for drug delivery purposes

7.2.3 Aim 3: To study the in vitro effects of functional polymersomes using HUVECs and SK-BR-3 tumorigenic cells

The effects of PEO-b-PCL vesicles on HUVECs and SK-BR-3 cells were examined separately. It was determined that the HUVECs incubated with PEO-b-PCL polymersomes remain 50% viable after 72 hours, even when incubated at the high concentration of polymer. At short times, SK-BR-3 cells appear to tolerate the PEO-b-PCL polymersomes, with viability as great as 50% after 12 hours. However toxicity is observed at longer times, where after 72 hours only 50% of cells cultures in the lowest polymer concentration are viable.

The cellular uptake of PEO-b-PCL by HUVECs and SK-BR-3 cells was determined using porphyrin polymersomes. The uptake of vesicles by these cell types was established over 5 hours and it was determined that the uptake is dependent upon both vesicles concentration and incubation time.

Lastly, the cytotoxic effects of drug loaded polymersomes on cell viability were investigated with cells cultured both separately and in co-culture. In general, toxicity was a function of both drug concentration and incubation times. Preliminary co-culture assays suggest that cells in co-culture appear to be less adversely affected initially by the drug loaded vesicles.

These *in vitro* experiments establish the potential of using polymersomes loaded with doxorubicin and combretastatin for the simultaneous (and independent) destruction of tumorigenic and endothelial cells.

7.2.4 Aim 4: To demonstrate the in vivo potential of polymersomes for imaging and drug delivery applications using athymic nude mice with xenograft tumors

Using NIR-emissive porphyrin PEO-b-PBD polymersomes, the biodistribution of vesicles was determined both at short times (up to 12 hours) and at long times (up to 9 days) using the eXploreOptix GEArt and LI-COR Odyssey, respectively. These studies demonstrate accumulation of vesicles at the tumor site within 4 hours, with the greatest accumulation after 24 hours. Furthermore, localization of the vesicles with the spleen and liver were observed *in vivo* and ex vivo studies also demonstrate accumulation in the kidneys and lungs. Subsequent studies carried out using NIR-emissive porphyrin PEO-b-PCL polymersomes show similar results.

The anti-tumor effects of doxorubicin loaded PEO-b-PCL polymersomes on tumor suppression *in vivo* were demonstrated using metrics such as tumor volume and mouse weight. Athymic nude mice were administered one of four treatments (doxorubicin polymersomes, DOXIL®, unencapsulated doxorubicin, and PBS) and it was determined that the DOX polymersomes was able to retard tumor growth in mice as well as DOXIL®, and better than free DOX. Furthermore, physical behavioral disposition of the treated mice, suggested that the polymersome may be a superior delivery vehicle for the drug.

The potential to image drug delivery through the use of *multi-functional* doxorubicin loaded porphyrin incorporated PEO-b-PCL polymersomes was highlighted. Mice were administered one of four treatments (DOX-porphyrin polymersomes, porphyrin polymersome, unloaded polymersomes, and free DOX). While the results of the study are not nearly as promising as was desired, the study does demonstrate the

ability to use bioresporbable vesicles loaded with drug for imaging and treating tumors highlighting their potential for theranostic applications.

7.3 Significance of Results

Through preliminary developmental studies, multi-drug loaded PEO-b-PCL and multi-functional PEO-b-PCL polymersome were successfully generated. These multi-drug loaded vesicles demonstrate potential utility for combination therapies where the simultaneous co-localization of the drug is imperative for effective therapy, for example when administering a vascular disrupting agent and a chemotherapeutic. If the anti-vascular agent is administered prior to the chemotherapeutic, the chemotherapeutic may never reach the tumor site because of vasculature disruption. The multi-functional porphyrin-doxorubicin PEO-b-PCL polymersome enables the drug loaded vesicles to be tracked *in vivo*. This novel ability is believed to prove exceedingly useful for monitoring therapeutic outcomes of after administration of therapy. In addition, this combination vesicle will greatly assist in drug biodistribution studies where the number of animals required can be greatly reduced since location of the drug over time can be tracked fluorometrically, obviating the need to sacrificing multiple animals at various time points for histological assessment on the excised organs.

7.4 Future Work and Investigations Towards the Development of a Clinically Relevant Fully-Biodegradable Multi-Functional Polymersome for *in vivo* Theranostic Applications

As demonstrated throughout this thesis, bioresorbable polymersomes hold considerable promise to be clinically relevant nanoparticles for the simultaneous delivery

of dual therapeutics and imaging agents. However, a few key modifications to the vesicles would enhance their clinical utility. Furthermore, additional experimentation is required to bring theses nanoparticles from bench to bedside. This section will highlight additional experiments deemed necessary to demonstrate the clinical applicability of multi-modality vesicles, future surface modifications to the vesicles, and suggest additional changes to experiments already performed.

7.4.1 Suggestions to Enhance Experiments Investigating the Anti-vasculature and Anti-tumor Potential of Combretastatin and Doxorubicin Loaded PEO-b-PCL Polymersomes on HUVECs and SK-BR-3 Cells in Co-culture

As discussed in Chapter 5, considerable sticking was observed when carrying out stained co-culture cell viability assays to determine the effects of doxorubicin and combretastatin separately or together on co-cultured cells. At the time of the experimentation, the dual color staining of cells using CellVue® stains from MTTI appeared to be a proper course of action for these preliminary experiments. However, post experimentation, considerable cell sticking was observed with HUVECs. It was determined that this sticking increases as the amount of time the nonviable cells remain in the wells increases; thus yielding false positive results (i.e. nonviable cells appear viable).

A dual-color fluorescence imaging based assay [38, 134], appears to be a promising alternative to the current assay. In this assay, one type of cells in the co-culture, the tumorigenic cells for example, will be transfected and selected such that they express green fluorescent protein (GFP). The co-culture, comprised of HUVECs and tumorigenic cells, will be exposed to the various polymersome treatments for a defined period of time. After administration of drug-loaded polymersomes, the cells will be

treated with propidium iodide to stain the nuclei and analyzed by dual-fluorescence confocal microscopy to determine the extent of treatment efficacy by examining the vascular network and survival of the tumor cells.

In addition to the dual-color fluorescent microscopy assay detailed above, if the morphological markers of cell death vary between the cell types, investigating morphological markers can be used to ascertain difference in cellular viability between each cell type. In addition, the upregulation of various cellular markers on the cell can be examined to further determine the cellular viability of each cell type.

Additionally, it may be advantageous to co-culture the endothelial and tumorigenic on cells a three-dimensional Matrigel, as this will simulate the tumor environment better than cell culture plates.

7.4.2 Suggestions for Future Surface Modifications to the Vesicles for Enhanced Therapeutic and Diagnostic Efficacy and Related Experiments

Tumor vasculature varies greatly from that of normal tissues. The endothelial cells lining the vessels of solid tumors, where angiogenesis is prevalent, upregulate α_v integrins, as well as receptors for various angiogenic growth factors [135]. These proteins, however, are not present or are present at very low levels in established normal blood vessels [135]. Thus, peptides directed at these upregulated proteins are good targets for cancer therapeutics. Ruoslahti and colleagues showed that upregulated $\alpha_v\beta_3$ integrins on tumor vasculature are active, available for binding by circulating RGD ligands, and expressed at levels sufficient for tumor targeting[135, 136]. Furthermore, α_v

integrins are expressed on many human carcinoma cells as well as tumor vasculature [135].

Peptides for homing to tumors (that can direct therapeutics to the tumor site) can enhance therapeutic efficacy and minimize adverse side effects [137]. This idea of enhanced therapeutic index with tumor-homing peptides was examined by Ruoslahti and coworkers who conjugated doxorubicin to an RGD peptide and administered the conjugated drug and free drug to nude mice with human tumor xenografts [135]. In addition to increased survival rate and decreased tumor size, nude mice treated with the dox-RGD conjugates exhibited less cardiac and liver toxicity than those treated with free DOX [135].

This data suggests that decorating the PEO brush surface of the fully-bioresobable polymersome loaded with combretastatin and doxorubicin with an RGD peptide capable of targeting tumor vasculature as well as cancer cells would enhance the localization of the vesicles at the tumor site and ultimately improve therapeutic efficacy.

Peptides targeting upregulated α_v-integrins can be conjugated to the PEO brush of the polymersome via various covalent and modular chemistries. Currently, Joshua Katz (Hammer and Burdick Laboratories) is working on the ability to functionalize the polymer chain ends through amidation chemistry, where by the amine of the peptide is conjugated to a carboxylic acid at the end of the PEO block to form an amide bond. Furthermore, the biotin-avidin binding represents a method of modular chemistry for peptide conjugation. A biotin molecule is attached to the PEO brush of the polymersome surface and an additional biotin molecule is attached to the end of the peptide. The

biotinylated polymersome and the biotinylated peptide are joined by an avidin molecule [21]. It should be noted that the attachment of peptides to the vesicle surface has been previously attempted by P. Peter Ghoroghichian [53] with limited success in maintaining vesicular structure with peptide attachment. This is likely because the conjugation of ligands to the polymersome surfaces can alter the composite polymer amphiphiles' hydrophilic-block-to-total-mass ratio leading to a change in structural morphology (e.g. from vesicles to micelles) [132]. Hence peptide attachment to polymer vesicles should be confirmed using both cryo-TEM, to images the vesicles, and well as fluorescence microscopy to confirm the presence of an aqueous reservoir.

Once peptide attachment to vesicles is confirmed, Enzyme-linked Immunosorbent Assay (ELISA) can be performed to ensure binding of the RGD peptide-conjugated polymersome with α_v integrins and to determine binding properties of the α_v integrin to the conjugated polymersome. Equilibrium binding of the RGD peptide-conjugated polymersomes to purified α_v integrins will be examined using an ELISA assay. RGD peptide-conjugated polymersomes, scrambled RGD peptide-conjugated polymersomes, and non-conjugated polymersomes will each be mixed with purified α_v integrins. After integrin binding, the sample will be purified to remove unbound integrin, and an antibody for the integrin (but not function blocking) will be added to each sample. Again the sample will be purified once binding had occurred. Lastly, a secondary antibody linked to an enzyme such as horseradish peroxidase (HRP) will be added and allowed to bind to the anti-integrin antibody. The sample will be purified, and the enzyme will be developed using a substrate solution. After a period of time, the reaction will be quenched and absorbance readings will be determined using an ELISA reader [53].

Higher absorbance values will be seen with increased enzyme in sample, thus correlating to increased integrin-RDG peptide binding.

Once these *in vitro* studies are completed, further *in vivo* work to demonstrate increased therapeutic outcomes as well as increased localization to the tumor site are necessary. Anti-tumor potential of the peptide-decorated drug loaded polymersomes can be assayed as a measure of tumor volume and mouse survival. The localization of these peptide conjugated vesicles can be demonstrated through vesicle tracking with the porphyrin fluorophore as shown in Chapter 6.

These enhancements and confirming studies can lead to the generation of a fully-bioresorbable vesicle with potential to directly and simultaneous effect tumor cells and the endothelial cells which grow up to support their existence.

7.4.3 Suggestions for Future Work and Experiments to Enhance In Vivo Component of this Thesis

Through the work described in this thesis, considerable advancements have been made in marrying the drug delivery and imaging applications of polymersomes. However, there are still challenges which must be overcome. First and foremost, the sizing of the vesicles is an extremely labor and time intensive task and a system to automate the extrusion process is essential if vesicle preparation is to be scaled up for clinical use.

In addition, the loading efficiency of DOX, when loaded into porphyrin incorporated vesicles, must be further enhanced and better controlled so that a substantial amount of drug can be delivered to the tumors. Currently, the loading is quite poor and

as such, only 1% of the dose deliver in the Therapeutic Studies was delivered in the Theranostic Studies. The addition of a targeting agent to the vesicle should enhance the localization of vesicles to the tumor site, decrease systemic delivery of the drug, and thereby increase the amount of drug delivered to the tumor. Once the loading efficiency of DOX in porphyrin-incorporated vesicles has been increased, the Theranostic Study described in Chapter 6 should be repeated as the potential to demonstrate the "imaging of drug delivery" has been demonstrated, and could be confirmed with an increase in drug concentration at the tumor site.

As eluded to in Chapter 6, it is envisioned that the bioresorbable vesicles generated from PEO-b-PCL diblock, might be able to link changes in fluorescence not only to the clearance of the vesicle, but also to degradation of the vesicle. While PEO-b-PBD vesicles are biocompatible, they are not known to be biodegrable. Thus, changes in fluorescence associated with the non-degradable PEO-PBD vesicles, would provide information about biodistribution and in vivo clearance of the vesicles while changes in fluorescence of the degradable PEO-PCL vesicles should provide information about clearance and biodistribution, as well as vesicle breakdown and subsequent drug delivery. Data in Chapter 4 demonstrated a decrease in porphyrin fluorescence as doxorubicin is released from the vesicle interior. To carry out this experiment, mice should be administered, PEO-b-PBD and PEO-PCL vesicles with porphyrin incorporated into the bilayer. The *in vivo* fluorescence should be tracked over time, and organs examined for fluorescence upon culmination of the study to determine vesicle location and breakdown.

Once these studies establish the ability to demonstrate vesicle degradation *in vivo* through changes in fluorescence, the drug delivery component should be added by administering doxorubicin loaded vesicles in both the biocompatible and biodegradable formulation. Post treatment, tumor volumes and fluoresce should be monitored *in vivo* at regularly established time points. At the culmination of the study, organs should be harvested and fluorescence measured. In addition to imaging whole organs for fluorescence signal from the porphyrin in the vesicles, these tumor should be sectioned, and sections should imaged for both DOX florescence [28] and porphyrin fluorescence. *Ex vivo* imaging of visible fluorophores is possible at sub-millimeter depths [114]. These studies will assist in fully capturing the essence of polymersomes for imaging drug delivery.

Lastly, in an effort to further develop multi-drug vesicles for clinical *in vivo* applications for the simultaneous delivery of drug to two different cell types, namely endothelial cells and tumorigenic cells, once clearance is granted for *in vivo* studies, in addition to demonstrating increased tumor suppression when combretastatin is delivered in combination with DOX, the tumor vasculature post delivery of the VDA should be examined. Mice should be administered chemotherapeutic vesicles with and without combretastatin, as well as blank vesicles to compare the therapeutic effects of the dual drug loaded vesicles against single drug vesicles and control (non-drug loaded) vesicles. Tumor volumes should be monitored daily, and mouse weights recorded every other day. At the culmination of the study, prior to sacrificing mice, if possible, mice should be administered Angiosense 680 IVM and the tumor vasculature examined using the Olympus IV-100 described in Chapter 6 for invasive *in vivo* examination of the tumor

vasculature. Once the vasculature dye has cleared, the mice should be sacrificed, tumors harvested, sectioned, and stained for vWf, CD34, CD31, which are known markers of blood vessels in order to get a better understanding of the effects of combretastatin on tumor vasculature.

7.5 CONCLUDING REMARKS

Considerable progress was made in establishing the utility of polymer vesicles for drug delivery and diagnostic applications. *In vitro* work was performed to characterize the effects of these vesicles on endothelial and tumorigenic cells. However, the ultimate experiments in establishing the significance of these vesicles in clinical biological applications were performed *in vivo* through collaboration with Dr. Murali. For future clinical use of the theranostic polymersomes, however, the efficiency of loading doxorubicin into porphyrin vesicles must be greatly enhanced, so that a significant dose of drug can be delivered to the tumor site. Furthermore, to fully realize the potential of multi-drug vesicles, the attachment of a vascular homing peptide to target the vesicles to the tumor would probably enhance therapeutic efficacy of the drug loaded vesicles. As a final permutation, to provide both dual therapeutic action as well as imaging capability, a vascular targeting peptide with known therapeutic value could be attached to the PEO brush surface of doxorubicin-porphyrin PEO-b-PCL vesicles, enabling the simultaneious imaging of drug delivery to both endothelial and tumorigenic cells.

7.6 REFERENCES

1. Discher, D.E. and A. Eisenberg, *Polymer vesicles.* Science, 2002. **297**(5583): p. 967-973.

2. Sengupta, S., et al., *Temporal targeting of tumour cells and neovasculature with a nanoscale delivery system.* Nature, 2005. **436**(7050): p. 568-572.
3. Sengupta, S., T. Kiziltepe, and R. Sasisekharan, *A dual-color fluorescence imaging-based system for the dissection of antiangiogenic and chemotherapeutic activity of molecules.* FASEB Journal, 2004. **18**(11): p. 1565-+.
4. Arap, W., R. Pasqualini, and E. Ruoslahti, *Cancer Treatment by Targeted Drug Delivery to Tumor Vasculature in a Mouse Model.* Science, 1998. **279**: p. 377-380.
5. Pasqualini, R., E. Koivunen, and E. Ruoslahti, *alpha v Integrins as receptors for tumor targeting by circulating ligands.* Nature Biotechnology, 1997. **15**(6): p. 542-546.
6. Ruoslahti, E., *Vascular zip codes in angiogenesis and metastasis.* Biochemical Society Transactions, 2004. **32**: p. 397-402.
7. Lin, J.J., et al., *Adhesion of antibody-functionalized polymersomes.* Langmuir, 2006. **22**(9): p. 3975-3979.
8. Ghoroghchian, P.P., *Emissive Polymer Vesicles: Soft Nanoscale Probes for In Vivo Optical Imaging*, in *Bioengineering*. 2006, University of Pennsylvania: Philadelphia. p. 364.
9. Levine, D.H., et al., *Polymersomes: A new multi-functional tool for cancer diagnosis and therapy.* Methods, 2008. **46**(1): p. 25-32.
10. Ahmed, F., et al., *Shrinkage of a rapidly growing tumor by drug-loaded polymersome: pH-triggered release through copolymer degradation.* Molecular Pharmaceutics 2006. **3**(3): p. 340-250.
11. Jain, R.K., L.L. Munn, and D. Fukumura, *Dissecting tumour pathophysiology using intravital microscopy.* Nature Reviews Cancer, 2002. **2**(4): p. 266-276.